STRATIGRAPHY, DEPOSITIONAL ENVIRONMENTS, PETROLOGY, DIAGENESIS, AND HYDROCARBON MATURATION RELATED TO THE RED FORK SANDSTONE IN NORTH-CENTRAL OKLAHOMA

By

KENNETH SCOTT ROBERTSON

Bachelor of Science

Edinboro State University

Edinboro, Pennsylvania

1977

Submitted to the Faculty of the
Graduate College of the
Oklahoma State University
in partial fulfillment of
the requirements for
the Degree of
MASTER OF SCIENCE
December, 1983

STRATIGRAPHY, DEPOSITIONAL ENVIROMENTS, PETROLOGY, DIAGENESIS, AND HYDROCARBON MATURATION RELATED TO THE RED FORK SANDSTONE IN NORTH-CENTRAL OKLAHOMA

Thesis Approved:

Zuhair al-Shaieb
Thesis Adviser

Gary J. Stewart

Arthur W. Cleaves

Norman N. Durham
Dean of the Graduate College

PREFACE

This study focuses on the stratigraphy, depositional environments, petrological characteristics, diagenetic sequences, and hydrocarbon maturation related to the Red Fork sandstone in north-central Oklahoma. Approximately 700 electric logs were used to construct nine regional cross sections and four diagnostic subsuface maps. These maps and cross sections were used to delineate the stratigraphy of the Red Fork sandstone. Depositional environment(s) were interpreted based upon vertical and lateral relationships generated from core descriptions, cross sections, log, net sand, and isopach maps. Petrologic and diagenetic analysis were established upon detailed thin section examination, bulk and extracted X-ray diffraction analysis, and scanning electron microscopy of the cores. Burial history and hydrocarbon maturation interpretations were based upon the depositional and tectonic history of the region, and vitrinite reflectance values obtained from the cores.

The writer wishes to express his sincere appreciation to his adviser, Dr. Zuhair Al-Shaieb, for his guidance and assistance throughout the study. Appreciation is extended to Dr. Gary Stewart for his critical review to the cross sections and maps. Gratitude is also extended to Dr. Authur Cleaves for patience in carefully editing the thesis.

The writer wishes to thank the Institue for Energy Analysis and its director Dr. Mize for funding during the study. Appreciation is extended to Cities Service Company which provided access to their well log files and cores, and to Ames Oil and Gas Company and Earth Energy Resources, Inc. which also provided cores. A note of thanks to KWB Oil Property Management, Inc. for providing financial assistance during the close of the study.

Special appreciation and thanks are extended to my parents, Kenneth H. Robertson and Jane H. Fortney for their understanding and support. Finally, special gratitude is expressed to my wife, Sandra, for her endless patience, constant encouragement, and many sacrifices.

TABLE OF CONTENTS

TABLE

LIST OF FIGURES

Figure Page

Figure Page

Figure Page

LIST OF PLATES

CHAPTER I

ABSTRACT

The Red Fork interval is a regressive deposit, bracketed by two transgressive marker beds. The base of the Pink Limestone defines the upper boundary, while the top of the Inola Limestone delineates the basal boundary. The regressive Red Fork interval is believed to have prograded in a southerly direction across the stable Cherokee Platform. The Red Fork sandstone was probably deposited in a complex fluvial-deltaic environment, including major and minor distributary channels and associated crevasse splay deposits. Depositional environment interpretation was based upon vertical and lateral sedimentological and stratigraphic characteristics that have been generated from core descriptions, regional cross sections, and various diagnostic subsurface contour maps.

Petrographic analysis of the bulk composition of the sandstone revealed large amounts of secondary porosity generated due to partial and or complete dissolution of various detrital constituents (primarily detrital feldspar).

The diagenetic sequence of the Red Fork sandstone appears to have progressed in three overlapping stages: (1) reduction of primary porosity and permeability by compaction and precipitation of authigenic cements, (2) enhancement of porosity

and permeability by dissolution of chemically unstable constituents, (3) reprecipitation of chemically stable authigenic constituents.

Red Fork sediments in the area of study were determined to have achieved a maximum depth of burial of approximately 8300 feet. The depth of burial was sufficent to generate the necessary pressure and temperature to transform the available organic matter to kerogen and eventually to oil.

CHAPTER II

INTRODUCTION

The study area is located on the Cherokee Platform in north central Oklahoma. It includes approximately 504 square miles and consists of 14 townships (T17N through T23N, R1&2E), in portions of Noble, Payne, Lincoln, and Logan Counties, Oklahoma (Fig. 1). The Red Fork sandstone is the primary unit of investigation and is included within the Red Fork interval, Krebs Subgroup, Cherokee Group, Desmoinesian Series, Pennsylvanian System. The Red Fork interval is generally delineated as the interval below the Pink Limestone and above the Inola Limestone (Fig. 2).

Objectives

The objectives of this study are: (1) to provide substantiating interpretations concerning the depositional environment(s) of the Red Fork sandstone, (2) to define the general composition and petrologic characteristics of the Red Fork sandstone, (3) to determine the types of porosity and the affects of authigenic clays on the porosity and permeability generated within the Red Fork sandstone, (4) to document the modifications and sequential diagenetic alterations that have affected the Red Fork sandstone, (5) to determine the maximum

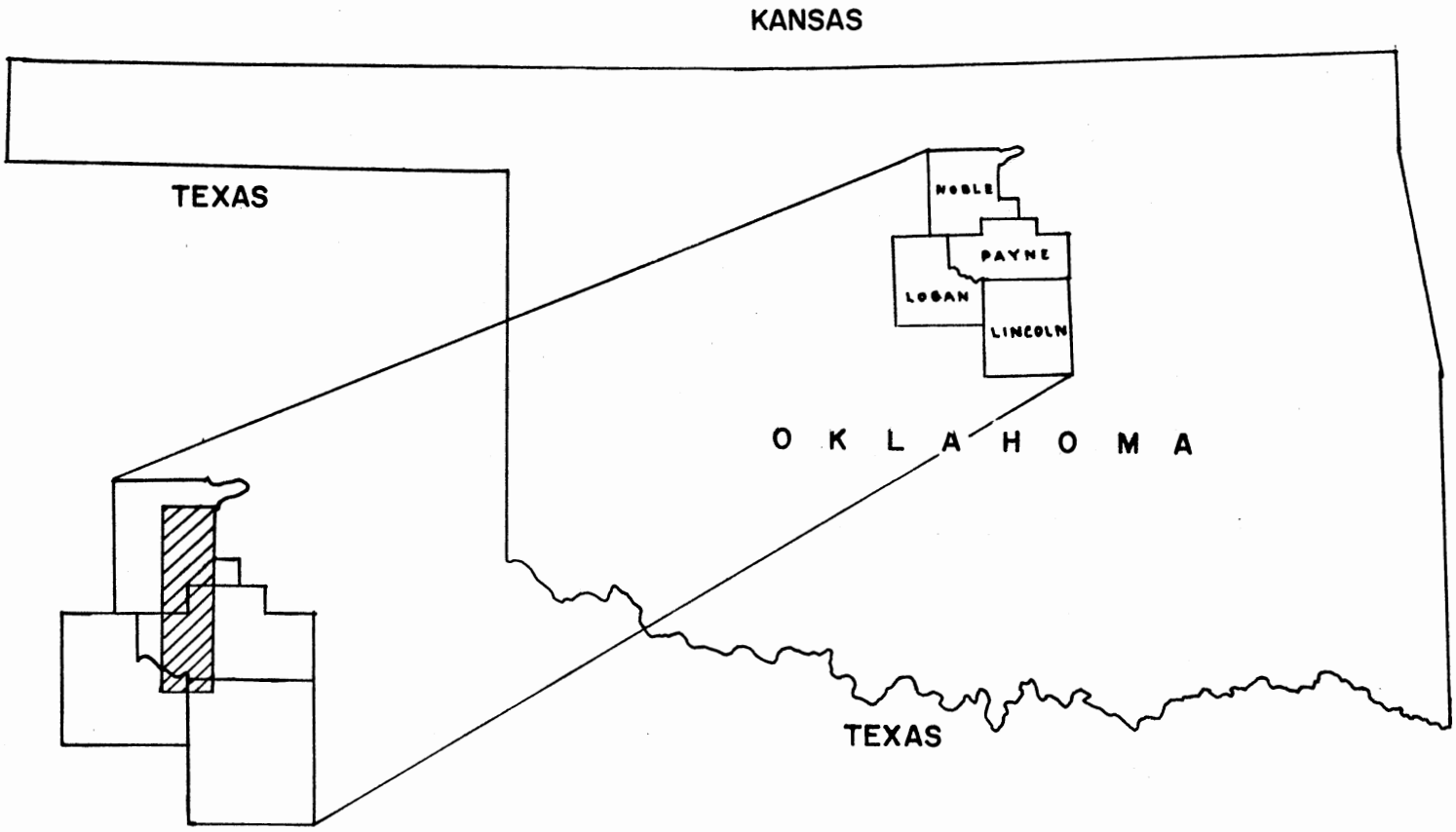

Fig. 1--Location map of the study area.

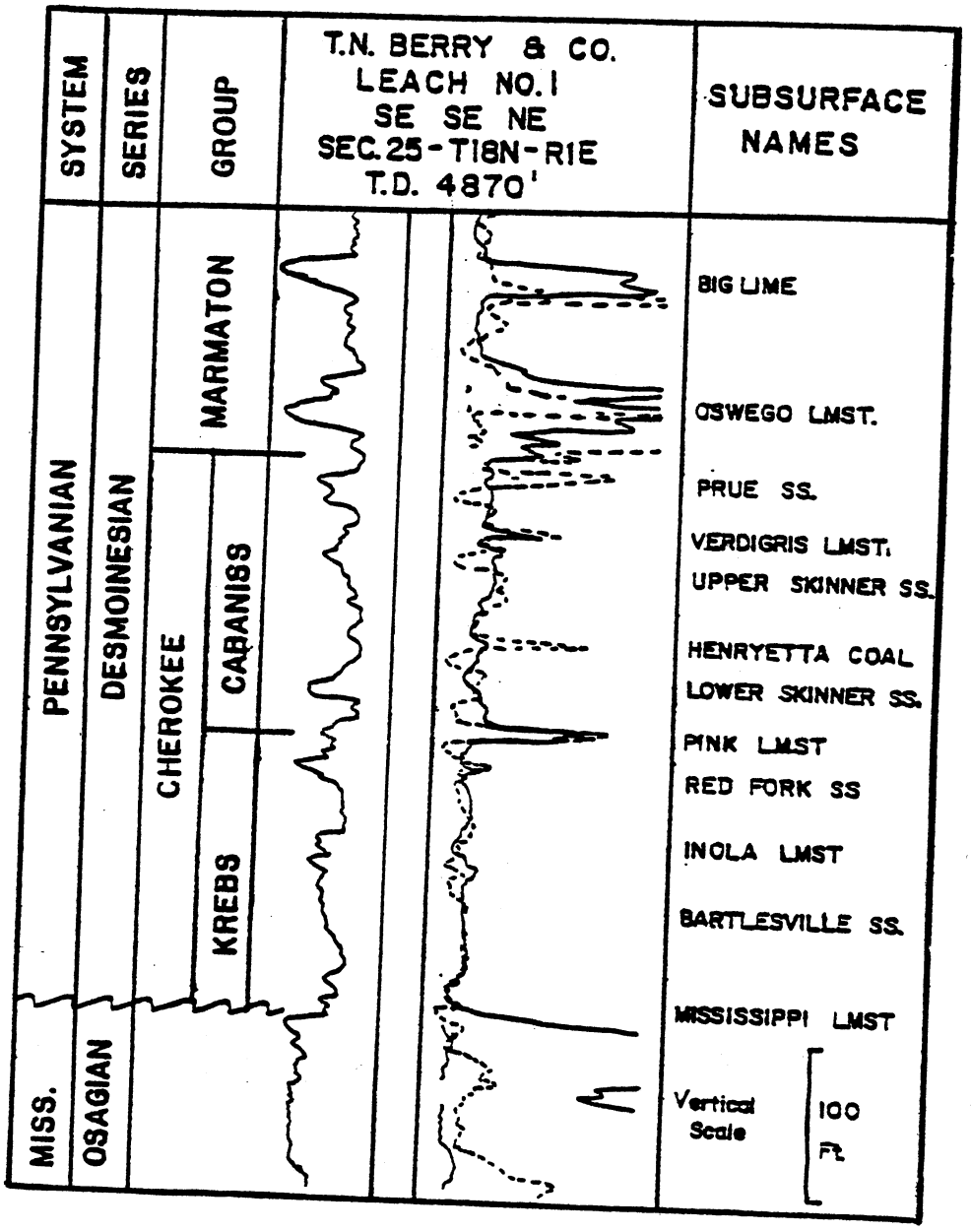

Fig. 2--Type electric log.

depth of burial and its relationship to hydrocarbon generation within the Red Fork reservoirs.

Methods

Data used in this study to determine the geometry, trends, and boundaries of the Red Fork sandstone was obtained through examination of 683 electric well logs. The data from these logs were compiled on data sheets with reference to sand thickness, log signature, and subsea tops of pertinent marker beds. Selected electric logs were used in preparation of nine regional stratigraphic cross sections. These cross sections were constructed for the establishment of a grid network, and for illustrating the stratigraphic and sedimentological relationships of the Red Fork sandstone.

A structural contour map was prepared using the top of the Pink Limestone as the reference datum. This map illustrates the present-day attitude of the Red Fork interval. An isopachous map of the interval was drawn in order to portray the paleotopography which may have influenced the deposition of the Red Fork. A net-sand map was constructed in order to delineate major depositional patterns. The interval between the top of the Pink Limestone and the top of the Inola Limestone, or their stratigraphic equivalents which contained any sand, was recorded. A greater than 20 millivolt cutoff from the shale base line, was used on the Spontaneous Potential curve to define the amount of sand present. A log map was constructed of the Red Fork interval to aid in the depo-

sitional interpretation and stratigraphic characteristics.

Three Red Fork cores were described in detail in order to define the vertical sucession of sedimentary features needed to interpret the depositional environment(s). Two cores from within the area of study, Cities Service Company, Rhodd #1, and the Earth Energy Resources Inc,, Coe Bailey #1, and one core from outside the area, Ames Oil and Gas Company, Rogers #2, were utilized. A total of fifty-four thin sections were employed in determing the petrographic characteristics, composition, porosity relationships and types, and diagenetic events of the Red Fork sandstone.

Bulk and extracted X-ray diffraction analysis was performed on selected samples, in order to determine the general composition, percentages, and identification of the clay fraction.

Scanning Electron Microscope (SEM) was employed for the identification of diagenetic minerals, and porosity verus mineral relationships. Numerous photomicrographs were taken to illustrate the more obvious diagenetic relationships.

Vitrinite reflectance data was obtained from selected Red Fork samples in order to determine the maximum depth of burial.

Previous Investigations

The Red Fork sandstone has been a prolific hydrocarbon producing interval on the Central Oklahoma Platform for many decades, and therefore has been the topic of numerous investi-

gations. Only studies which are directly related to the boundaries of the study area will be included in the following discussion.

The stratigraphic position of the Red Fork was defined by Jordan (1957) as that unit which lies below the Pink Limestone and above the Inola Limestone of the Cherokee Group. Jordan also mentioned that the surface equivalents of the Red Fork sandstone and the Pink Limestone are the Taft sandstone and the Tiawah Limestone, respectively. The term Cherokee Group was defined by Haworth and Kirk (1894) as a sequence of black shale between the Pennsylvanian Oswego Limestone and the Mississippian rocks in Cherokee County, Kansas (Withrow, 1968). Oakes (1953) subdivided the Cherokee Group of east-central and northeastern Oklahoma into the "Krebs Group" and "Cabaniss Group". In 1956 the term Cherokee Group was readopted back into the formal stratigraphic nomenclature, and the Krebs and Cabaniss Groups were demoted to subgroups (Howe, 1956). Previous studies which have influenced work on the Cherokee Group include stratigraphic and depositional studies by Bass (1934 & 1935), Bass etal. (1937) and petrologic work initiated by Leatherock (1937).

The first reference of the Red Fork was made by Hutchinson in 1911, for a shallow producing sand body which was located near the town of Red Fork, Oklahoma (Jordan, 1957).

In a subsurface investigation conducted by Clements (1961, p.13) in portions of north-central Noble and south-central Kay Counties, Oklahoma; he stated, "The Red Fork sand-

stone is a shallow marine deposit that has accumulated in the synclinal areas and the nature of the occurrence of the sand seems to fit best the strike valley theory proposed by Busch (1959).". McElroy (1961) analyzed the Desmoinesian series in north-central Oklahoma by constructing regional isopach and lithofacies maps. These maps were used to interpret the stratigraphic relationships of the formations and their association with the structural geology of the region. Clayton (1965) described the paleodepositional environments of the Cherokee sands in central Payne County Oklahoma. Clayton (1965, p.38) concluded that, "The position of the channel sand of Red Fork age is predetermined to a great extent by the position of the drainage channels on the pre-Pennsylvanian erosion surface.". Hawissa (1965) interpreted the depositional environments of the Bartesville, Red Fork, and lower Skinner sandstones, in portions of Lincoln, Logan, and Payne Counties, Oklahoma. Hawissa surmised that the Red Fork sandstone in his area was deltaic in orgin. A regional investigation of the Marmaton and Cherokee Groups on the east side of the Nemaha Ridge in north-central Oklahoma, was compiled by Cole (1969). Scott (1970) presented a detailed stratigraphic study of the Cherokee Group in northern Noble County, Oklahoma. Scott (1970, p.40) concluded that, "The Cherokee sands were deposited in distributary channels of a deltaic environment.". Shipley (1975) described the depositional environments and paleotopographic influences on the Cherokee Group in western Payne County, Oklahoma. Shipley (1975, p.32)

stated, "The trends of thick Red Fork sandstone within the study area represent deposition in channels which were probably major and minor distributaries of a deltaic system.". Candler (1976) presented a stratigraphic analysis of the middle and upper Cherokee sands in southern Noble County, Oklahoma. Candler (1976, p. 24) submitted that, "The data available suggest that in the study area the Red Fork sandstone is a lower deltaic-plain facies with interdistributary fine-grained sandstones and minor distributary channel or crevasse splay deposits.".

Several other studies that were indirectly related to this thesis, yet provide valuable contributions to this investigation include: Lowman (1933), Weirich (1953), Branson (1954), Howe (1956), Benoit (1957), Stringer (1957), Graves (1955), Berg (1969), Dogan (1970), Hudson (1969), Astarita (1975), Krumme (1975), and Glass (1981).

CHAPTER III

STRUCTURAL FRAMEWORK

Regional Setting

The regional setting of the study lies within the Cherokee Platform (Central Oklahoma Platform) of Oklahoma. The area of investigation is bounded by the Arbuckle Uplift and Arkoma Basin to the south, the Ozark Dome to the east, the Bourbon Arch to the north, and the Nemaha Ridge to the west (Fig. 3).

Regional strucure is depicted by the Pink Limestone structure map (Plate 10) and indicates a general north to northwest strike and a gentle westward dip. The rate of dip varies slightly from 40 to 60 feet per mile, except were interupted locally by flexures. The rugged Mississippian unconformity surface is believed to have caused the gentle flexures within the Red Fork interval. The study area roughly parallels the Nemaha Ridge, which lies approximately twenty miles to the west. This dominant structural trend is believed to have been a controlling factor on the deposition of the Red Fork sandstone studied.

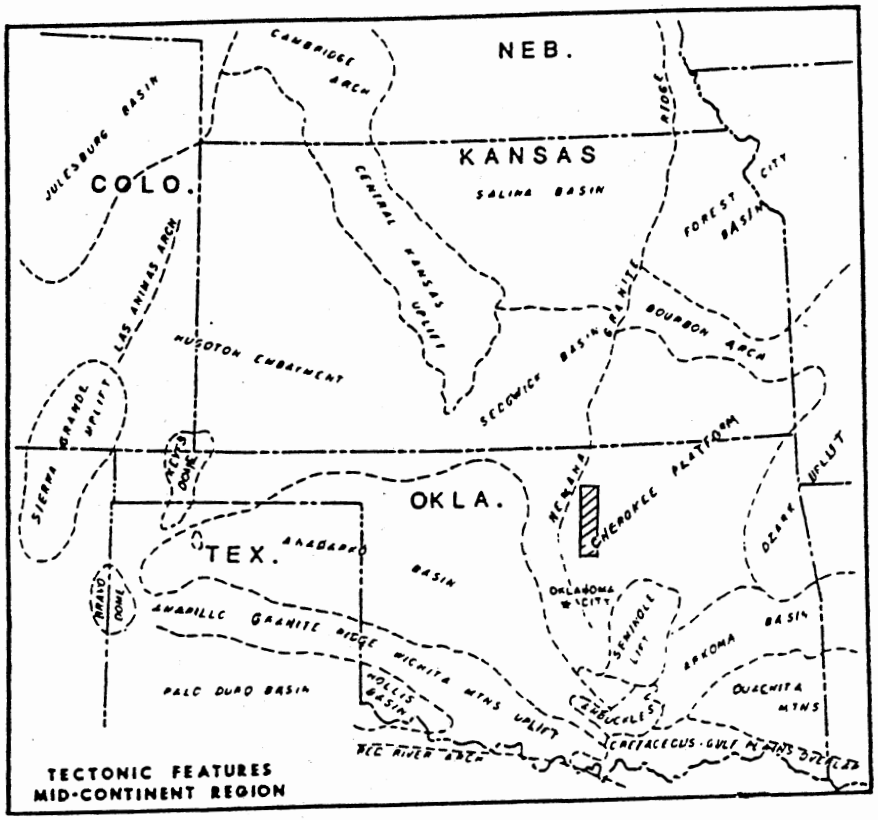

Fig. 3-- Generalized tectonic map showing location of study area (Cities Service Company, 1983).

Local Setting

A structural contour map was constructed on the top of the Pink Limestone. The Pink Limestone was used as a reference because of its close proximity to the Red Fork and because it is a consistant marker bed which is easily recognizable throughout the study area. Because the Pink Limestone lies directly over the Red Fork interval it provides the best representation of the structural configuration of the Red Fork.

Structure map based on the top of the Pink Limestone shows a north to northwest strike and a general westward dip at the rate of approximately 50 feet per mile. The dip is occasionally disrupted by flexures that are oriented in a general east-west pattern, and closures which are present in a dominantly north-south arrangement. A significant structural closure is located in portions of Sections 7,18,19,20,28,29, 32,33-T22N-R2E. A smaller closure associated with the aforementioned structure is located to the southwest, in portions of Sections 31,36-T22N-R2E, and Section 6-T21N-R2E. There are two small closures which are located in T20N-R2E. The larger of the two is located in portions of Sections 15 and 16-T20N -R2E, while the smaller is positioned in fractions of Sections 28,29,32 and 33-T20N-R2E. These two small closures are believed to be the result of tectonic movement. Numerous west-southwest plunging noses occur throughout the study area. These nosings are thought to be primarily created by regional tectonic movement. No large scale faulting was recognized.

CHAPTER IV

STRATIGRAPHIC FRAMEWORK

Introduction

The Red Fork interval in the north-central Oklahoma Platform (Fig. 3) is the middle member of the Cherokee Group (Fig. 2). Jordan (1957) defines the Cherokee Group to include all strata from the top of the Mississippian to the base of the Oswego Limestone (Fort Scott) of late Desmoinesian age. Stratigraphicly, the Cherokee Group is represented by a series of cyclic deposits of sand and shale, disrupted periodically by laterally persistent deposits of limestone. These limestone marker beds are thought to represent extensive periodic transgressions of the Cherokee Sea onto the platform. The Brown Limestone was the first transgressive unit to be deposited in the Cherokee Group, followed by the Inola Limestone, Pink Limestone, and the Verdigris Limestone (Fig. 2). The limestone marker beds are the basis on which the Cherokee Group is subdivided. The base of the Oswego Limestone marks the top of the Cherokee Group and represents an overall transgression.

Jordan (1957) defines the Red Fork as the interval from the base of the Pink Limestone (surface equivalent Tiawah Limestone) to the top of the Inola Limestone. The Taft sandstone is the stratigraphic surface equivalent to the Red Fork.

The Burbank sand was initially believed to be the stratigraphic equivalent to the Red Fork in the upper part of the Boggy Formation. However, Jordan (1957, p. 30) noted: "Recent stratigraphic work suggest that the Burbank sand could be equivalent to the lower part of the Boggy Formation or both the Red Fork and the Bartlesville."

The base of the Cherokee Group lies unconformably upon an undulating erosional surface of Mississippian age. A regional study by Cole (1969) of the Cherokee and Maramaton Groups demonstrated the unconformity at the base of the Cherokee Group. Isopach maps constructed by Cole (1969) display a general thickening of the Cherokee strata to the south-southeast, thereby indicating the direction of the paleoslope. The direction of paleoslope and interval thickening suggests the receiving basin lie to the south-southeast of the study area.

Correlations

Seven east-west and two north-south regional stratigraphic cross sections were constructed in a grid network to illustrate the stratigraphic and sedimentological relationships of the Red Fork sandstone (Plates 1-9). The Pink Limestone was selected as the datum for all of the stratigraphic cross sections because it is laterally persistant throughout the study area and lies directly over the Red Fork interval (Fig. 2). The index map illustrating the locations of the cross sectional traces is shown in Figure 4.

The Pink and Inola limestones were used as key strati-

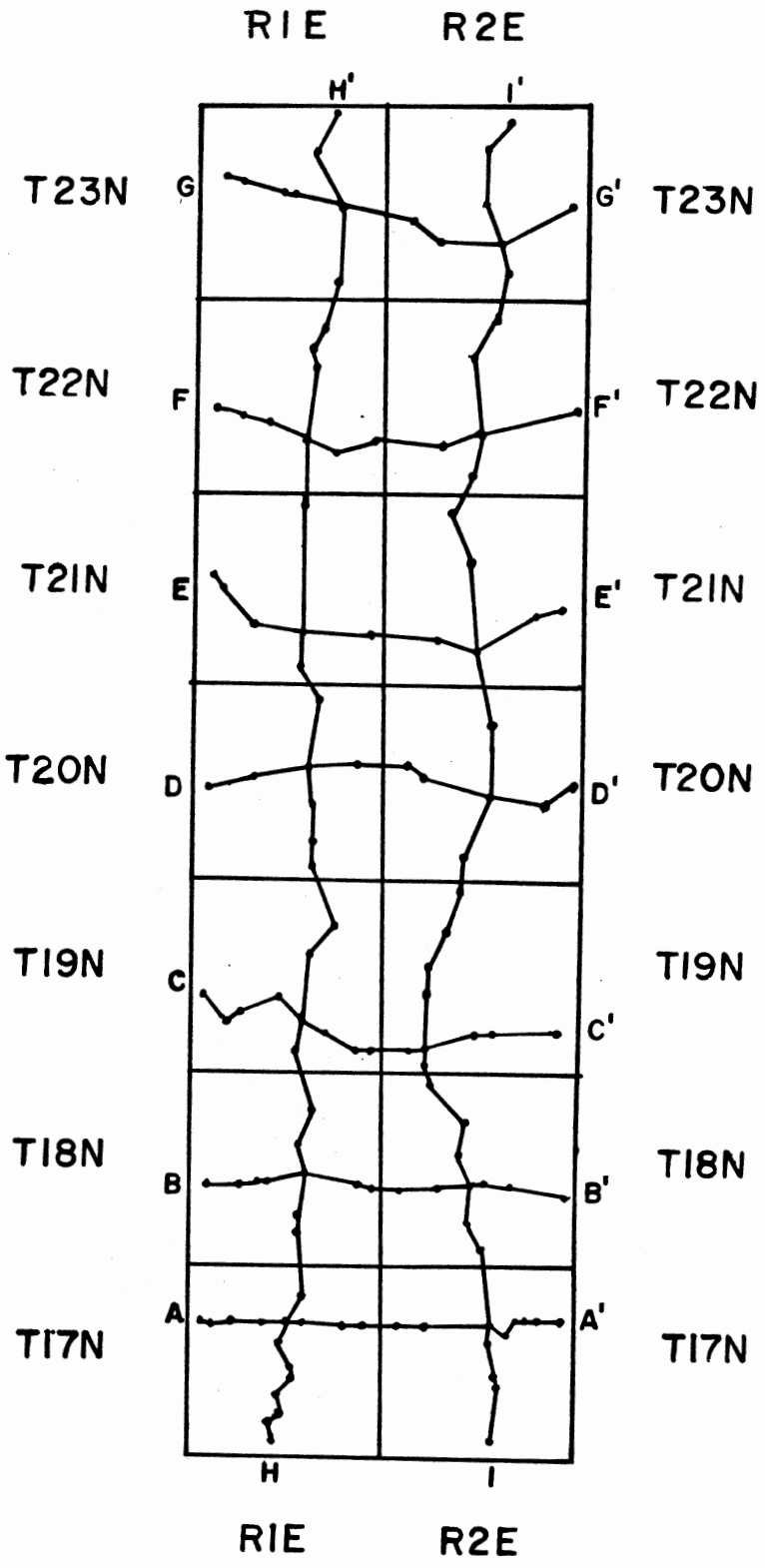

Fig. 4--Index map of stratigraphic cross sectional traces.

graphic markers to distinguish the boundaries of the Red Fork interval. The gross lithology of the Pink Limestone is grey to tan, fine to medium crystalline limestone containing pink crystals of calcite (Jordan 1957). Thickness of the Pink Limestone varies from five to ten feet throughout the study area. The composition of the Inola Limestone commonly is grey to tan, finely crystalline, semi-dense and fossiliferous (Jordan 1957). Regionally, the Inola Limestone is persistent, except locally where the Red Fork sandstone has eroded the underlying shale units and occasionally the Inola Limestone. The Inola is characterized on electric-logs by a reversed or low resistivity. The Pink Limestone usually is recognized by a high resistivity response. The Pink and Inola Limestone represent transgressive stratigraphic intervals, while the Red Fork denotes a regressive depositional phase.

Red Fork sandstone deposits were divided into two types, as channel or non-channel, based upon their characteristic log shapes. Channel deposits commonly exhibit a log response that shows an abrupt basal and lateral contacts, indicating erosion of the underlying strata. Non-channel and or overbank deposits were distinguished by sharp erosive base and laterally gradational contacts. Regional and local cross sections illustrate the thickness and stratigraphic position of the sand deposit. Log, net-sand and isopach maps assist in the interpretation of the geometry and distribution of channel and non-channel deposits.

Stratigraphic Cross Sections

Seven east-west cross sections display an increase in the thickness of the Red Fork interval from west to east (Plates 1-7). Plate 7 shows the interval ranging in thickness from 70 feet in well number 247 to over 200 feet in well number 62. The slight thinning of the Red Fork interval to the west reflects the presence to the eastern flank of the Nemaha Ridge. McElroy (1961) describes the Nemaha Ridge as, " post Mississippian belt of faulted anticlines; pre-Pennsylavain rocks are truncated across the summits.". Both Cole (1969) and Berg (1969) concluded that the Nemaha Ridge was a positive feature during Red Fork time. Berg (1969) noted the absence of large concentrations of sandstone west of the Nemaha Ridge, suggesting that it may have acted as a sediment barrier. Trangressive onlap of the lower Cherokee Group to the west is suggested in Plates 1 through 7 (Fig. 4).

The two regional north-south cross sections demonstrate a south-southeast increase in the thickness of the Red Fork interval (Plates 8 & 9). Plate 9 shows the interval thickening from 70 feet in the north to slightly over 200 feet in the south. This indicates that the receiving basin was to the southeast of the study area, probably the Arkoma Basin. Cole (1969) and Scott (1970) both suggested that the paleodrainage system of the Cherokee Group had a dominant southeasterly component.

Plate 1 (A-A') is an east-west cross section extending

across T17N-R1&2E (Fig. 4), which demonstrates the lateral variations of the Red Fork sandstone. Well 232 shows the downcutting of the Skinner sandstone, and subsequent erosion of the Pink Limestone. Channel downcutting of the Red Fork sandstone, and erosion of the Inola Limestone is illustrated in wells 54 and 62. The sand thickness in each of these wells is approximately 140 feet. Log signature of these two wells exhibit a modified blockly to serrated log response, suggesting the degree of vertical stacking which probably took place. Note in Plate 1 that the accumulation of thick sand deposits occurs in the paleotopographic lows of the Mississippian erosional surface. This evidence indicates that deposition of the Red Fork sandstone was influenced by the rugged erosional surface.

Wells 66, 64 and 58 in Plate 1 illustrate blocky log patterns which are indicative of a channel deposit. Absence of the Inola marker bed was probably caused by the erosive downcutting of the Red Fork channel.

Plate 2 (B-B') is an east-west cross section across T18N-R1&2E. This plate illustrates thin, isolated deposits of sand averaging 10 to 15 feet in thickness. Wells 282 and 284 show the relative stratigraphic position and funnel-shaped log response. This type of sand deposit is indicative of a non-channel or overbank deposit.

The stratigraphic marker beds used in the cross sections are well illustrated in Plate 2. The Pink Limestone is laterally persistent and is characterized by a high resistivity

response. Correlation of the Inola Limestone was achieved by observing the reversed log response of the resistivity and spontaneous potential curves.

Plate 3 (C-C') is an east-west cross section extending across T19N-R1&2E. The western half of the cross section shows a variety of log shapes. These responses represent thin isolated deposits of sand ranging in thickness from 5 to 15 feet. The eastern half of Plate 3 displays blocky log responses which range in thickness from 20 to 30 feet. Stratigraphicly, these Red Fork sand deposits occur in the middle of the interval and are suggestive of smaller distributary channels.

Plate 4 (D-D') is an east-west cross section constructed across T20N-R1&2E. Minor occurrences of sand (15 to 20 feet) appear in wells 460 and 488. These two wells demonstrate funnel- shaped log responses which show a gradational base and abrupt upper contacts. The Red Fork interval in the remaining wells of Plate 4 consist mainly of shale and siltstone, with minor occurrences of sand.

Well 485 of Plate 4 displays channel downcutting of the Skinner channel sand and subsequent erosion of the Pink Limestone. Note that the Pink Limestone is present in the adjoining wells.

Plate 5 (E-E') is an east-west cross section extending across T21N-R1&2E. Thin sand deposits, usually not exceeding 10 feet in thickness, occur in the middle of the Red Fork interval. Plate 5 indicates the presence of the rugged paleotopography on the top of the Mississippian Unconformity. This

cross section illustrates that the Red Fork interval throughout this area is comprised primarily of shales and siltstones.

Plate 6 (F-F') is an east-west cross section constructed across T22N-R1&2E. Minor sand deposits ranging from 10 to 15 feet thick are present in a few wells, however most of the wells are comprised of shale and siltstone. Well 547 illustrates a modified bell-shaped curve, which is indicative of a channel deposit. This channel is probably an extension of the Ceres field to the north (Plate 12).

Plate 7 (G-G') is the northernmost east-west cross section which extends across T23N-R1&2E. Wells 632 and 635 illustrate a major deposit of Red Fork sand. The sand in these wells is approximately 50 feet thick and the log curves exhibit a bell-shaped pattern indicative of a channel deposit. These wells are a representative sample of the Red Fork sandstone in the Ceres field. East of the Ceres field thin sand units (generally less than 15 feet) are present, however the majority of the Red Fork interval consists of shales and siltstones.

Plate 8 (H-H') is a regional cross section comprised of 35 wells and extends across T23N through T17N-R1E. Wells 564, 557, and 551 located in T23N-R1E illustrate the bell-shaped log response indicative of a channel deposit. Absence of the Inola Limestone in the these wells was probably due to the channeling of the Red Fork sandstone. The sand displayed in wells 564, 557 and 551 is approximately 50 feet thick.

Funnel-shaped log responses can be seen in wells 472 and 447, these sand deposits do not exceed 15 feet in thickness.

This non-channel sand deposit, stratigraphicly occurs in the middle of the Red Fork interval.

The southern portion of Plate 8 illustrates the complexities which can arise when erosion or non-deposition of a marker bed has occurred. Wells 177,176,118,117, and 107 contain sand deposits which are difficult to determine whether the sand unit is entirely Red Fork or Skinner. Commingled Red Fork sand Skinner sand deposits were probably due to the stacking of the sand units, making differentiation of the sand units difficult. Absence of the Pink Limestone in wells 177, 176 and 118 suggest that channel downcutting of the sand body has caused the erosion of the marker bed. Since the Skinner sand overlies the Pink Limestone, the downcutting probably was achieved by a Skinner channel.

The Inola Limestone is not present in wells 117 and 107 of Plate 8. Absence of the Inola Limestone was probably due to the channel downcutting associated with the thick sand bodies illustrated in wells 117 and 107. Log characteristics imply that the sand deposits are of the channel variety. The stratigraphic position of the sand body suggests that the deposit occured during Red Fork time.

Plate 9 (I-I') is regional north-south cross section comprised of 32 wells and extends across T23N through T17N-R2E (Fig. 4). Wells 493, 486, 475, and 418 contain Red Fork sand deposits ranging in thickness from 15 to 25 feet. The sand in these wells occurs approximately at the same stratigraphic position. Well 475 exhibits an abnormally high spon-

taneous potential deflection. This blockly log pattern illustrates abrupt contacts indicative of the avulsed distributary channel.

Wells 363 and 347 demonstrate a bell-shaped log response, which displays an abrupt basal contact and a gradational upper contact of a channel deposit. The sand units are approximately 50 feet thick. Erosion of the Inola Limestone was probably due to the channel downcutting of the Red Fork sandstone in well 347.

Thick accumulation of Red Fork sand is evident in wells 321 and 67. Well 321 is 100 feet thick and well 67 is 60 feet thick. The downcutting of the Red Fork sand body probably caused the erosion of the Inola marker bed.

Erosion of the Pink Limestone by channeling of the overlying Skinner sandstone is demonstrated in wells 55 and 5.

CHAPTER V

DEPOSITIONAL ENVIRONMENT

Introduction

The depositional environment of the Red Fork Sandstone in this area of study was interpreted to be part of a larger fluvial-deltaic complex. Interpretation was based on evidence from the following: detailed examination of three cores which penetrated the Red Fork sandstone, a regional log map, nine regional stratigraphic cross sections, an isopach map of the Red Fork interval, and a net-sand isopach map.

Examintion and interpretation of the data reveals: 1) vertical succession of sedimentary structures indicative of cut and fill channel deposition (Figs. 7,9 and 11), 2) channels are elongate and perpendicular to depositional strike (Plates 11 and 12); 3.) sand trends are dominately arranged in north-south direction; 4) isolated absences of the basal Inola Limestone marker, probably due to the channel downcutting of the Red Fork sandstone (Plate 13); 5) sharp basal and lateral contacts which are indicative of channel deposition (Plate 13); 6) complicated geometry (Southern region) reflecting the presence of multistoried sand units which display an array of trends (Plates 12 and 13); 7) underlying shale contains abundant carbonaceous debris, mica and pyrite. Brachipod

fragments and molds of shells were noted in the basal shale unit of the Cities Service Company, Rhodd #1 (Fig. 5). Core data reveals that the Red Fork sandstone was deposited in a reducing environment.

The evidence presented tends to support the interpretation that the Red Fork sandstone was deposited in a fluvial-deltaic environment.

Discussion

For the sake of simplicity the study has been divided into three regions; Northern, Central, and Southern. The Northern region is comprised of T23&22N-R1&2E; the Central region consists of T21,20&19N-R1&2E; and the Southern region is comprised of T18&17N-R1&2E.

The Northern region illustrates a variety of environments as demonstrated by the log signature map (Plate 13). The net-sand map shows a major sand deposit trending southward through the center of T23N-R1E. The log signature of this deposit resembles a bell-shaped pattern, which implies an erosive base and a gradual fining upward sequence. The Cities Service Company, Rhodd #1 (Sec.9-T23N-R1E) core was taken from this trend and described in detail. The core displays a basal channel lag conglomerate at the base, which fines upward into very fine grain sand at the top of the genetic unit (Fig. 7). With the exception of the previous mentioned channel, the remaining portion of the Northern region consists primarily of shale with minor stringers of sand. This region is representive of

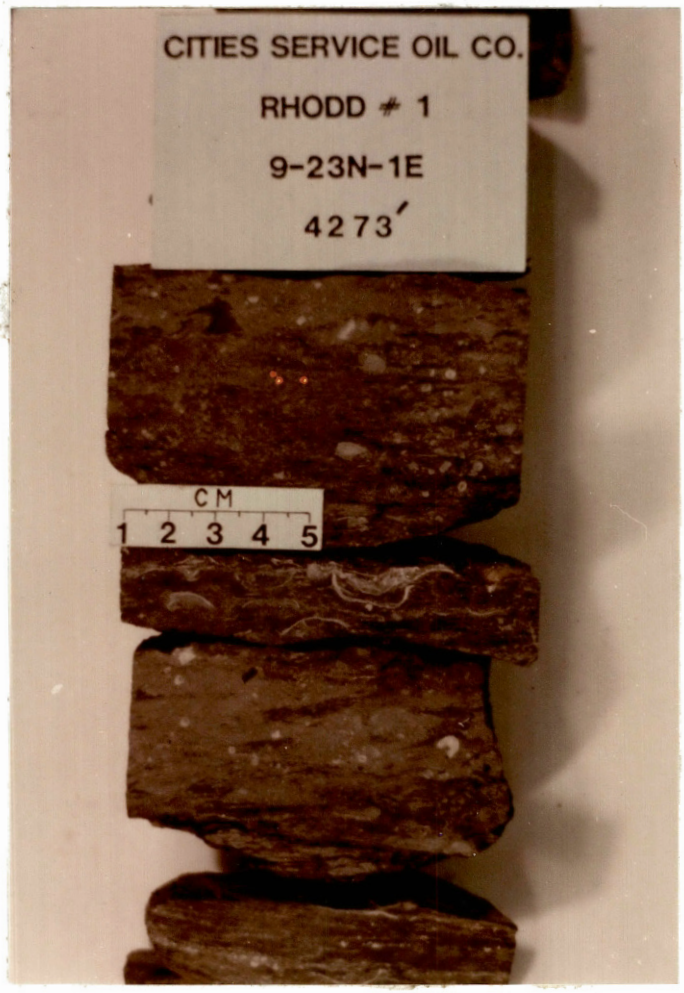

Fig. 5 -- Organic rich shale containing fragments of brachipods and coral.

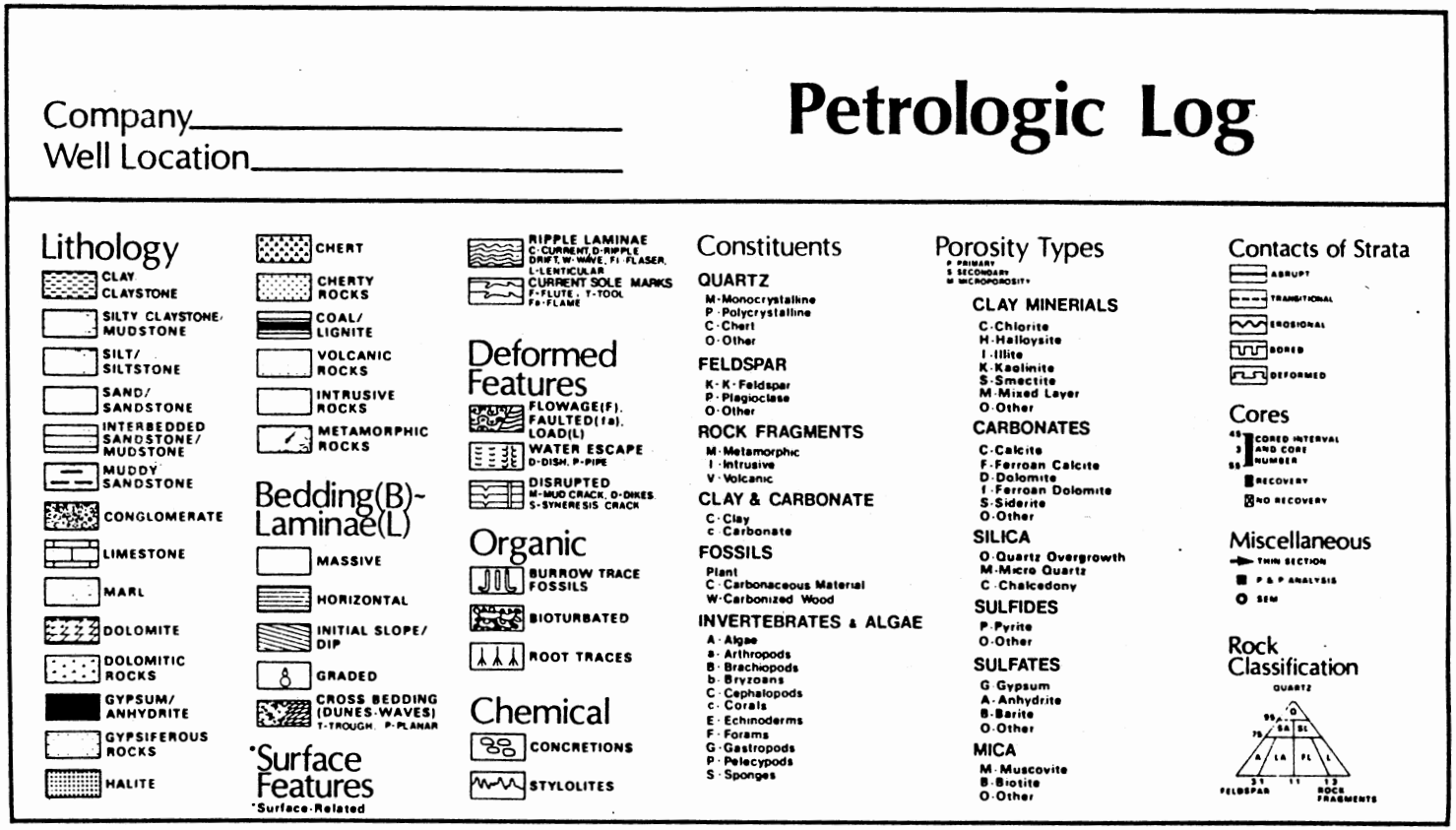

Fig. 6--Key for core descriptions, (Figs. 7,9 and 11).

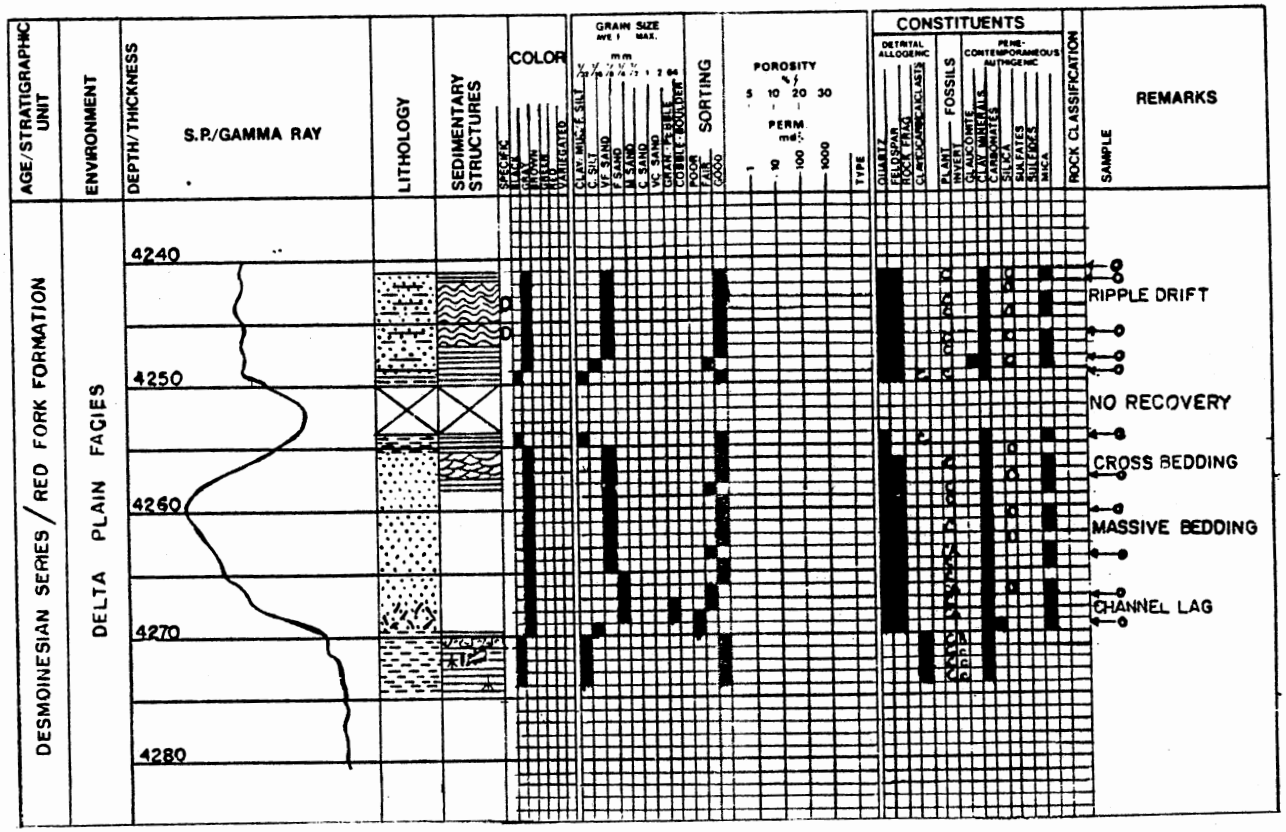

Fig. 7--Core description of the Cities Service Company, Rhodd #1 (NE NE NE Sec. 9-T23N-R1E).

a deltaic plain environment.

The Central region consists of T21,20&19N-R1&2E and contains an assortment of sand deposits ranging from major and minor distributary channels to associated crevasse splays. The isopach map of the Red Fork interval (Plate 11) and the net-sand map (Plate 12) illustrate the major geometric configuration of the Red Fork interval. The net-sand map reveals an arrangement of isolated pods and elongate sand patterns that trend in a predominant north-south direction. Figure 7 displays a large distributary sand body which lies to the east of the Central region. This large distributary sand body probably controlled the deposition of the Red Fork sandstone in the study area. Portions of this distributary system are included in the area of study.

Examination of the log map (Plate 13) in conjunction with the net-sand map (Plate 12) demonstrates the variety of sand deposits which occur in the Central region. An example of a large isolated sand deposit, is an isolated pod which exists in portions of Sections 12,13,23,24,25 and 26 of T19N-R1E, and in portions of Sections 7,18,19 and 20 of T19N-R2E (Plate12). This deposit demonstrates a substantial concentration of sand where a channel bifurcates downdip. The log map of this area displays a modified "blocky" log signature which is indicative of an abandoned channel. The log signature illustrates a sharp basal contact implying an erosive base, and a sharp upper contact that is suggestive of an avulsed distributary channel.

Plates 3,4&5 are east-west cross sections which extend

across the Central region. The sand bodies displayed in these cross sections commonly are lenticular with sharp basal and lateral contacts. The stratigraphic relationships of the Red Fork sandstone in this area were discussed in greater detail in Chapter IV.

Interpretation of the available data suggest that the Red Fork sandstone was deposited in a delta plain environment. Sand deposits associated with this environment of deposition include major and minor distributary channels and crevasse splays.

The Red Fork sandstone in the Southern region (T18&17N-R1&2E) is part of a larger channel system to the east (Fig. 8). The sandstone studied in this area represents a complex arrangement of multistoried, bifurcating and anastoming channels which form a broad north-south trending belt (Plate 12). The increase in thickness is due to the downcutting and vertical stacking of the distributary channels. As the log map reveals (Plate 13), the stacked channels can be detected by observing the "blocky" log signature in the southeast portion of the Southern region.

The Earth Energy Resources, Inc., Coe Bailey #1 (Sec. 11-T17N-R2E) core was taken from the Southern region and described in detail. Figure 9 displays a vertical stacking of genetic sand units. Grain-size analysis of each of these genetic sand units illustrates a slight fining upward sequence with fine grain sand at the base grading into very fine grain sand at the top of the unit. This textural arrangement is commonly

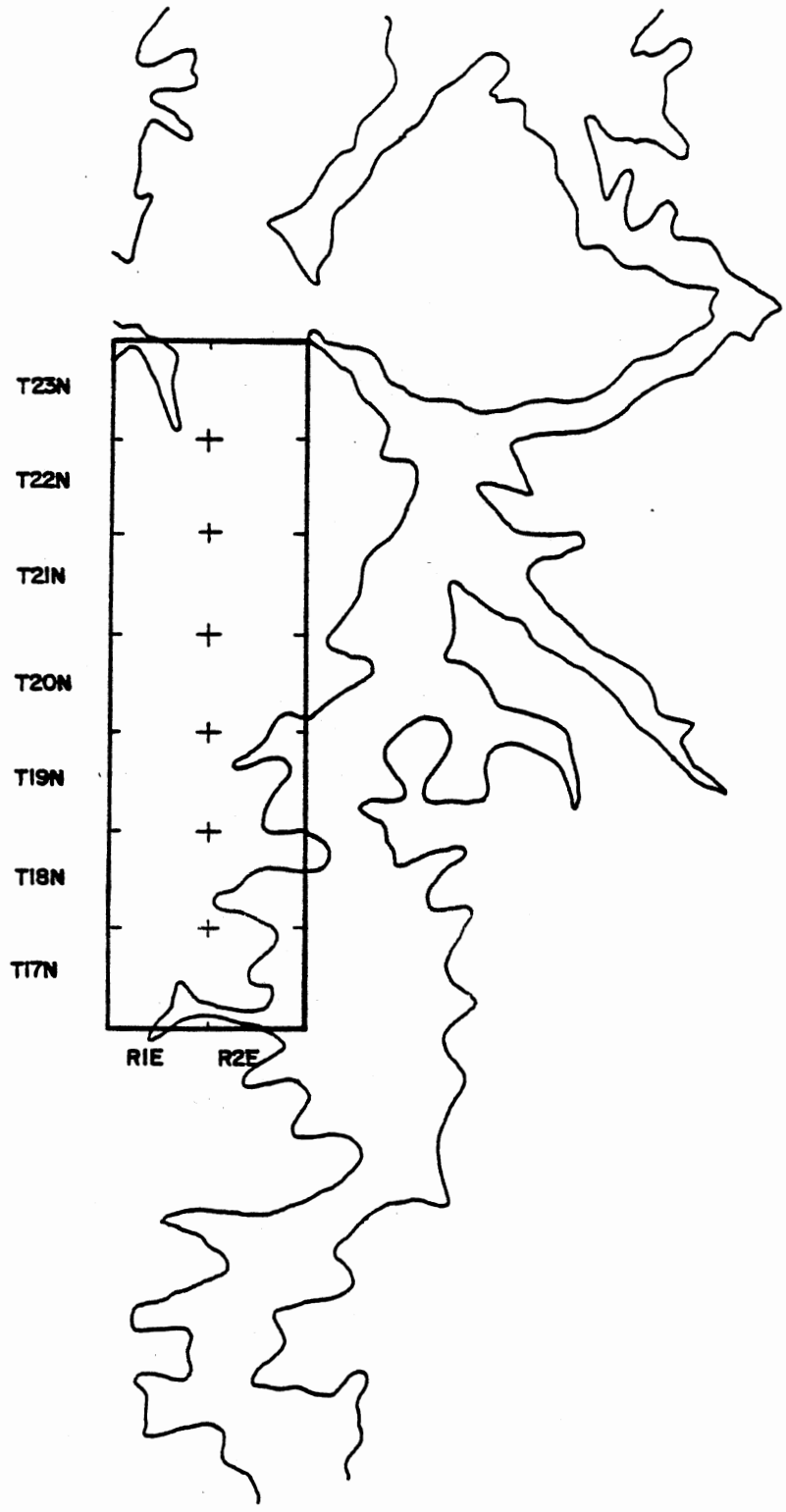

Fig. 8 -- Diagram illustrating sand thickness greater than 40 feet. (Modified from Cole, 1969)

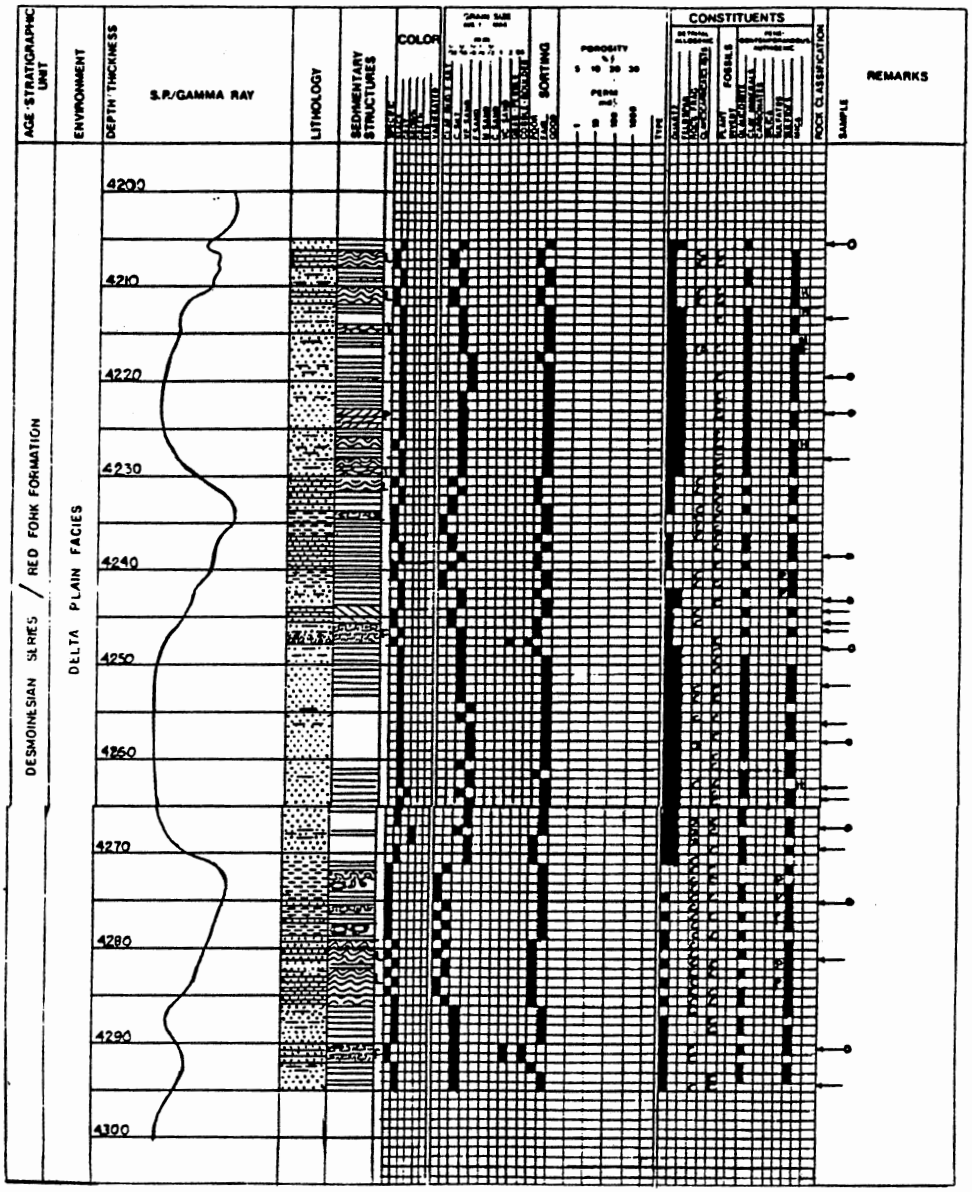

Fig. 9--Core description of the Earth Energy Resources, Inc., Coe Bailey #1, (NW NW SW Sec. 11-T17N-R2E).

found in distributary channels associated with delta plain facies. The vertical succession of sedimentary structures observed in the Coe Bailey #1 include massively bedded sandstone at the base grading upward into horizontal bedded sandstone at the top. The gradual change in sedimentary structures indicates a general decrease in stream energy, which commonly occurs as stream approaches a new base level. Interstratification of sand and shale sequences observed at the top of each sand unit probably represents abandonment and infilling of the channel and the interdistributary area.

Plates 1&2 are east-west cross sections which extend across the Southern region. The eastern half of Plate 1 illustrates multistoried sand units which have developed at the expense of the underlying strata. Note that the thicker accumulations of sand were deposited in paleotopographic lows of the Mississippian erosional surface.

Interpretation of the data gathered from the Northern, Central and Southern regions indicates that the Red Fork sandstone was deposited in deltaic plain environment. Dominance of fine and very fine grain sand coupled with the subrounded nature and high degree of sorting of the sediment, indicates deposition a significant distance from an uplifted source or from a provence of uniform, submature sediments. Examination of the Red Fork isopach map (Plate 11) constructed displays a general thickening to the south-southeast, thereby indicating the direction of the paleoslope. The net-sand map (Plate 12) illustrates major sand trends oreinated in a north

-south direction, perpendicular to depositional strike. The two aforementioned lines of evidence tend to suggest that the source of Red Fork sediments was from the north.

Sedimentary Features

Sedimentary features of the Red Fork sandstone are based upon the detailed examination of three cores (Fig.10): Cities Service Company, Rhodd #1 (Sec.9-T23N-R1E)(Fig. 7); Earth Energy Resources, Inc., Coe Bailey #1 (Sec.11-T17N-R2E)(Fig. 9); Ames Oil & Gas Company, Rogers #2 (Sec.13-T22N-R4E)(Fig. 11). The most commonly observed sedimentary structures in order of abundance are: horizontal bedding and laminations, massive bedding, interstratification of sand and shale (wavy and lenticular laminae), small scale trough cross bedding and medium scale plannar cross bedding. A vertical sequence of sedimentary structures generally appeared as follows: (1) a lower zone of massively bedded sandstone containing clay clasts, and or ripup fragments of the underlying shale unit (Fig. 12); (2) the massively bedded sandstone commonly grades into horizontally bedded sandstone; (3) the upper zone of the sand interval exhibits small to medium cross bedding. The Cities Service Company, Rhodd #1 displayed ripple drift laminae in the upper portion of the sand body. Multiple stacked sand units were usually separated by cyclically deposited layers of interbedded sand and shale. The interbedded sand and shale exhibit both horizontal and wavy to lenticular bedding. Within each of the sand packages small scale cross bedding was noted, usually

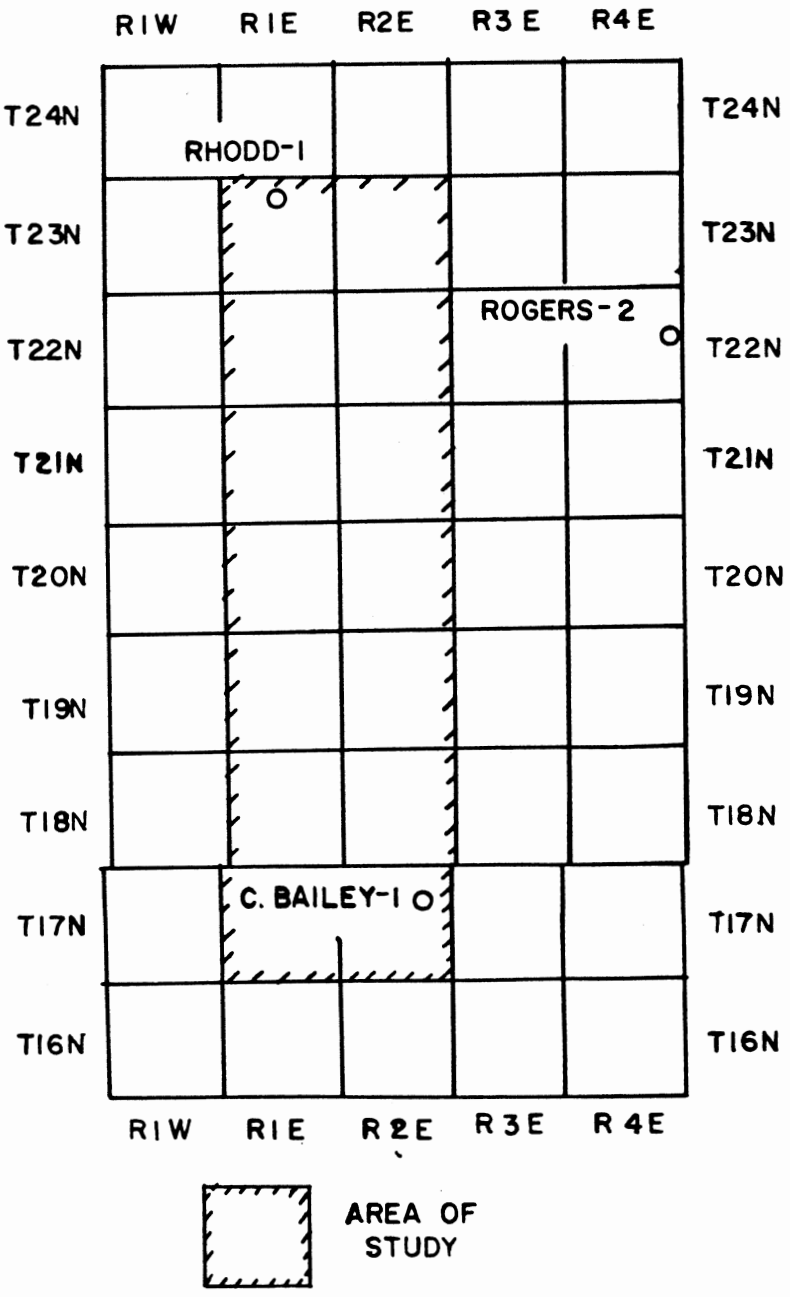

Fig. 10--Diagram illustrating location of cores used in study.

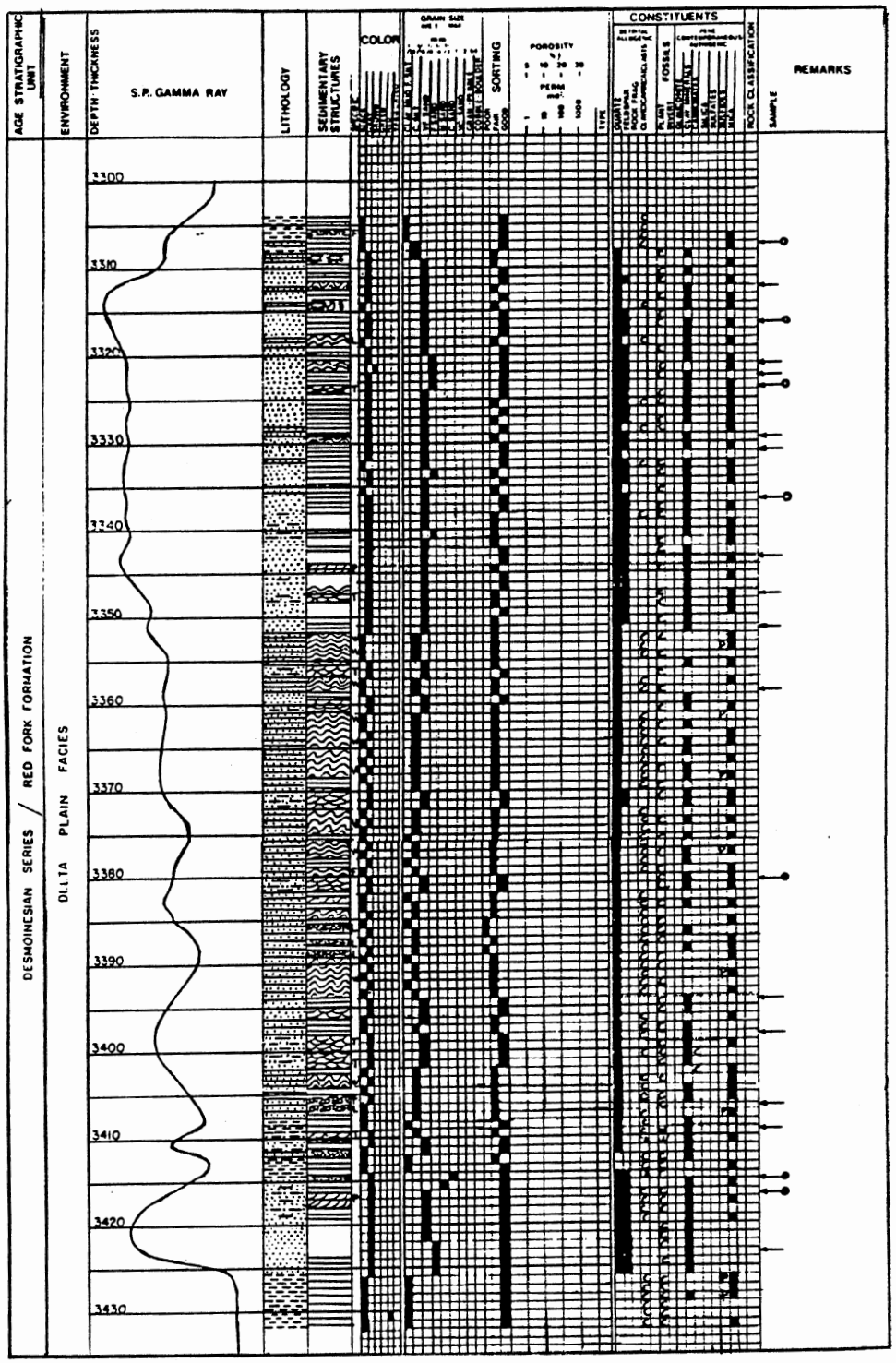

Fig. 11--Core description of Ames Oil and Gas Company, Rogers #2,(SE NE NW Sec 13-T22N-R4E).

Fig. 12--Photograph of channel-lag conglomerate.

accompanied by a minor fining upward sequence. This type of deposit probably represents minor crevasse splays which are cyclically deposited between black organic rich shale of a interdistributary bay or marsh environment (Fig. 9, 11).

Horizontal Bedding

Horizontal bedding and laminations are the most common sedimentary structure noted in all three cores. While horizontal lamination is usually restricted to interstratified sands and shale sequences (Fig. 13), it is also found in some of the thicker sand intervals. Horizontal bedding is associated with zones of well developed sand thickenesses, and is commonly found disrupting the massive bedding of the lower sand zones. The change in sedimentary structures reflects the change in the amount of stream energy available to transport the sediment. Therefore the change represents a wanning current flow, which is a feature that commonly exists in distributary channels.

Massive Bedding

Massive bedding is present in all the cores logged (Fig. 7,9,11) and usually occurs near the base of the sand interval. The Cities Service Company, Rhodd #1 core exhibits nearly fifty percent massively bedded sandstone (Fig. 14).

Interstratification

Interstratification is most common in the Ames Oil & Gas

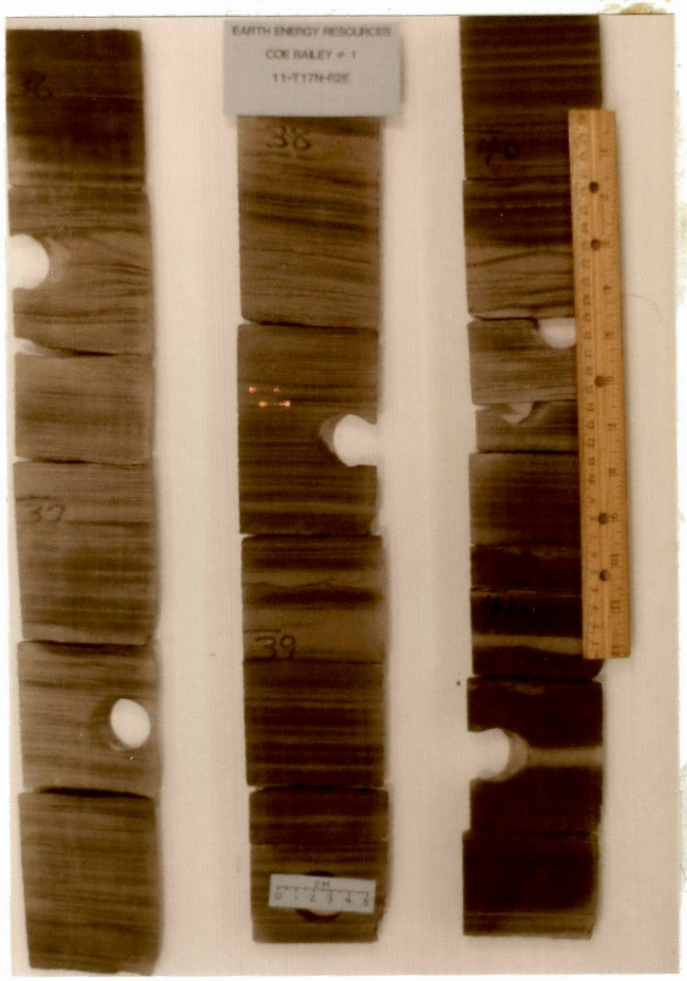

Fig. 13--Photograph of horizontally laminated (bedded) sand and shale sequences.

Fig. 14--Photograph of massively bedded sandstone.

Company, Rogers #2, Sec.13-T22N-R4E (Fig. 11), and less frequent in the Earth Energy Resources, Inc., Coe Bailey #1, Sec. 11-T17N-R2E (Fig. 9). The core descriptions of these two cores illustrates that the larger sandstone units are usually bounded by intervals of interstratification. Wavy interstratification was the dominant variety of interbedding recognized in the cores desrcibed (Fig. 15). Small scale cross bedding was exhibited in the sand rich portions of the interstratified sequences. Abrupt erosional contacts coupled with the above information suggest that these structures are the result of over-bank deposits.

Medium and Small Scale Cross Bedding

Medium and small scale cross bedding was present in the three cores studied. Small scale cross bedding and laminations were prevalent in intervals of interstratification. Medium scale cross bedding generally occurrs in intervals of well developed sand (Fig. 16). The medium scale cross bedding probably represents a sand dune migrating down current.

Erosional-Reactivational Surfaces

Erosional-reactivation surfaces were observed in the Ames Oil and Gas Company, Rogers #2 and the Earth Energy Resources, Inc., Coe Bailey #1 cores (Fig.s 11 and 9). This sedimentary feature was frequently associated with the interstratified layers, creating sharp boundaries between sediments of differing lithology. The boundaries of multistoried sandstone units are defined by erosional-reactivation surfaces (Fig. 17).

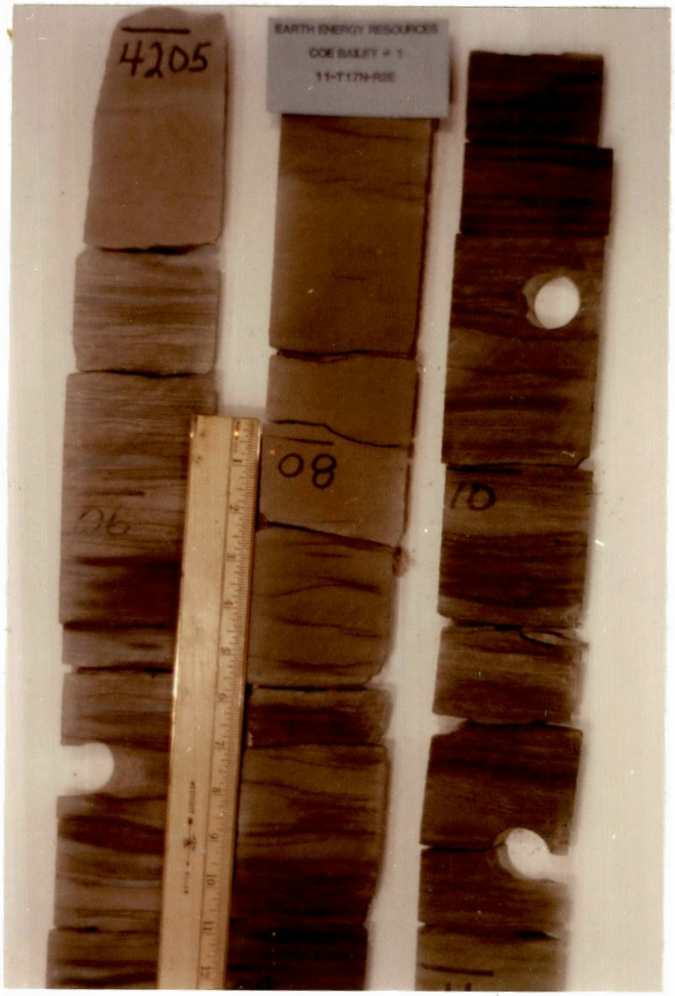

Fig. 15--Photograph of wavy to parallel bedding.

Fig. 16--Photograph of medium scale cross bedding.

Fig. 17--Photograph of interstratified zone exhibiting erosional -reactivation surfaces.

Initial Dip/Slope

Depositional dip was interpreted in the Earth Energy Resources, Inc., Coe Baily #1 core at a depth of 4244 - 4246 feet. The deposit was probably formed as a result of channel downcutting which caused a portion of the bank to slump into the active channel and be preserved. The deformed features at the base of the unit, the relative stratigraphic position of the deposit, and the fining upward of the shale rip-up fragments support the interpretation for a bank-slope deposit (Fig. 18).

Deformed Features

Deformed features were observed in all three cores. Flowage and loading features occur primarily in the shale rich intervals (Fig. 19). These two varieties of deformed features are generally present below thick sequences of well developed sand units. Flowage and loading features were probably a result of differential compaction of thick sand bodies overlying more easily compressible shale units.

Organic Features

Organic features were recognized primarily in the shale rich portions of the cores examined. Bioturbated sediments (Fig. 20), root traces, and trace fossils were generally found in the uppermost shale unit of each genetic sand body. Bioturbation was commonly associated with the thinly bedded interstratified intervals (Fig. 17). Fossils were identified

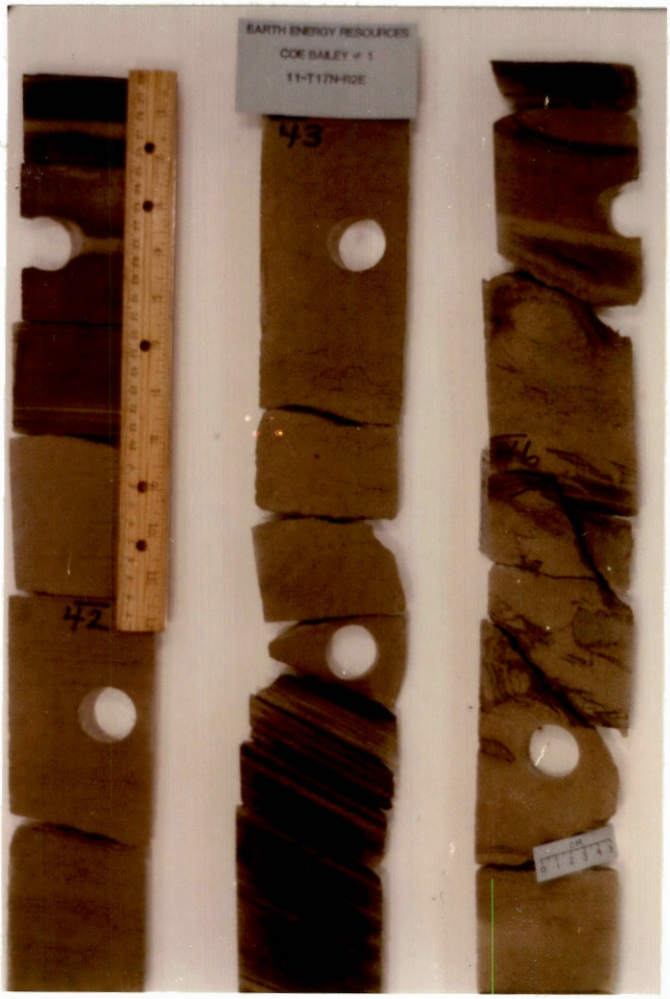

Fig. 18--Photograph interpreted as a bank slope deposit.

Fig. 19--Photograph depicting flow-age and loading features.

Fig. 20--Photograph illustrating a bioturbated interval.

in the lowermost shale unit of the Cities Service Company, Rhodd #1 core (Fig. 7). Productid brachipods, coral fragments and root traces were recognizable throughout the black shale interval (Fig. 5). The organic features listed support the interpretation of a delta plain environment.

CHAPTER VI

DISTRIBUTION OF THE RED FORK SANDSTONE

Introduction

In order to delineate distribution patterns of the Red Fork sandstone three maps were constructed: a log map of the interval, an isopach map, and a net-sand map. The log map was used as an interpretative tool, based upon the characteristics of the short normal curve and the spontaneous potential curve. The log characteristics were used in combination to define the trends and distribution of the Red Fork sandstone. This type of map was useful in determining sandstone trends and inferring environments of deposition.

The isopach map of the Red Fork interval was constructed using the top of the Pink Limestone and the top of the Inola Limestone. When the Inola Limestone was not present the base of the Red Fork sandstone was used as the lower marker bed. The isopach map was used to illustrate the general thickening and thinning of the interval throughout the area of study. The isopach map reveals a general increase in thickness from 80 feet in the northwest to over 200 feet in the southeast.

The net-sand map shows the net thickness of the Red Fork sandstone and assists in delineating the major channels. Net-sand was defined as units with a deflection from the shale

base line greater than 20 millivolts of the spontaneous potential curve. The total thickness from each well was tabulated and plotted.

Trends and Widths

The trends of the Red Fork sandstone indicate a prevailing north-south orientation. The widths vary depending upon whether one is dealing with a single or multistoried unit. Because of the stratigraphic and geometric complexities of the Red Fork sandstone the study area was divided into three regions.

The Northern region (T23&22N-R1&2E) contains a single genetic sand unit which extends southward into the study area for approximately twelve miles (Plate 11). This elongate trend ranges in width from 5000 to 7500 feet (Plate 12).

The Central region (T21,20&19N-R1&2E) illustrates broad elongate trends which tend to bifurcate downdip. Smaller isolated pods of sand appear to be arranged in a north-south direction. The widths of the major trends varies from 2500 to 12,500 feet (Plate 12).

The Southern region (T18&17N-R1&2E) displays a complex pattern of multistoried, bifurcating, anastomosing channels forming a broad north-south trending belt. The Red Fork sandstone in the southeast portion of the Southern region is part of a larger distributary system to the east (Fig. 8). The broad belt in the southeast portion exhibits major digitations which extend southward. The digitations range in width from 4000 to 7000 feet (Plate 12).

Thickness

The Red Fork isopach map reveals a general increase in thickness from 80 feet in the northwest to 200 feet in the southeast. The net-sand map reflects similar trends in thickness from 40 feet in the northwest to over 120 feet in the southeast. The general increase in thickness from the northwest to the southeast suggests that the receiving basin for Red Fork sediments was to the southeast. Examination of the log map (Plate 13) in the southeast portion of the study area illustrates the increase in sand thickness is due to the multistoried nature of the deposit. The frequence of stacking appears to increase towards the larger complex of channels to the east (Fig. 8).

Boundaries

Major Red Fork sand bodies exhibit sharp lateral and basal contacts bounded by shale (Plate 13 T23N-R1E). Basal contacts are abrupt and are associated with a basal channel lag conglomerate or a fine grained sandstone. Upper contacts are generally gradational, fining upward into a very fine-grained sandstone or silt (Fig. 7,9). Areas which have thick accumulation of sand (Plate 12,13 T17N-R2E) result from the downcutting of the Red Fork sandstone, and subsequent erosion of the Inola Limestone.

CHAPTER VII

PETROLOGY

Introduction

Petrographic analysis of the Red Fork sandstone includes thin section examination from three cores (Fig.10): (1) Cities Service Company, Rhodd #1, (Sec.9-T23N-R1E) from which eleven thin sections were examined, (2) Earth Energy Resources, Inc., Coe Bailey #1, (Sec.11-T17N-R2E) of which twenty-two thin sections were studied, and (3) Ames Oil and Gas Company, Rogers #2 (Sec.13-T22N-R4E) from which twenty-one thin sections were examined. Bulk and extracted x-ray diffraction analysis was preformed on selected samples throughout the cores described. The scanning electron microscope was employed to illustrate textural relationships and identify various authigenic minerals.

Three, one-hundred point counts were made of each thin section. The data was normalized and plotted according to Folk's (1968) sandstone classification. The Rhodd #1 and Rogers #2 plotted as a sublitharenite (Fig. 21&22) whereas the Coe Bailey #1 was classified as a lithic arkose (Fig. 22). The lithic rock fragments observed in thin section included shale, chert, and low grade metamorphic rock fragments. Potassium feldspar and varieties of sodic plagioclase were identified, with potassium feldspar being the more abundant. Quartz was

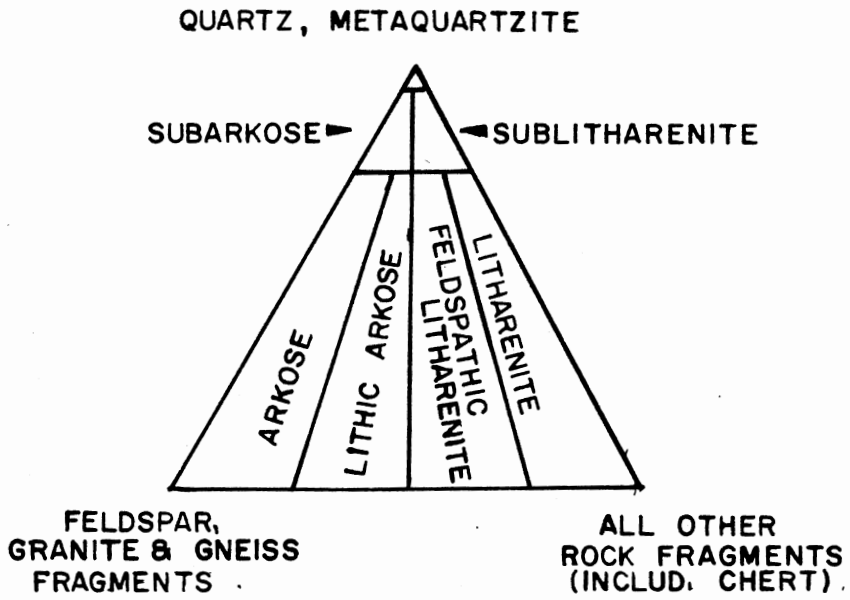

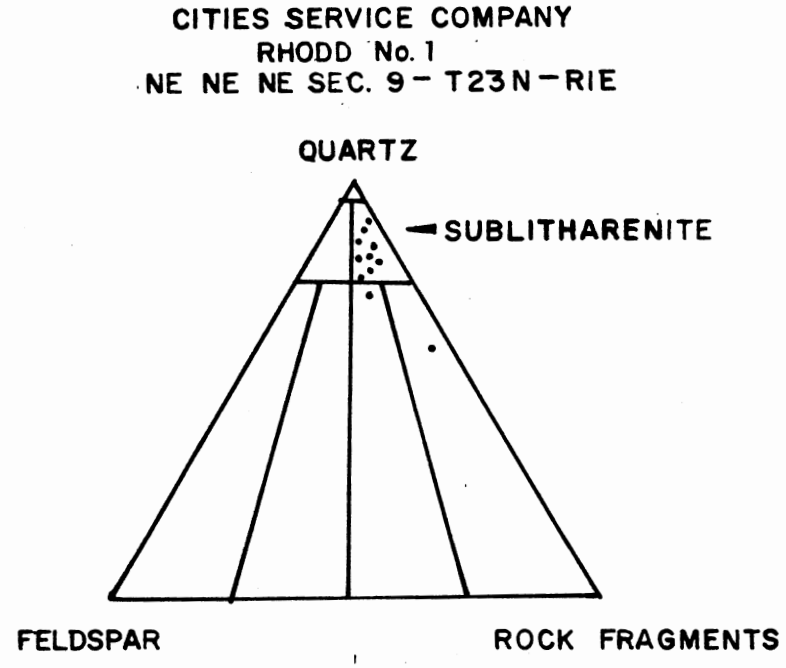

Fig. 21--Classification of Red Fork sandstones, (Modified after Folk, 1968).

EARTH ENERGY RESOURCES, INC.
COE BAILEY No. 1
NW NW SW SEC. 11 - T17N-R2E

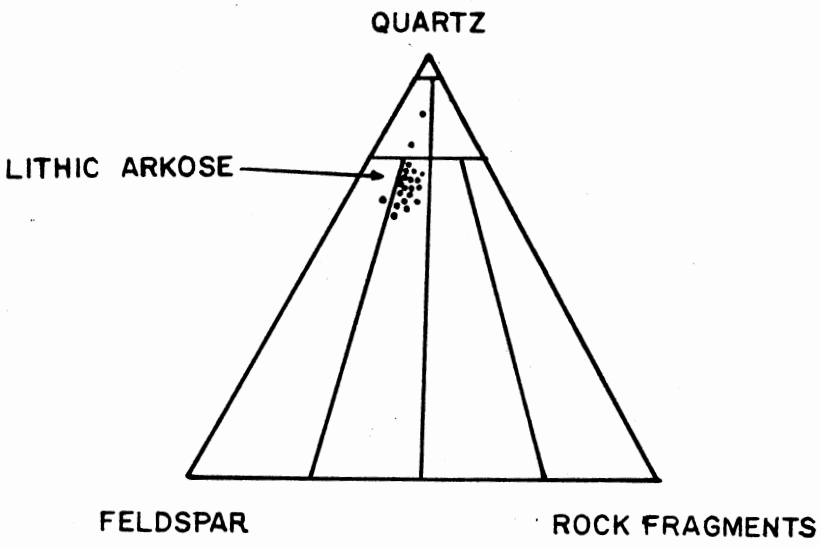

AMES OIL & GAS COMPANY
ROGERS No. 2
SE NE NW SEC. 13 - T22N-R4E

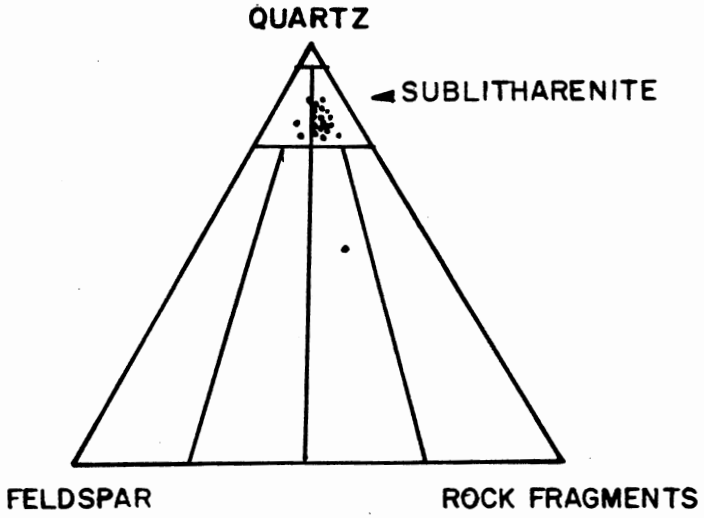

Fig. 22--Classification of Red Fork sandstones, (Modified after Folk, 1968).

commonly the dominant detrital constituent with the average being 75 percent.

Texture

In both the Rhodd #1 and Coe Bailey #1 cores, there is a general upward decrease in grain size in each of the genetic sand units (Fig. 7 and 9). The fining-upward sequence ranges from fine-grained sand at the base to very fine-grained and silt size particles at the top. The Rogers #2 exhibited a general uniform grain size (fine-grained) throughout the core.

Textural analysis of the Red Fork sand revealed that each genetic sand interval was moderately well sorted, with subangular to subrounded grains. The low percentage of detrital matrix combined with the above evidence indicates that the Red Fork sandstone is a submature deposit.

Detrital Constituents

The Red Fork sanstone was comprised of mainly three detrital constituents: (1) quartz, (2) feldspars, and (3) rock fragments. Three, one-hundred point counts were made on fifty-three thin sections. The data was normalized to a three component system so as to illustrate the gross lithology of each Red Fork core. Figure 21 shows the normalized composition of the detrital constituents using Folk's (1968) sandstone classification. The most significant contrast is among the Rogers #2 and the Coe Bailey #1, the increase in the amount of feldspar and the relative decrease in the amount of

rock fragments gave rise to two distinct lithologies.

Quartz

Detrital quartz was the major framework grain observed within the Red Fork sandstone. Two tpyes of detrital quartz were distinguished: (1) monocrystalline and (2) polycrystalline (Fig. 23). Monocrystalline quartz grains were the most abundant by a ratio of ten to one.

The Rhodd #1 showed an average of 53% total detrital quartz with the range extending from 42% to 66%. Normalized results of the quartz, feldspar, and rock fragments brought detrital quartz to 78%. The total detrital quartz of the Coe Bailey #1 ranged from 19% to 60%. Normalized results altered the detrital quartz percentage to 71%. The Rogers #2 displayed an average of 51% with the range extending from 14% to 72%. Computed normalized results brought the detrital quartz to 80%.

Rock Fragments

Rock fragments made up 10 to 15% of the framework grains. The majority of the rock fragments were metamorphic and sedimentary clasts of chert and shale. Minor quanities of igneous rock fragments were present throughout the Red Fork sand interval.

Shale rip-up clasts and impure chert fragments were the most common types of sedimentary rock fragments. Many of the lager shale rip-up clasts can be traced to an underlying shale unit of similar lithology. Deformed clay clasts composed of allogenic clays were squeezed to form a pseudo-matrix.

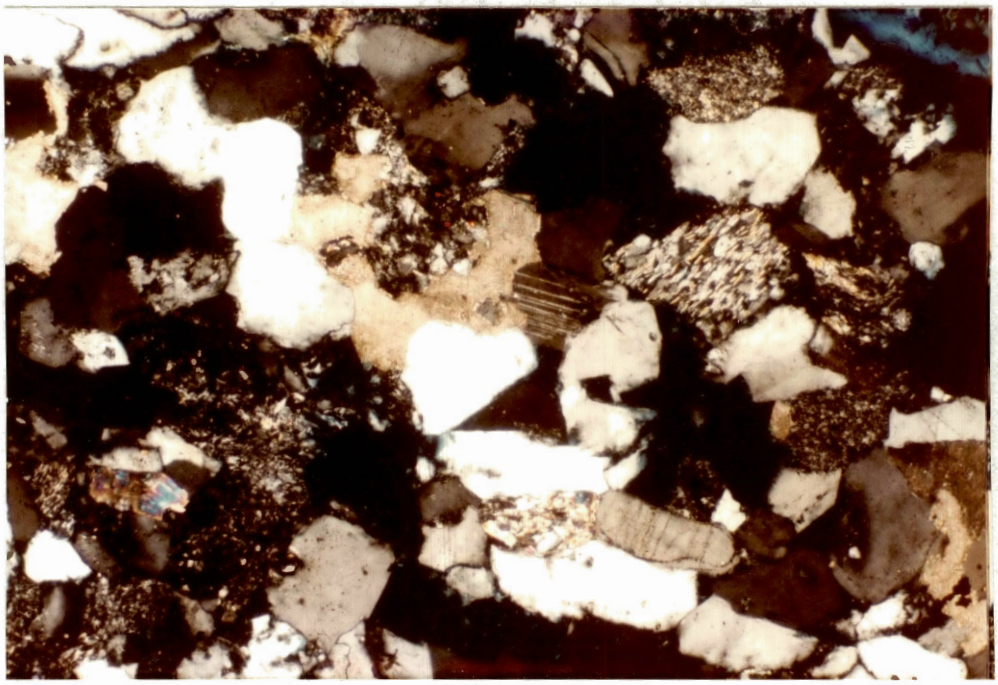

Fig. 23--Photomicrograph of polycrystalline and monocrystalline quartz. Magnification 10X, Crossed Nicols, Rhodd #1, Depth 4260.6'

Metamorphic rock fragments observed include chlorite and mica shists, phyllite, and fragments of slate. Many of these rock fragments exhibit ductile deformation possibly as a result of increased depth of burial and of past tectonic activity. Some metamorphic rock fragments were contorted to produce a pseudo-matrix between adjoining detrital grains (Fig. 24).

Cities Service Company, Rhodd #1 core revealed an average of 10% total rock fragments with the range extending from 6% to 26%. Normalized computations altered the percentage to 15%. Total rock fragments observed in the Earth Energy Resources, Inc., Coe Bailey #1 core range from 4% to 8% and average at 6%. Normalized computations showed the Coe Bailey #1 core to have an average of 10% rock fragments. The Ames Oil and Gas Company, Rogers #2 core contained an average of 7%, and the range extended from 5% to 10%.

Feldspar

Feldspar made up approximately 3 to 11% of the total composition of the Red Fork sandstone. The primary types of feldspar observed in order of abundance are: (1) potassium feldspar (commonly untwinned) and, (2) sodium rich plagioclase. The plagioclase grains exhibited various extinction angles from carlsbad to albite twinning, thus indicating the composition varies between oligoclase and andesine. Many feldspar grains illustrated varying degrees of diagenesis, from partially dissolved grains to complete dissolution. Other alteration effects observed include serictization,

Fig. 24--Photomicrograph displaying ductile deformation of a mica schist fragment. Magnification 20X, Plane Polarized Light, Rogers #2, Depth 3336.6'.

replacement by either authigenic clays, calcite, or secondary quartz. Feldspar composition played an integral part in the formation of secondary porosity.

Feldspar content of the Rhodd #1 core ranged from 3% to 7% and averaged 5%. Computed normalized results increased the feldspar content to 7%. The Coe Bailey #1 core ranged from 4% to 14% feldspar, with the average being 11%. Normalized results increased the feldspar content to 19%. The Rogers #2 core showed a range between 4% and 8% feldspar, the average calculated to 6%. Computed normalized results increased the feldspar content to 9%.

Other Detrital Constituents

Other detrital constituents in the Red Fork sandstone include muscovite, carbonaceous debris, collophane, sphene, zircon, and glauconite. The range of these accessory detrital constituents varied from a trace to 10% of the total lithology. Muscovite and carbonaceous detritus were deposited along primary bedding planes and subjected to ductile deformation. Collophane occurred in irregular, patchy deposits throughout the Red Fork interval. Detrital glauconite occurred in trace amounts and commonly formed a pseudo-matrix. Sphene and zircon were the two most common heavy minerals identified in the Red Fork sandstone. The grains were subrounded, very fine-grained to silt sized and occurred in sporadic isolated patches (Fig. 25).

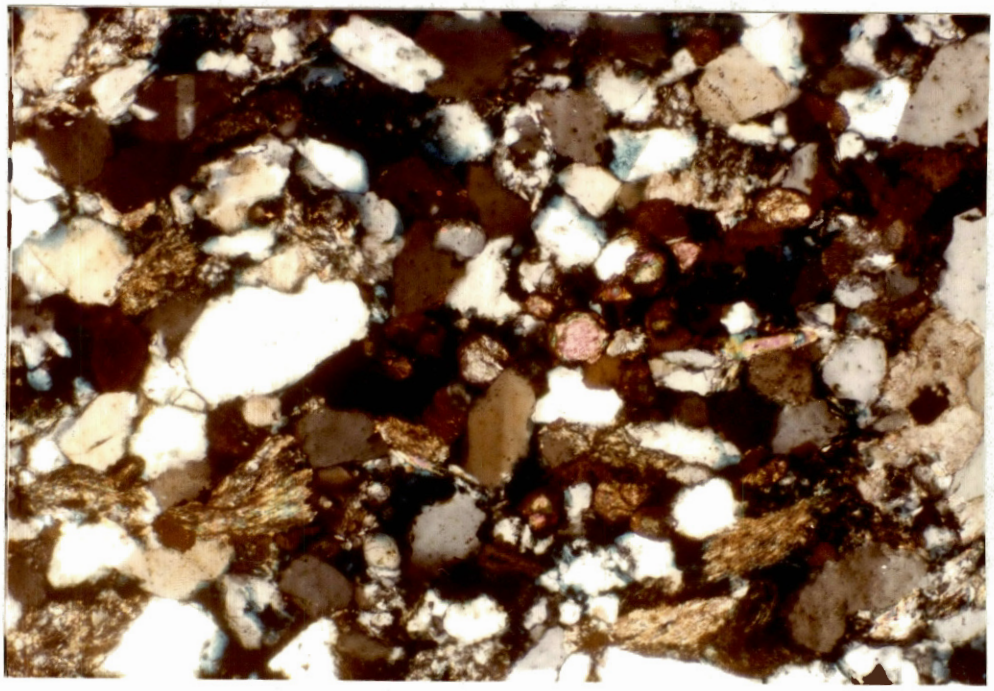

Fig. 25--Photomicrograph exhibiting an isolated patch of sphene and zircon. Magnification 10X, Crossed Nicols, Rogers #2, Depth 3322.4".

Detrital Matrix

Two types of detrital matrix were identified: (1) chlorite and (2) illite. The detrital matrix content fluctuated from trace amounts upward to 51% of the total composition. Illite was the most common matrix by a ratio of approximately three to one. Both chlorite and illite displayed a high degree of ductile deformation. Squeezing of the detrital matrix between the framework grains reduced primary porosity and permeability. However, later stages of diagenesis partially and or completely dissolved the detrital matrix which gave rise to secondary porosity.

Authigenic Constituents

Primary authigneic constituents observed include quartz overgrowths, authigenic clays, calcite, leucoxene, and pyrite. These constituents generally served to reduce effective porosity and permeability.

Quartz overgrowths range in abundance from trace to 5% of the total lithology. Silica overgrowths were commonly found coating detrital quartz grains. Detrital quartz grains served both as a source of dissolved silica and as loci for precipitated secondary quartz. Silica overgrowths are dependent upon pore fluid chemistry. A basic pore fluid will disolve silica whereas an acidic pore fluid will precipitate silica. Thereby the silica overgrowths reflect episodic growth patterns, which in turn document the fluctuating changes in pore fluid chemistry. Figure 26 shows corrosion of a quartz grain, while figure

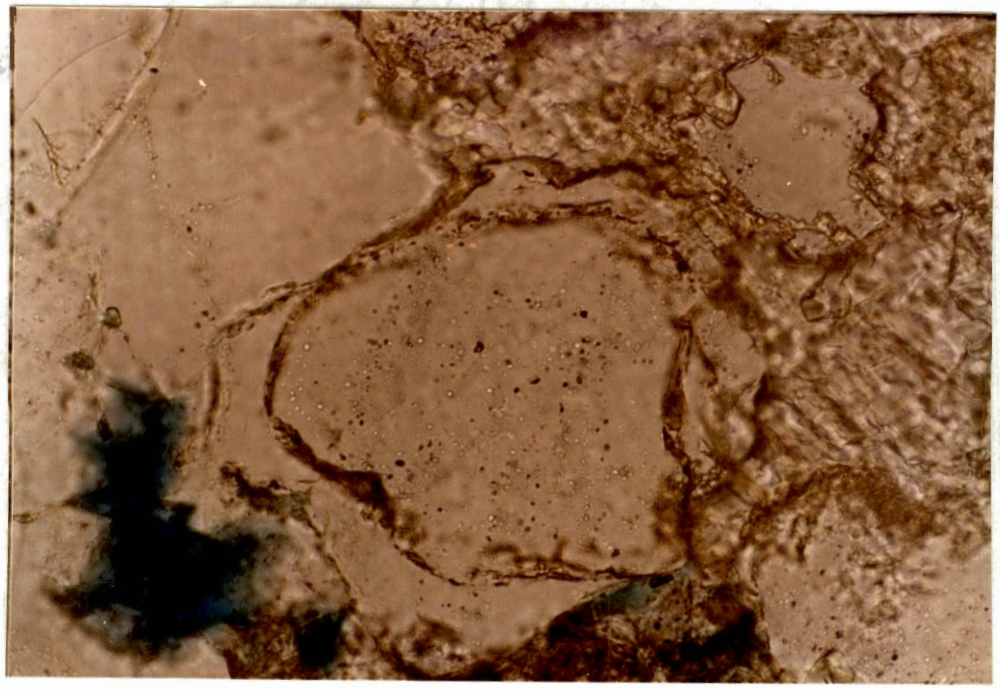

Fig. 26--Photomicrograph of carbonate cement replacing detrital quartz. Magnification 40X, Plane Polarized Light, Rhodd #1, Depth 4257.6'.

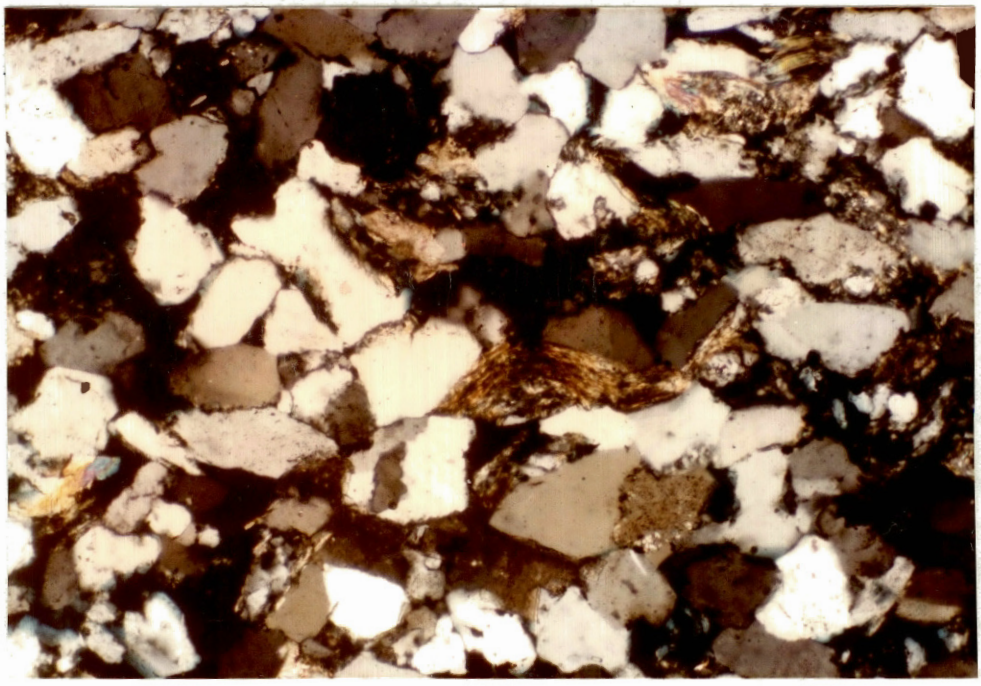

Fig. 27--Photomicrograph of syntaxial quartz overgrowths as a cementing agent. Magnification 10X, Crossed Nicols, Rogers #2, Depth 3343.4'.

27 illustrates syntaxial quartz overgrowhts in optical continunity. The quartz overgrowths serve in cementing the grains together and reducing primary porosity. Three probable sources for silica are: (1) pressure solution of quartz grains, (2) dissolution of feldspars, and (3) dissolution of clay minerals.

Authigenic clay minerals were determined by three methods: (1) detailed petrographic analysis, using blue epoxy stained thin sections, (2) scanning electron microscope (SEM), and (3) X-ray diffraction analysis of the extracted clay fraction. Each extracted clay sample was subjected to a natural, heated, and glycolated process. The X-ray diffractogram recorded the peaks of the various clays from 2 phi to 16 phi (Fig. 28).

The Red Fork sandstone contains three types of authigenic clays: (1) pore filling kaolinite, (2) pore lining and pore bridging illite, and (3) pore lining chlorite. The SEM demonstrated the delicate morphology and spatial distribution of the authigenic clays. Semi-quantitative analysis of x-ray diffraction data showed kaolinite as being the most prevalent authigenic clay by a ratio of 2:1:1, while illite and chlorite occurred in relatively equal proportions.

Authigenic kaolinite was identified by its distinctive morpology and characteristic 7.14 angstrom peak (Fig. 28). The scanning electron microscope illustrated abundant authigenic kaolinite, which occurred as pseudo-hexagonal booklets (Fig. 29). Microporosity has resulted by the precipitation of large amounts of authigenic kaoloinite crystals within oversized pore spaces (Fig. 30).

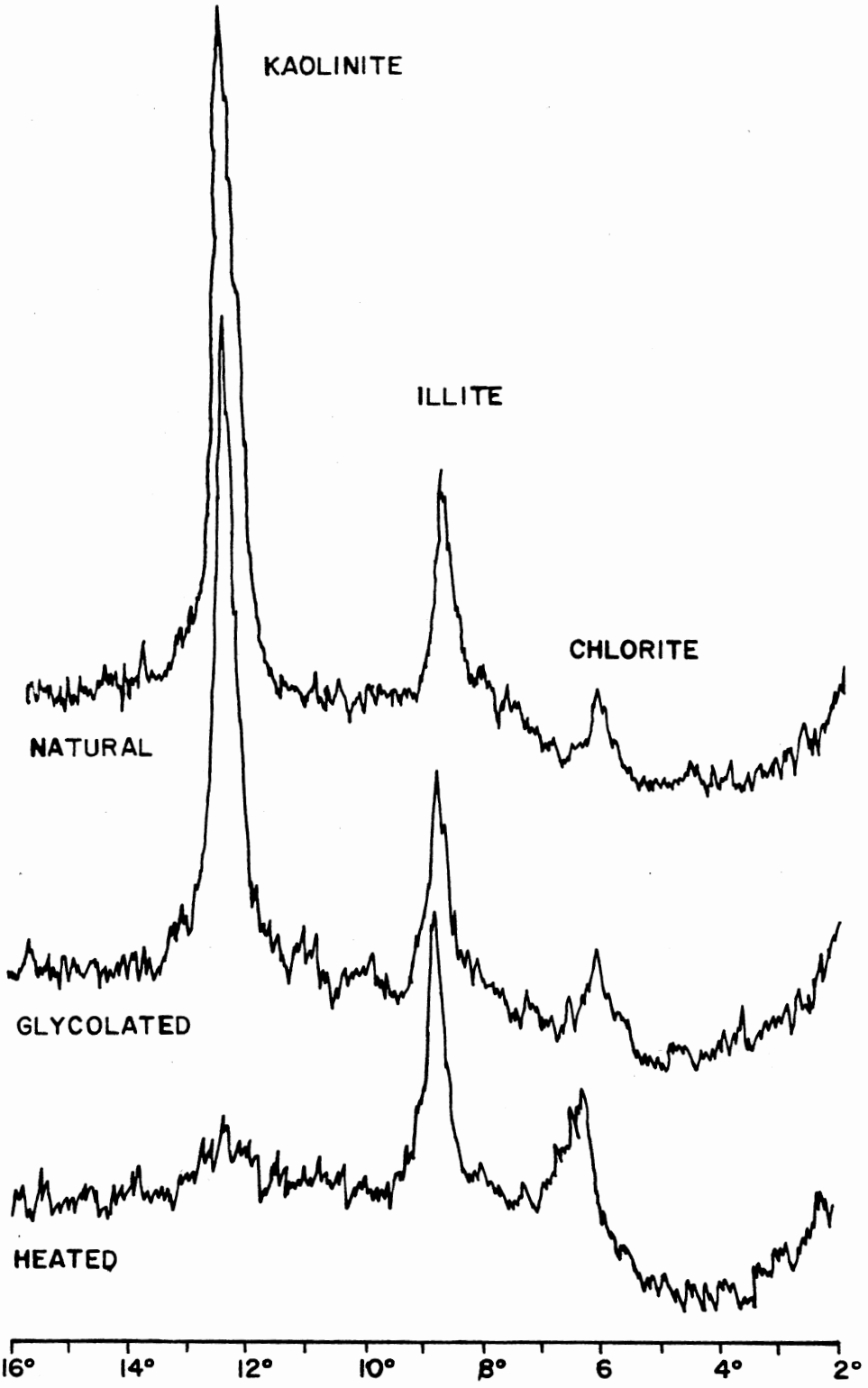

Fig. 28--X-ray diffraction analysis of extracted clay fraction from Coe Bailey #1, depth 4248.2'.

Fig. 29--Scanning electron photomicrograph of authigenic kaolinite. Magnification 2000X, SEM, Coe Bailey #1, Depth 4223.2'.

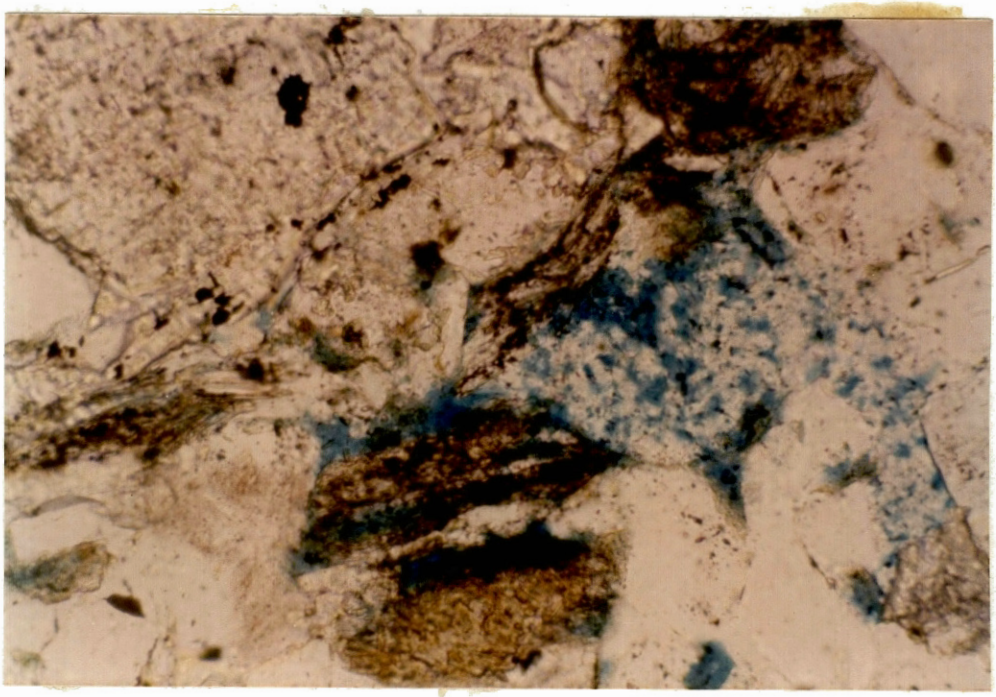

Fig. 30--Photomicrograph displaying large authigenic booklets of kaolinite filling an oversized secondary pore. Magnification 20X, Plane Polarized Light, Rogers #2, Depth 3322.4'.

Authigenic illite occurrs in the Red Fork sandstone as either lining grains or bridging across grains. Figure 31 illustrates the delicate lathe-like projections which extend outward into the pore space. Illite's delicate morphology dictates a high surface area, which has a dramatic affect in decreasing effective porosity and increasing irreducible water saturation. Thin section analysis showed illite to represent approximately 25 percent of the authigenic clays.

Authigenic chlorite was identified by the scanning electron microscope and x-ray diffraction techinques (Fig. 27). Figure 32 shows the characteristic end-to-face habit of authigenic chlorite. The figure also demonstrates the pore lining occurrence of authigenic chlorite. Semi-quanitative analysis of the x-ray diffraction data reveals that chlorite represents 25 percent of the total authigenic clay content.

Calcite cement observed in thin section ranged in abundance from a trace to 14% of the total lithology. In many instances calcite cement occurred in irregular patches close to thick sequences of shale. Figure 33 shows the corrosion of surrounding quartz grains which were in contact with the calcite cement. Calcite cementation probably occurred as a later diagenetic event which assisted in reducing the porosity of the Red Fork sandstone.

Fig. 31-- Scanning electron photomicrograph of authigenic illite. Magnification 2400X, SEM, Coe Bailey #1, Depth 4263.0'.

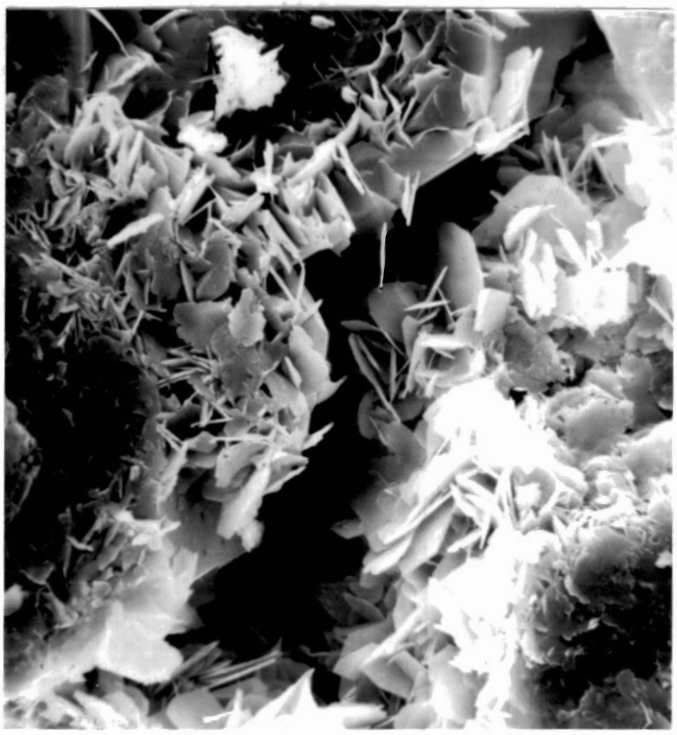

Fig. 32--Scanning electron photomicrograph of authigenic chlorite. Magnification 1800X, SEM, Rhodd #1, Depth 4241.4'.

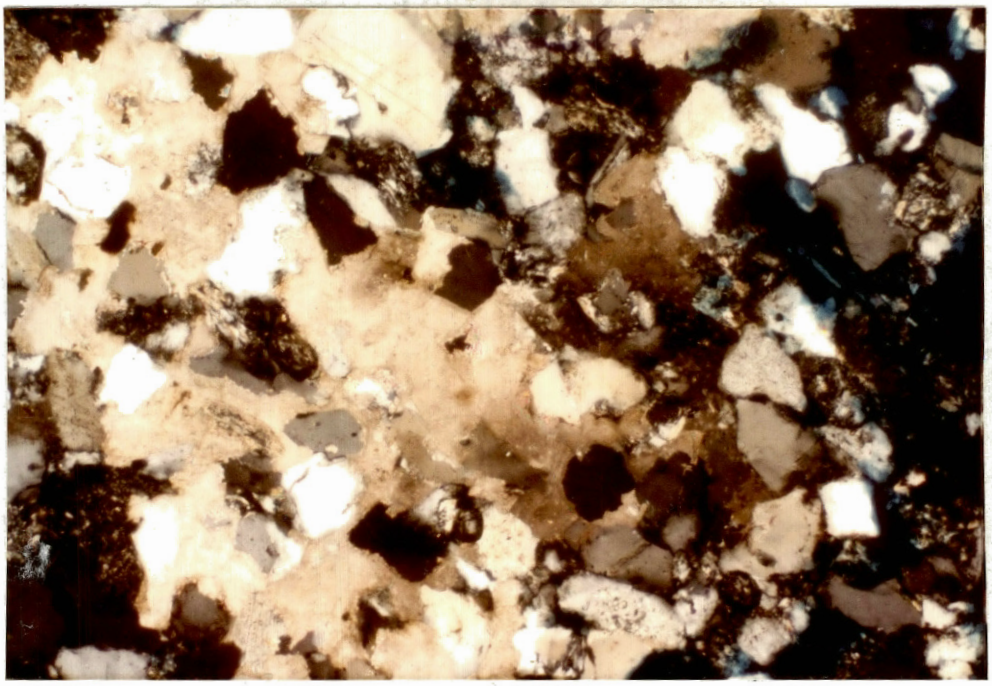

Fig. 33--Photomicrograph of carbonate cement binding detrital constituents. Magnification 10X, Crossed Nicols, Rhodd #1, Depth 4267.3'.

CHAPTER VIII

POROSITY

Introduction

The Red Fork sandstone contains two principle types of porosity: (1) primary and, (2) secondary. Volumetrically, secondary porosity exceeds primary porosity by a ratio of approximately 3 to 1. The tremendous difference in the amount of secondary porosity was due to the partial and or complete dissolution of various detrital constituents.

Porosity types observed in the Red Fork sandstone were identified by scanning electron microscopy and detailed petrographic analysis. Thin sections were prepared by impregnating the slabs of sandstone with blue epoxy. The procedure was preformed so that the size and geometry of the pore spaces would be defined. The scanning electron microscope provided intricate details of the evolution of secondary porosity and the problems which affect the permeability of the Red Fork sandstone.

Primary Porosity

Interparticle porosity was the most abundant type of primary porosity identified within the sandstone. An average of two percent interparticle porosity was computed, with the range extending from a trace to five percent.

Quartz overgrowths, calcite cementation, and the ductile deformation of the detrital matrix combine to reduce primary porosity. Figure 34 shows interparticle porosity being reduced by the formation of quartz overgrowths and the precipitation of carbonate cement.

The size of interparticle pore spaces present in the Red Fork generally ranges from 0.05 to 0.10mm. These pore spaces are not extensively interconected. Porosity and permeability values are commonly low only when primary porosity exsists. The writer believes that primary porosity played an important role in the generation of secondary porosity. Primary porosity assisted by providing avenues in which pore fluids could migrate and preferentially dissolve various constituents, thereby giving rise to secondary porosity.

Secondary Porosity

Secondary porosity in the Red Fork sandstone can be attributed to the extentsive amounts of partial and or complete dissolution of detrital constituents. Petrographic analysis of secondary porosity exhibits an overall average of six percent, while the range fluctuates from zero to twenty-two percent. The size of pores formed within the interval varied from 0.04 to 0.19mm. It appears that much of the secondary porosity depends upon the inital size of the grain and the amount of dissolution which has taken place.

Five different types of secondary porosity were identified (1) partial dissolution, (2) oversized pores and floating

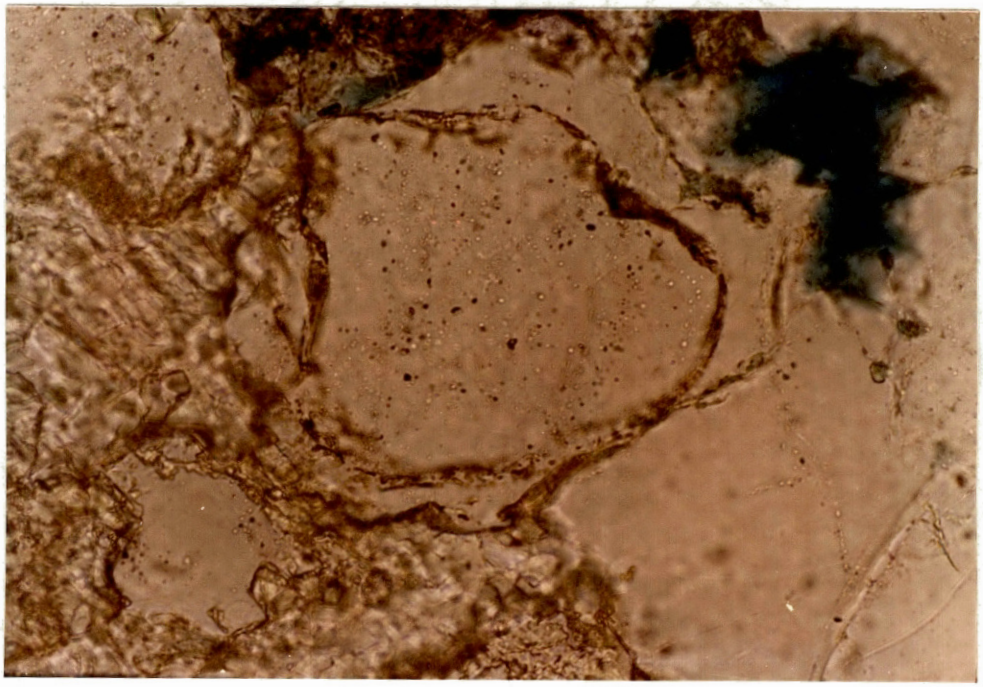

Fig. 34--Photomicrograph illustrating reduction of primary porosity by precipitation of silica and carbonate cements. Magnification 40X, Plane Polarized Light, Rhodd #1, Depth 4257.6'.

grains, (3) honeycombed grains, (4) elongate pores and, (5) corroded grains. These five types of porosity were identified using petrographic criteria proposed by Schimidt, McDonald and Platt (1977) and Choquette and Pray (1970). Much of the secondary porosity was due to the dissolution of feldspar grains. The removal of calcite and silica authigenic cements also appeared to enhance the generation of secondary porosity. Zones within the Red Fork sandstone which contain high percentages of detrital matrix have correspondingly low porosity values. The amount of primary porosity was reduced because the detrital matrix was squeezed between framework grains.

Partial dissolution of feldspar was the dominant type of secondary porosity recognized within the Red Fork interval. Figure 35 exhibits extensive developement of secondary porosity and subsequent formation of microporosity. Note corroded edges of grains surrounding the pore space and the partial dissolution of fragments within the secondary pore. The figure also demonstrates the affect that authigenic kaolinite has had on reducing effective porosity and permeability by filling and clogging the pore space and throat.

Elongate pores and oversized pores with floating grains are common secondary porosity types identified within the Red Fork sandstone. Figure 36 illustrates both varieties of porosity. Notice the amount and extent of secondary porosity generated. Some of the larger secondary pores generated contain relict grain fragments. When both porosity types are present within the Red Fork sandstone, the effective porosity and permeability are increased. However, the values are usually

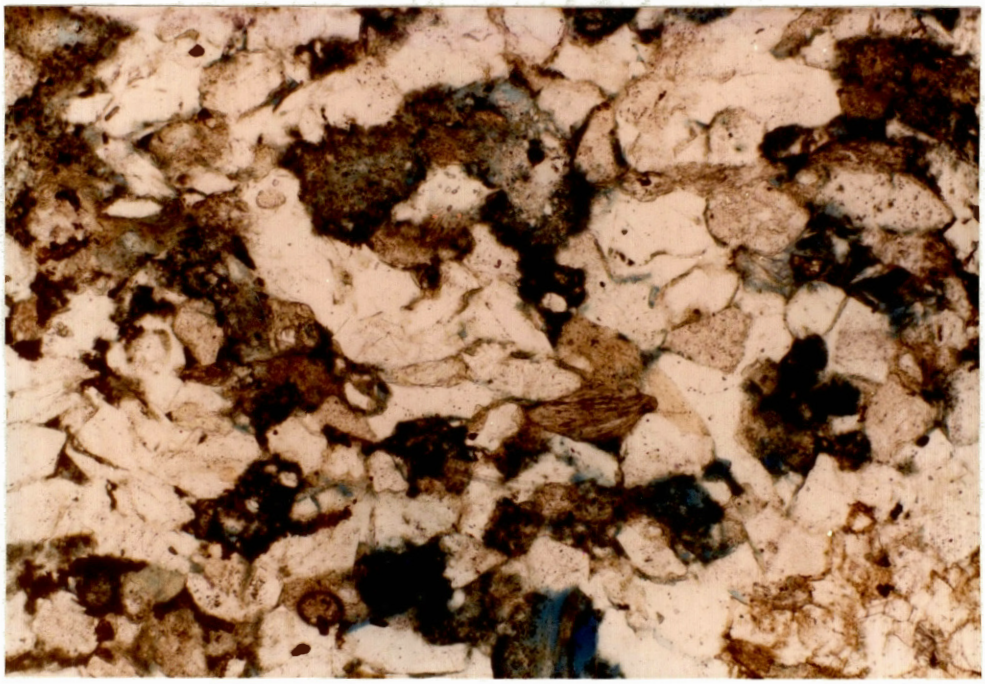

Fig. 35--Photomicrograph exhibiting microporosity generated in the Red Fork sandstone. Magnification 10X, Plane Polarized Light, Rhodd #1, Depth 4248.4'.

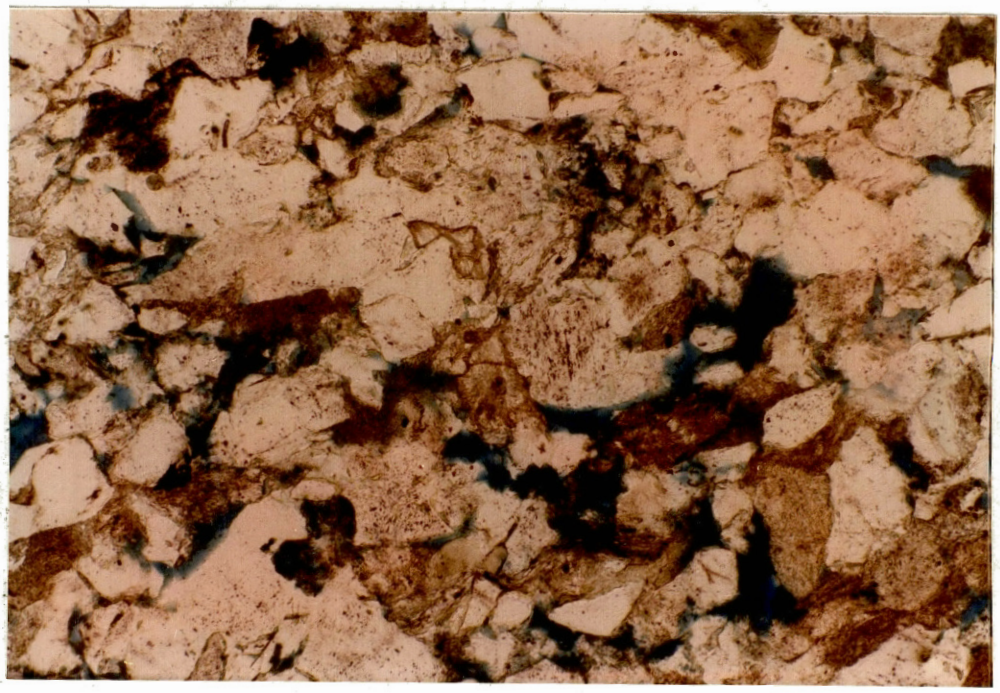

Fig. 36--Photomicrograph of elongate and oversized pores. Magnification 10X, Plane Polarized Light, Rhodd #1 Depth 4257.6'.

reduced by the precipitation of authigenic clays within the pore throat and space.

Honeycomb porosity is the result of incomplete dissolution of a constituent. Figure 37 exhibits a large detrital feldspar grain which was partially dissolved. Notice the preferred dissolution along clevage traces and fractures which have developed on the grain. Figure 37 also illustrates that the initial size of the detrital grain directly reflects the size and geometry of the secondary pore. Honeycomb porosity is an important porosity type of the Red Fork sandstone because of the large amounts of microporosity which have been generated.

Other detrital grains such as clay clasts and glauconite contributed to the formation of secondary porosity. Figure 38 shows a mud clast partially dissolved and altering to authigenic chlorite.

The secondary porosity generated in the Red Fork sandstone appears to have been controlled primarily by the initial lithology. The zones with the higher percentages of secondary porosity are a function of the complete and or partial dissolution of detrital feldspar. Figure 39 illustrates the amount of secondary porosity which has evolved due to the dissolution of detrital constituents. Notice in the figure the shape and amount of interconnected pores, which can be identified by the oil filling and lining the secondary pores.

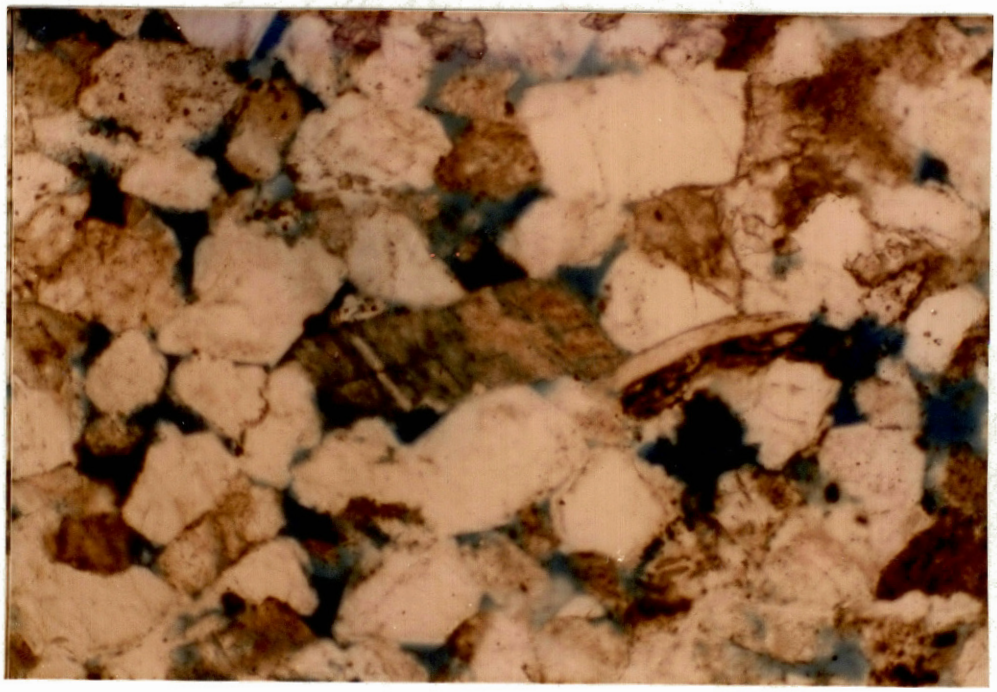

Fig. 37--Photomicrograph illustrating preferential dissolution of a detrital feldspar grain. Magnification 10X, Plane Polarized Light, Coe Bailey #1, Depth 4269.4'.

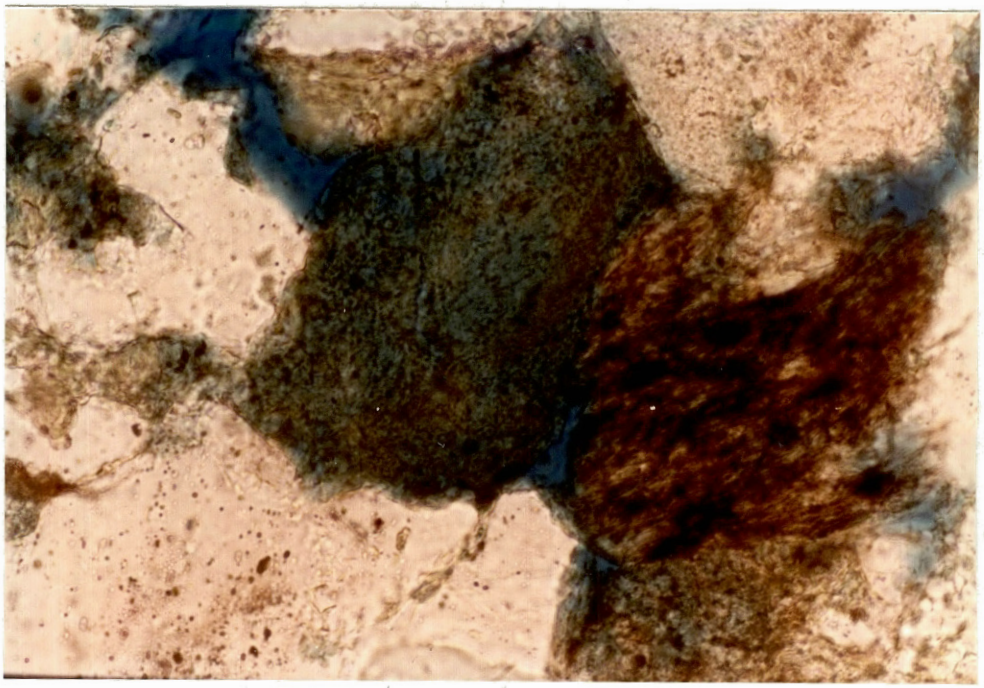

Fig. 38--Photomicrograph showing a detrital mud clast altering to authigenic chlorite. Magnification 40X, Plane Polarized Light, Rhodd #1, Depth 4257.6'.

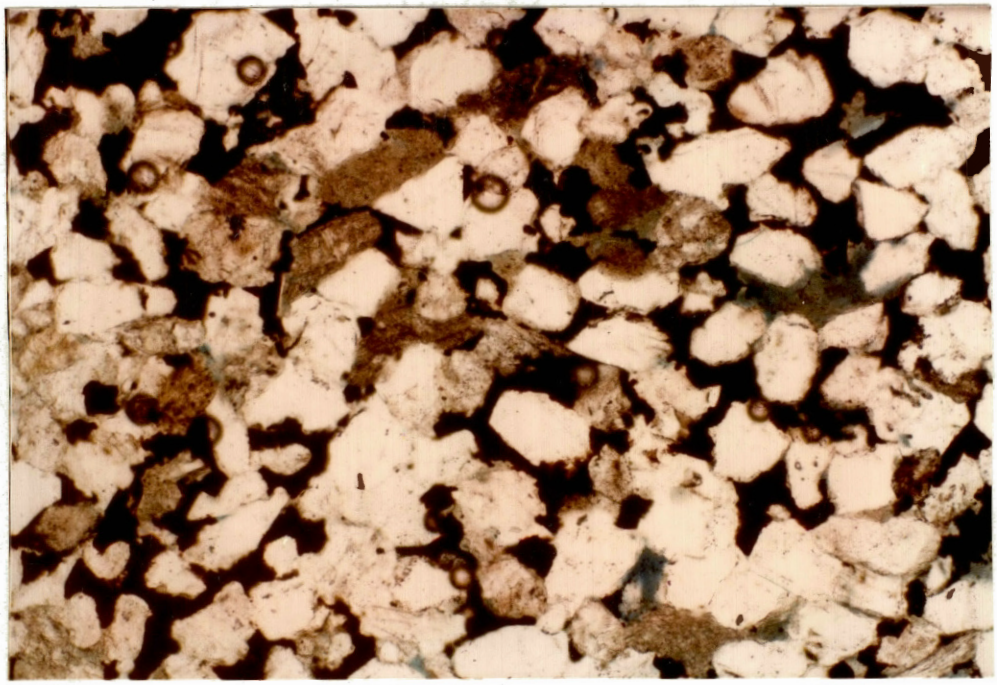

Fig. 39--Photomicrograph of oil lining and filling secondary pores generated by the partial and or complete dissolution of detrital constituents. Magnification 10X, Plane Polarized Light, Coe Bailey #1, Depth 4223.3'.

CHAPTER IX

DIAGENESIS

Introduction

The sequence of diagenetic events has greatly influenced the reservoir quality of the Red Fork sandstone. Modifications of the orginal depositional fabric include: (1) reduction of primary porosity and permeability by compaction and cementation (Fig. 40), (2) enhancement of porosity and permeability by dissolution of chemically unstable constituents and cements, (3) reprecipitation of chemically stable authigenic constituents. These modifications of the Red Fork sandstone are based upon petrographic analysis, X-ray diffraction data, and scanning electron microscopy criteria. Interpretation of the evidence reveals a complex diagenetic history of the Red Fork sandstone.

Dissolution Features

Dissolution of quartz grains was observed throughout the sand intervals studied, however only in minor quanities and usually in association with carbonate cement (Fig. 41). The dissolution of quartz was probably the result of compaction and pore fluid chemistry. Corrosion and etching of quartz grains were probably augmented by the presence of alkaline

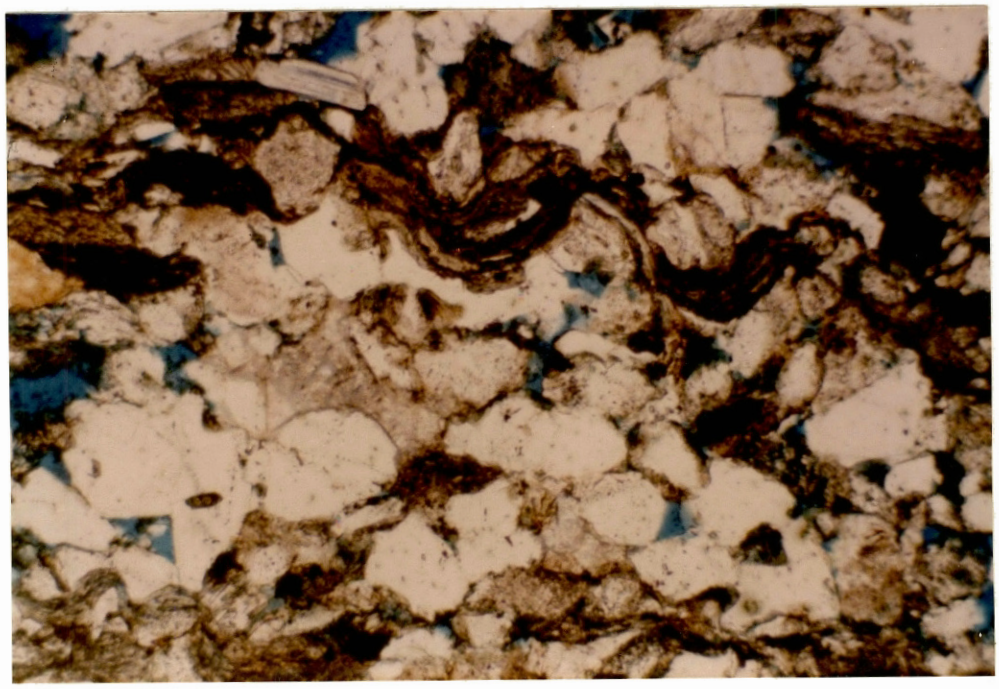

Fig. 40--Photomicrograph depicting ductile deformation of detrital matrix due to compaction. Magnification 10X, Plane Polarized Light, Rogers #2, Depth 3323.8'.

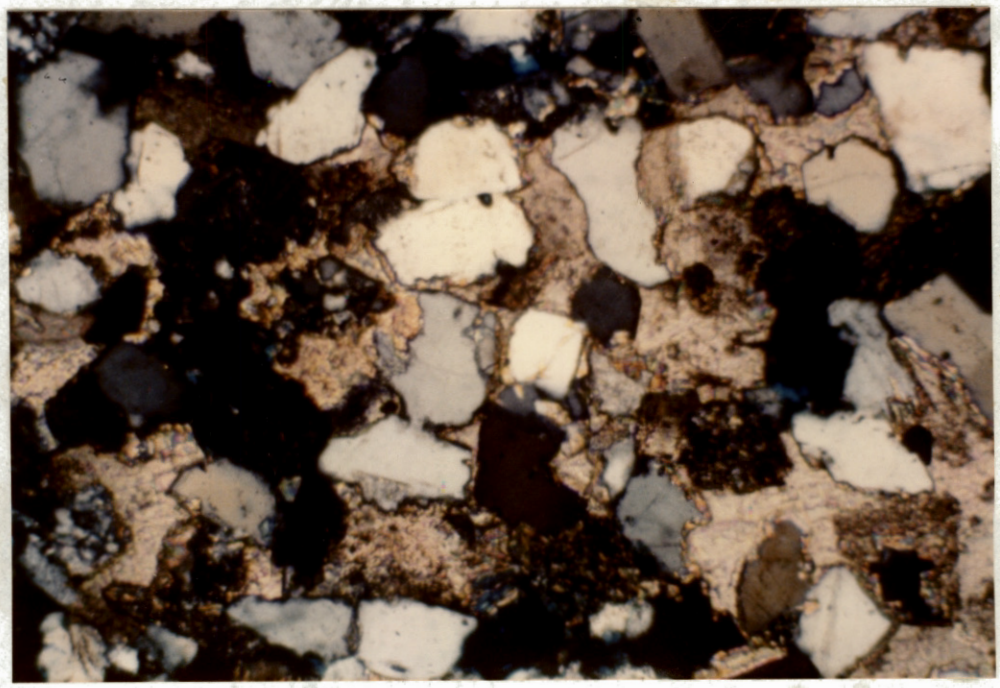

Fig. 41--Photomicrograph of corroded quartz grains due to precipitation of carbonate cement. Magnification 10X, Crossed Nicols, Rhodd #1, Depth 4264.1'.

pore fluids.

The primary diagenetic event of the Red Fork sandstone was the partial and or complete dissolution of detrital feldspar grains (Fig. 42). The dissolution of feldspar was responsible for much of the secondary porostiy generated throughout the sandstone interval. Figure 43 shows a detrital feldspar grain being preferentially dissolved along its cleavage traces. Partial dissolution of feldspar was commonly observed, and accounts for the large amounts of microporosity. The scanning electron photomicrograph (Fig. 44) illustrates relict features of a partially preserved crystallographic planes, thus demonstrating a late stage diagenetic event. The preferential leaching of detrital feldspar grains appears to have been a function of the chemical and structural elements of the mineral as well as the ph of the pore fluids.

Precipitates

Silica

Precipitation of silica cement was recognized as an early diagenetic event. Silica precipitation commonly occurred as syntaxial quartz overgrowths on detrital quartz grains. Figure 45 is a scanning electron photomicrograph displaying euhedral quartz terminations growing into a preexisting pore space. The overgrowths serve as an effective binding mechanism for cementing the grains together. Figure 46 illustrates silica cement binding detrital quartz grains. The dust rims help to denote the original grain boundary. Because the original grains are

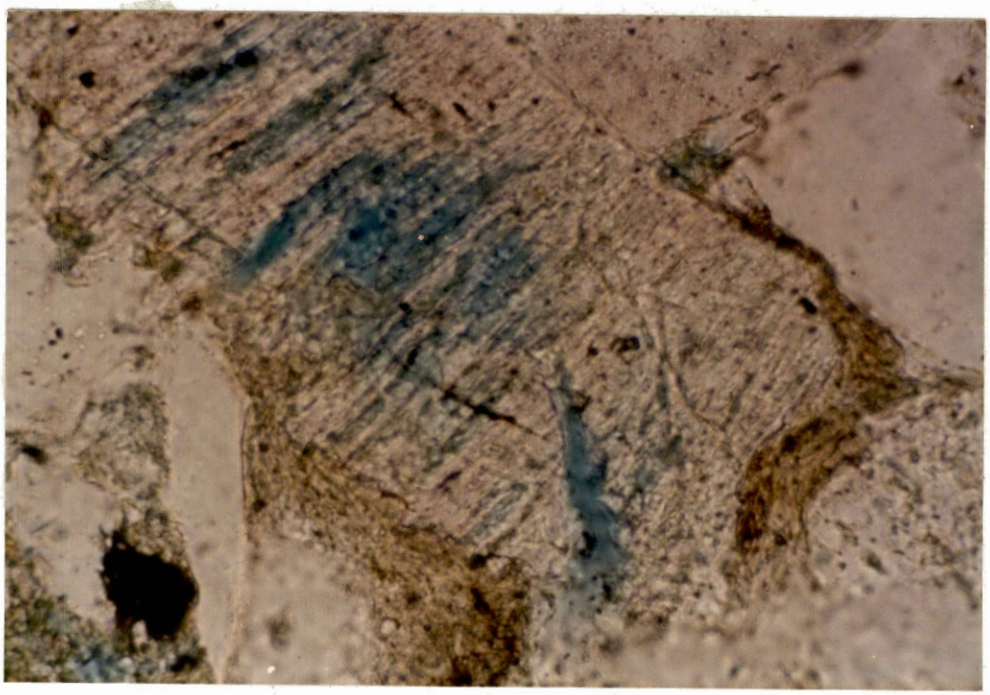

Fig. 42--Photomicrograph of partially dissolved detrital feldspar grain. Magnification 40X, Plane Polarized Light, Coe Bailey #1, Depth 4263.0'.

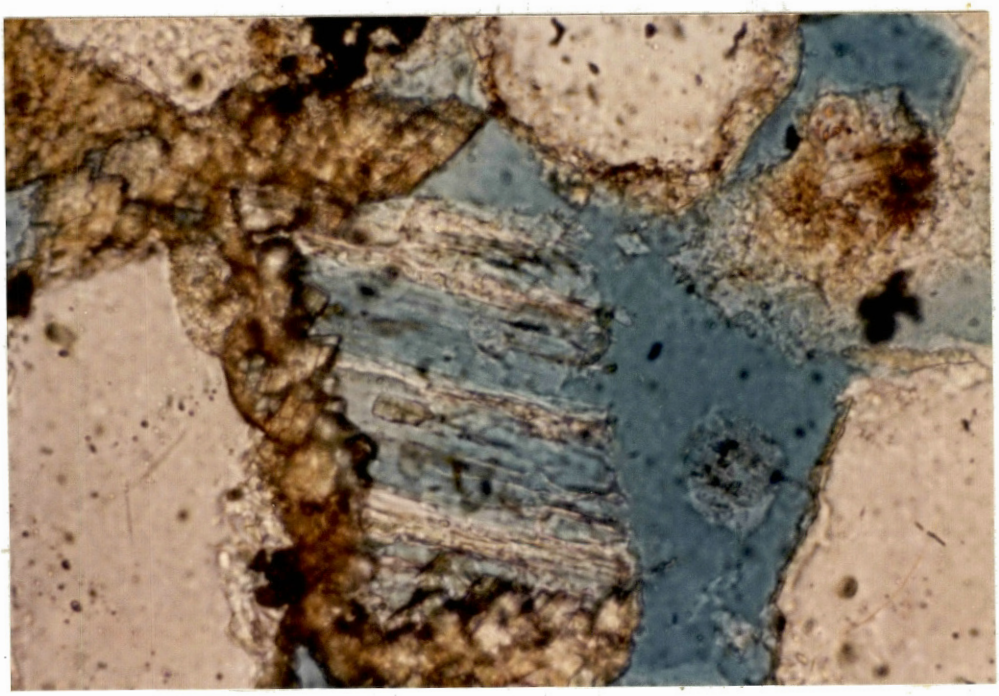

Fig. 43--Photomicrograph of a detrital feldspar grain showing preferential dissolution along cleavage traces. Magnification 40X, Plane Polarized Light, Coe Bailey #1, Depth 4213.3'.

Fig. 44--Scanning electron photomicrograph of a partially leached feldspar grain. Magnification 1600X, Coe Bailey #1, SEM, Depth 4223.2'.

Fig. 45--Scanning electron photomicrograph of euhedral quartz terminations. Magnification 2000X, SEM, Rhodd #1, Depth 4257.6'.

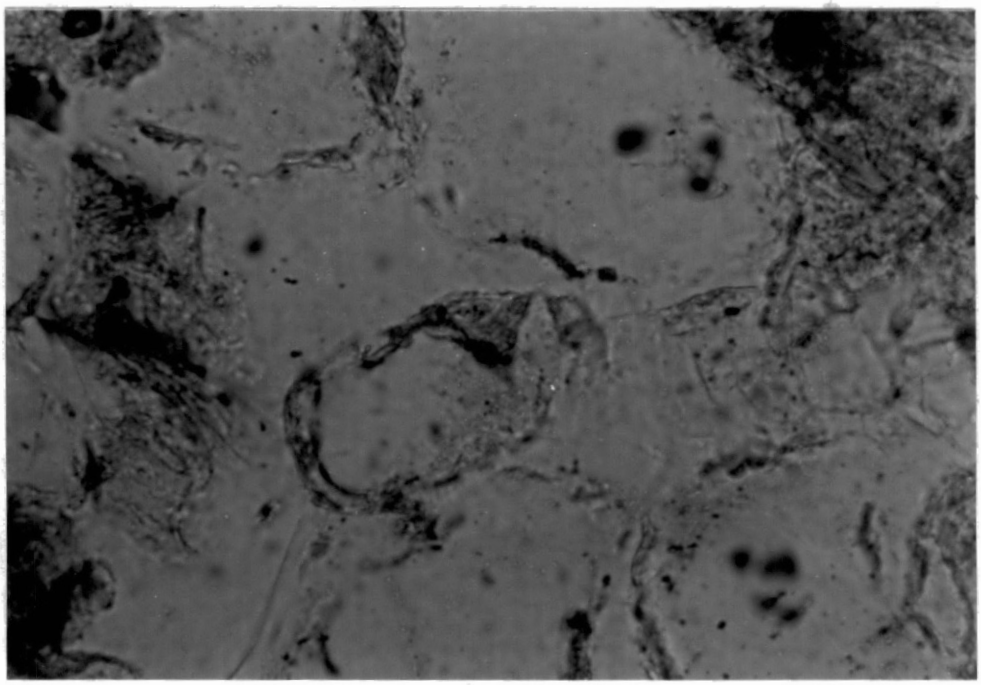

Fig. 46--Photomicrograph of silica cement binding detrital constituents. Note dust rims which delineate original grain boundaries. Magnification 40X, Plane Polarized Light, Rhodd #1, Depth 4248.4'.

not touching, the silica cement was believed to be void filling, and not the result of pressure solution. Figure 47 shows an irregular mossaic texture of detrital quartz grains exhibiting extensive silica diagenesis. The grains display irregular grain boundaries which were later extended by silica precipitation.

Detrital quartz grains and silica overgrowths display etching and corrosion locally, probably due to a change in pore fluid chemistry, from slightly basic to acidic. An acidic environment is conducive to the precipitation of silica, whereas a basic environment causes silica to go into solution. Figure 48 demonstrates the amount of corrosion of the quartz grains due to the precipitation of cabonate cement. Possible sources of silica include: hydrolysis of feldspar, alteration of clay minerals, precipitation from sea water, and pressure solution from silica rich minerals.

Carbonate

Thin section analysis indicates a general increase in carbonate cement as thick sequences of shale are approached. Compaction and dewatering of the shales is probably responsible for the subsequent release of the carbonate into the adjoining sandstone. This cement was effective in binding detrital constituents and reducing porosity, as shown in figure 48. Later stage diagenetic event however allowed for pore fluid chemistry to become slightly acidic. As the fluid became acidic it dissolved a portion of the carbonate cement,

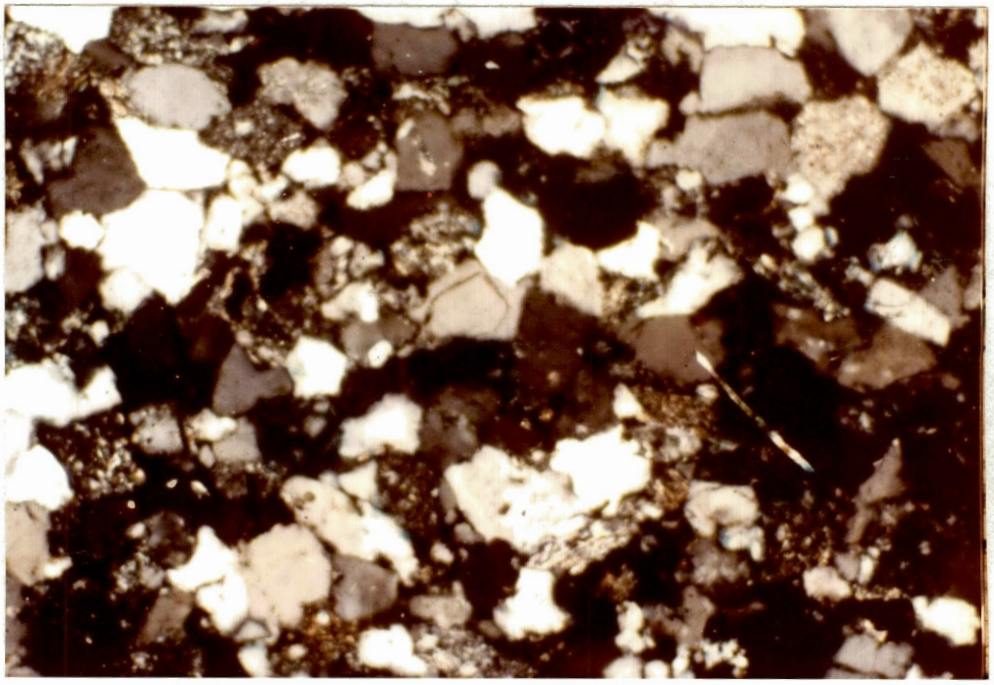

Fig. 47--Photomicrograph of detrital quartz grains showing an irregular mossiac texture due to severe silica diagenesis. Magnification 10X, Crossed Nicols, Rhodd #1, Depth 4248.4'.

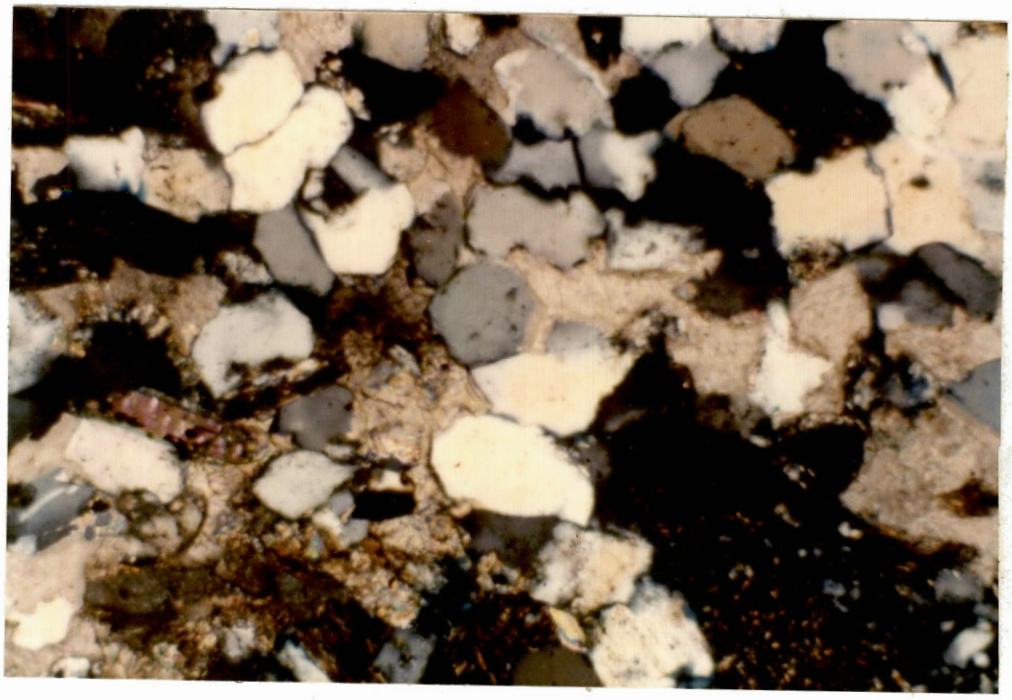

Fig. 48--Photomicrograph of carbonate cement effectively reducing porosity. Magnification 10X, Crossed Nicols, Rogers #2, Depth 3398.5'.

thereby creating porosity and enhancing permeability.

Carbonate cement is precipitated in basic solutions, and dissolved in acidic solutions. The inverse relationship exsists with reguard to the stability of silica constituents. Figure 48 demonstrates the corrosion of quartz overgrowths in association with carbonate cement. This textural relationship is common throughout the Red Fork sandstone.

Authigenic Clays

Three dominant types of authigenic clays were identified: (1) kaolinite, (2) illite, and (3) chlorite. Reduction of the porosity and permeability throughout the sandstone intervals is in part due to the precipitation of these authigenic clays. The clays were observed lining, filling, and bridging pore spaces and throats, which creates microporosity, decreases macroporosity, and lowers effective permeability.

Authigenic kaolinite was the dominant clay identified, and commonly occurred filling enlarged secondary pores (Figure 49). Because of authigenic kaolinite's occurrence and large crystal habit (pseudo-hexagonal booklets) (Fig. 5), it can pose a serious production problem. Figure 51 demonstrates the pore filling occurrence of authigenic kaolintie. The formation of kaolinite causes effective porosity to be reduced and creates microporosity.

Migration of fines is a production problem inherent to kaolinitic reservoirs. The problem is caused by high fluid turbulence, associated with completion and production techniques. The high rates cause the booklets to break off and

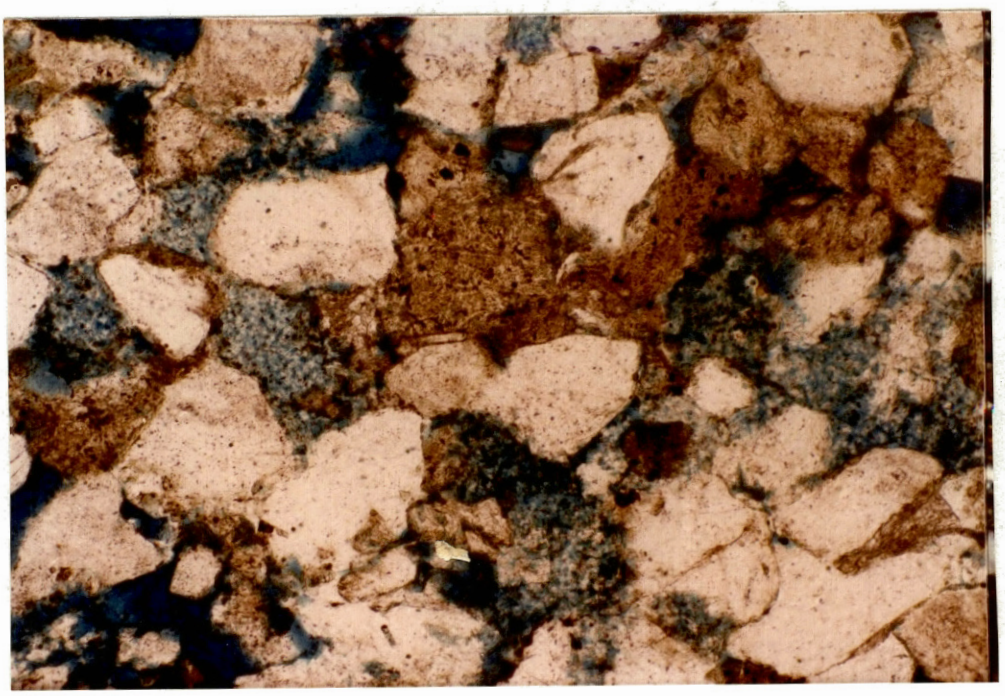

Fig. 49--Photomicrograph of authigenic kaolinite filling enlarged secondary pore spaces. Magnification 10X, Plane Polarized Light, Rogers #2, Depth 3416.8'.

Fig. 50--Scanning elctron photomicrograph of authigenic kaolinite. Magnification 1800X, SEM, Coe Bailey #1, Depth 4219.4'.

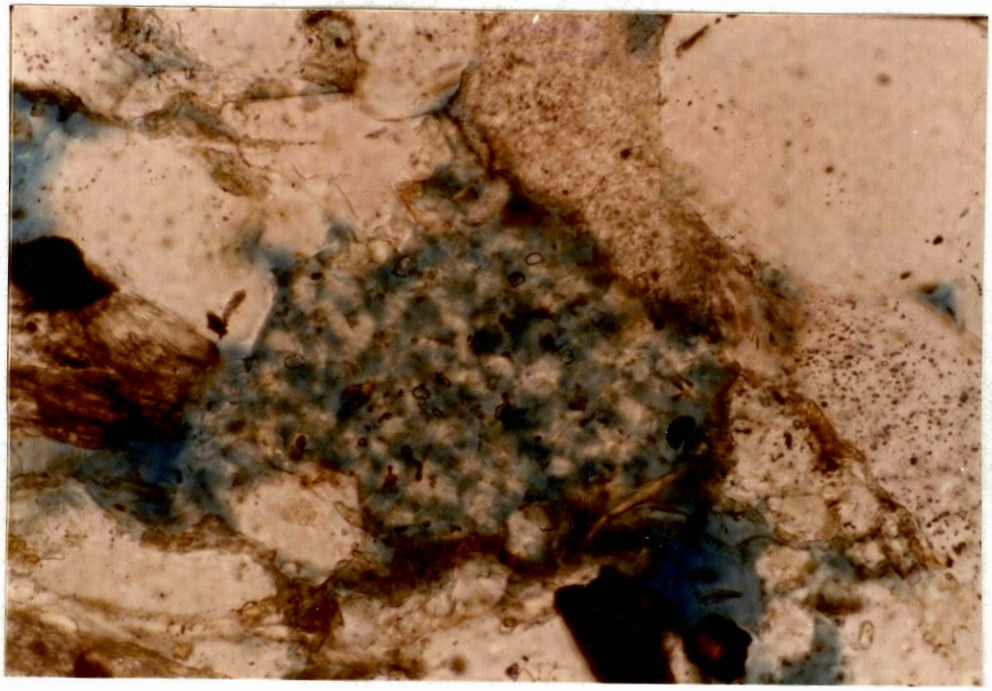

Fig. 51--Photomicrograph of authigenic kaolinite creating microporosity. Magnification 40X, Plane Polarized Light, Rogers #2, Depth 3321.2'.

migrate to the pore throats. The pore throats then become occluded and permeability is reduced. By using a variety of clay stabilization agents (polyhydroxy aluminum), and by decreasing production flow rates the problem can be diminished (Almon and Davies, 1978). However, these procedures should be carried out early in the history of the well, so that damage can be kept to a minimum and the reservoir be effectively produced.

Authigenic illite occurs in the Red Fork sandstone as either a pore lining or pore bridging hydrated silicate. Figure 52 illustrates the delicate crystal habit (lathe-like projections) and high surface area. Because of authigenic illite's morphology and occurrence, large amounts of microporosity have been created. The high surface area created by illite's crystal habit, causes free water to be bound to the clay surface. This phenomemon results in high irreducible water saturations. Pittman (1979) states that electric log calculations show water saturations too high, and permeability too low to produce hydrocarbons.

During high fluid turbulence, the delicate lathe-like projections tend to break off, clump together, and migrate to the pore throat. The pore throat becomes restricted and permeability is reduced. This problem can be avoided by using an oil base or potassium chloride mud during the drilling and completion of the well. However, if formation damage has already occurred, a weak mixture of hydrochloric acid initially, followed by a hydrofluoric solution can help to elevate the problem (Almon and Davies, 1978).

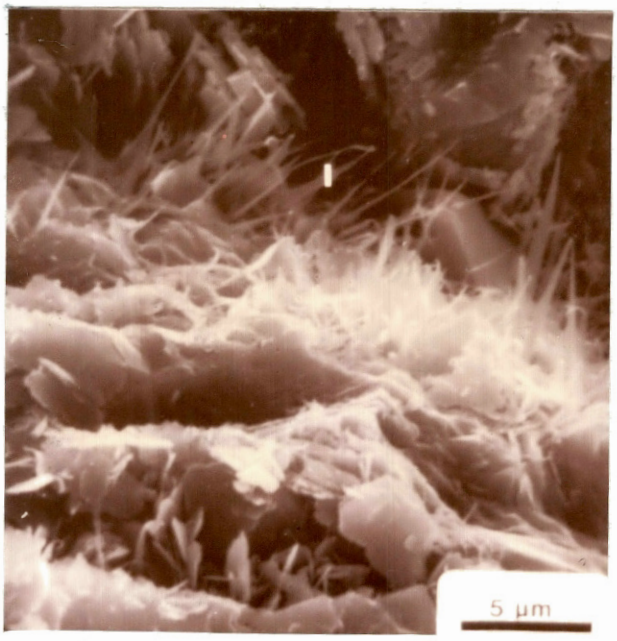

Fig. 52--Scanning electron photomicrograph of authigenic illite. Magnification 2000X, SEM, Coe Bailey #1, Depth 4267.4'.

Petrographic and scanning electron microscopy of the Red Fork sandstone reveals precipitation of authigenic chlorite. SEM analysis demonstrates that authigenic chlorite generally occurs as either a pore lining or pore filling clay. Figure 53 illustrates the edge to face crystal habit which is typical of authigenic chlorite. Figure 54 is a photomicrograph of authigenic chlorite rimming an enlarged secondary pore space.

Authigenic chlorite contains high amounts of iron and magnesium, which can be liberated when exposed to HCL acid. The iron ion is liberated and reprecipitated as ferric hydroxide ($Fe(OH)_2$), which forms large crystals. The formation of crystallin ferric hydroxide is effective in blocking or restricting pore throats, which can reduce the permeability of the producible horizon. The ferric hydroxide problem can be avoided if an oxygen scavenger and an iron chelating agent are used in combination with a mild acid. If damage to the formation has already occurred and ferric hydroxide has precipitated, removal can be enhanced by a mixture of (5%) HCL and (5%) HF acid, plus an iron chelating agent and a oxygen scavenger (Almon and Davies, 1978).

Alteration Products

Alteration products found within the Red Fork sandstone include authigenic clays, pyrite, and leucoxene. Dissolution of detrital constituents furnished the necessary chemical elements to form the alteration products.

Authigenic clays were an alteration product of the dissolution of detrital feldspars. The clays were identifed by

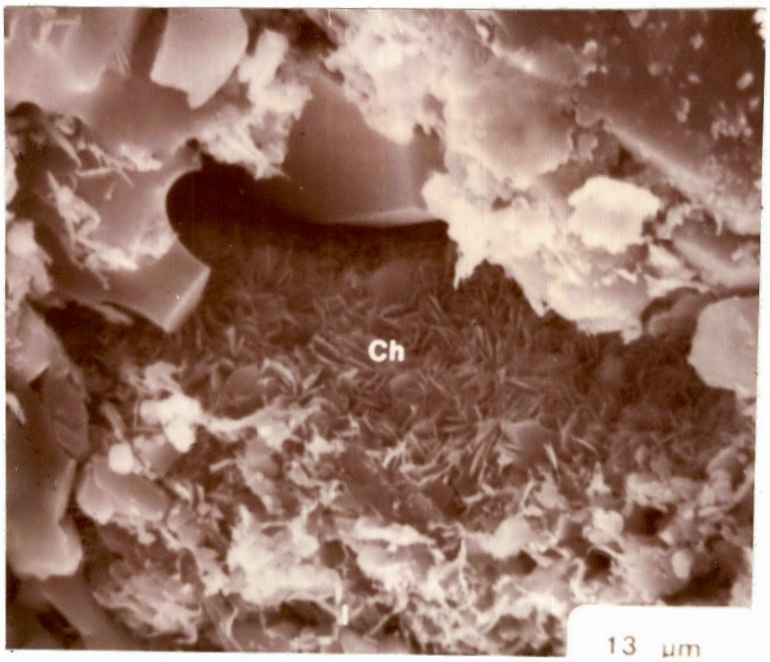

Fig. 53--Scanning electron photomicrograph of authigenic chlorite. Magnification 1700X, SEM, Coe Bailey #1, Depth 4243.3'.

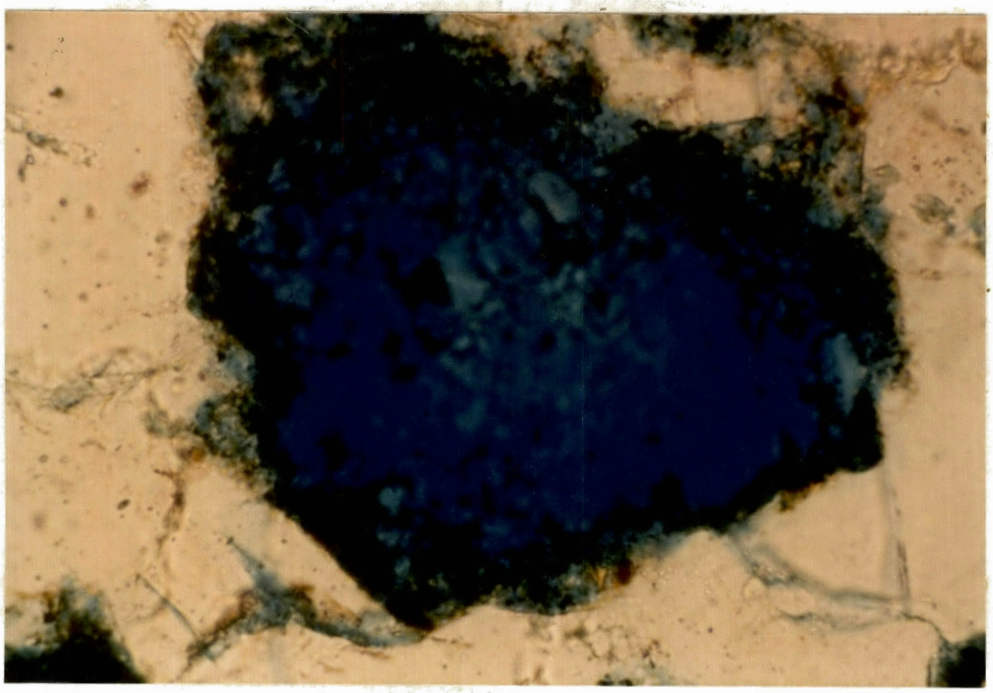

Fig. 54--Photomicrograph of authigenic chlorite lining a secondary pore space. Magnification 40X, Plane Polarized Light, Rhodd #1, Depth 4264.1'.

scanning electron microscopy, thin section analysis, and X-ray diffraction techniques. Figure 55 is an X-ray diffractogram of a typical specimen of Red Fork sandstone. The sample is the extracted clay size fraction, which was subjected to 500°C (heated for 30 minutes), glycolation, and natural states. These tests were run in order to positively identify the clay size fraction. The SEM and thin section photographs of the authigenic clays previously described illustrate their complex morphologies and occurrences. Their delicate crystal habit clearly indicates their in-situ generation. The following reactions help to explain the dissolution of feldspars to authigenic clays: (Al-Shaieb and Shelton, 1981, p.2436)

$$\underset{\text{K-feldspar}}{2KAlSi_3O_8} + 2H_2CO_{3aq} + 9H_2O = \underset{\text{Kaolinite}}{Al_2Si_2O_5(OH)_4} + 2K^+ + \underset{\text{Silicic Acid}}{4H_4SiO_4} + 2HCO_3^-$$

$$\underset{\text{K-feldspar}}{3KAlSi_3O_8} + 2H_2CO_3 + 2H_2O = \underset{\text{Illite}}{KAl_3Si_3O_{10}(OH)_2} + 2K^+ + \underset{\text{Silicic Acid}}{6H_4SiO_4} + 2HCO_3^-$$

Authigenic pyrite was observed throughout the Red Fork interval, as either highly disseminated framboidal pyrite or as an authigenic cement. Figure 56 is a microphotograph using reflected light in that the brassy luster of the disseminated pyrite could be displayed. The figure also shows minor amounts of leucoxene (off-white in color). Figure 57 demonstrates authigenic pyrite as a late stage diagenetic cement.

Leucoxene occurred sporadically and in trace amounts throughout the sandstone units studied. This alteration product was probably formed as the result of dissolution of feldspars

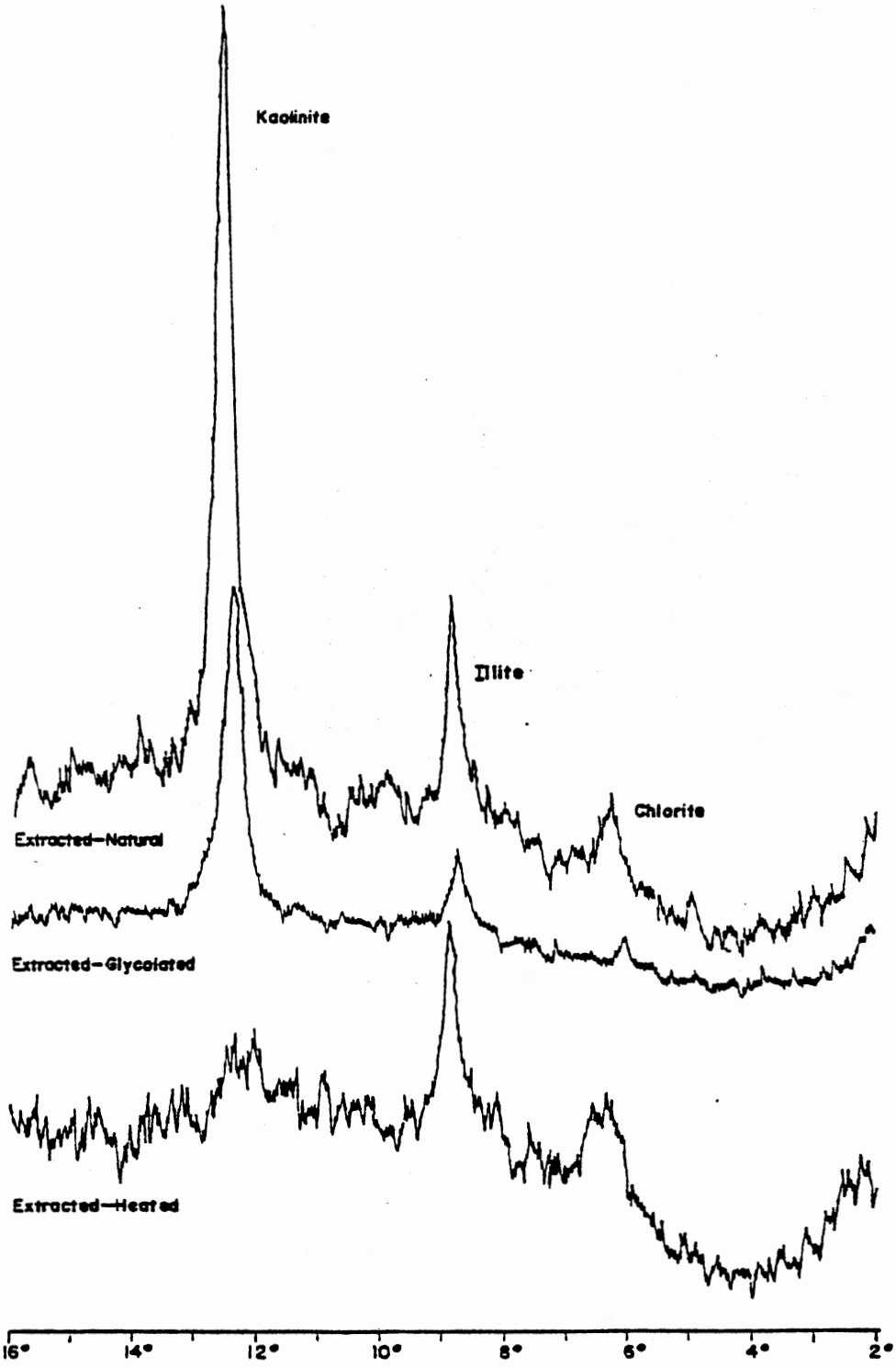

Fig. 55-- X-ray diffraction analysis of extracted clay fraction from Coe Bailey#1, Depth 4223.2'.

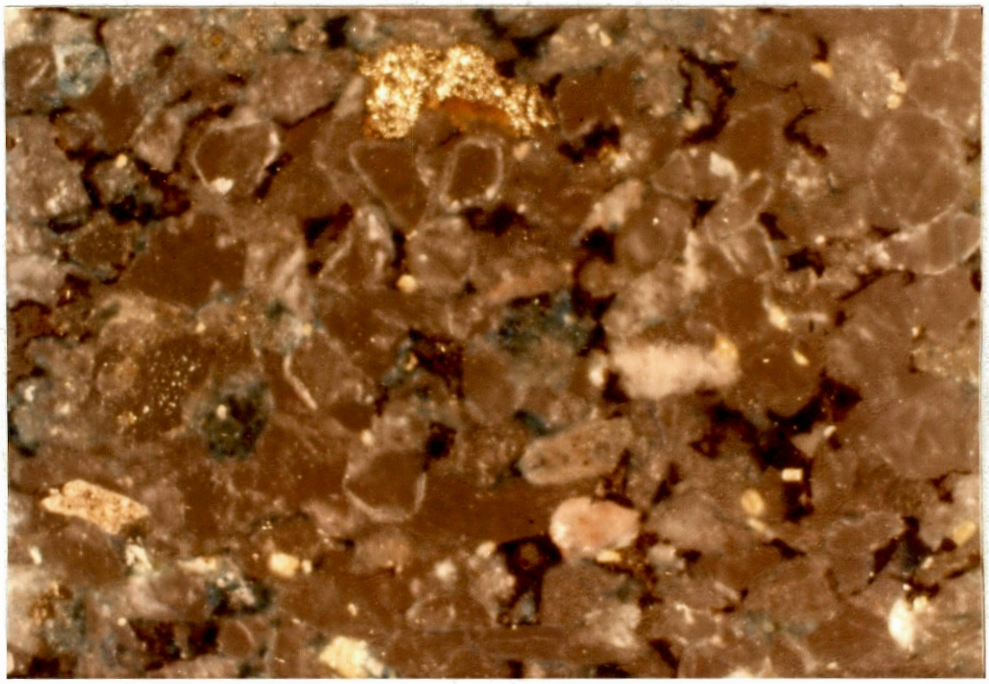

Fig. 56--Photomicrograph of authigenic pyrite (brassy yellow) and leucoxene (cotton wool-white). Magnification 10X, Reflected Light, Rhodd #1, Depth 4248.4'.

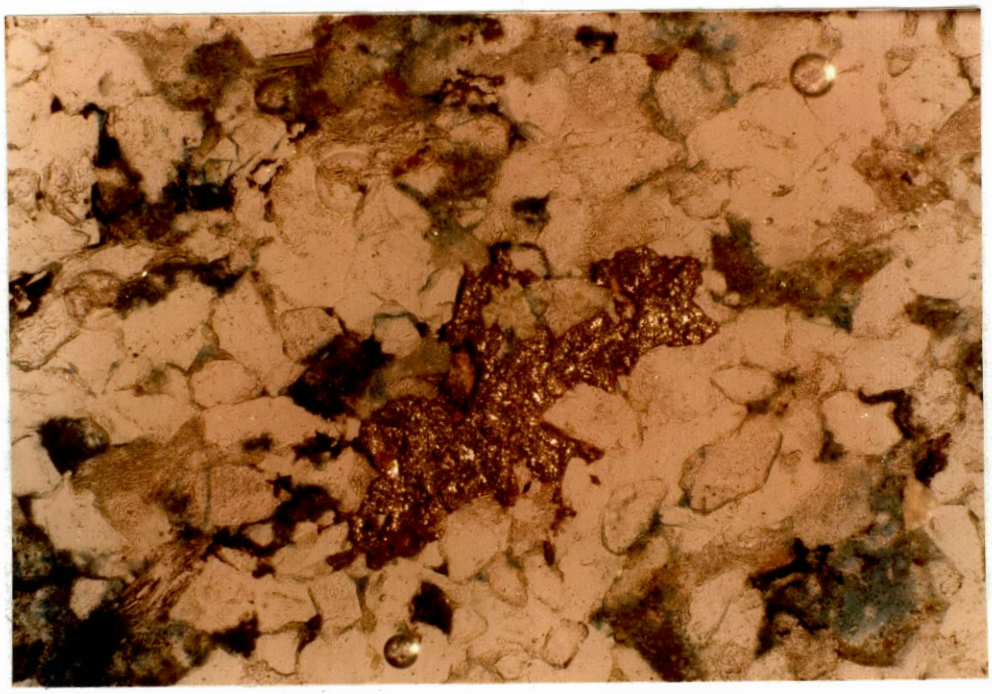

Fig. 57--Photomicrograph of authigenic pyrite cementing detrital constituents. Magnification 10X, Reflected Light, Rhodd #1, Depth 4248.4'.

and or titanium rich minerals. Figure 56 illustrates the sporadic appearance of leucoxene. Leucoxene appears white, like cotton wool in reflected light. The SEM and EDAX were used to show the morphology and relative chemical formula (Figs. 58 and 59).

Diagenetic History

Scanning electron microscopy and detailed thin section analysis were the basis for the interpretation and chronological sequence of the diagenetic events (Fig. 60).

Quartz overgrowths and silica cementation were the initial diagnetic events of the Red Fork sandstone. After the precipitation of silica, and increased burial, the ph of the pore fluids became slightly basic. Along with increasing temperature and lithostatic pressure, the carbonate cement was precipitated. The basic environment in which the carbonate cement was precipitated caused the corrosion and dissolution of the previously precipitated silica.

Dissolution of unstable detrital constituents (primarily feldspar) occurred as a result of the changing pore fluids. This diagenetic event was the most significant because of the generation of secondary porosity. Authigenic clays were probably formed during this period as a result of the dissolution of the unstable constituents. The authigenic clays precipitated are formed in a variety of chemical environments and therefore reflect the changing conditions of the pore fluids.

Hydrocarbon migration appears to have occurred during or

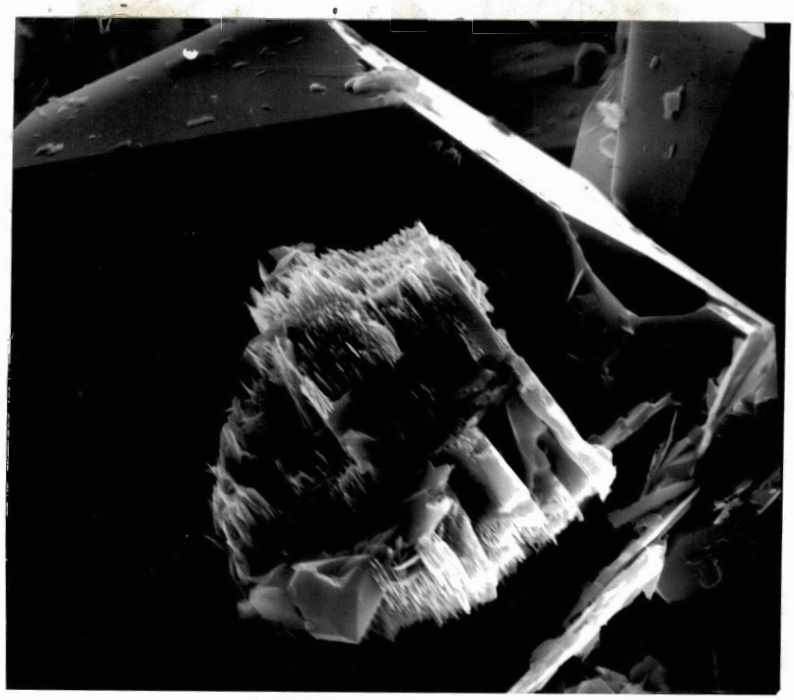

Fig. 58--Scanning electron photomicrograph of leucoxene. Magnification 2400X, SEM, Rogers #2, Depth 3409.0'.

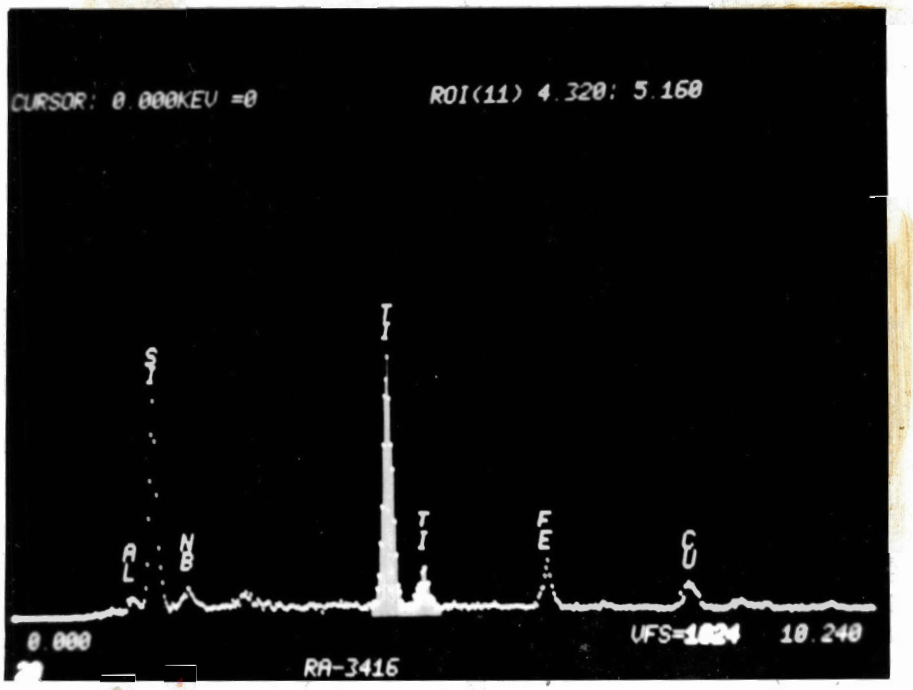

Fig. 59--Photograph of the EDAX showing the relative chemical composition of figure 58, (leucoxene). Magnification 1X, EDAX, Rogers #2, Depth 3409.0'.

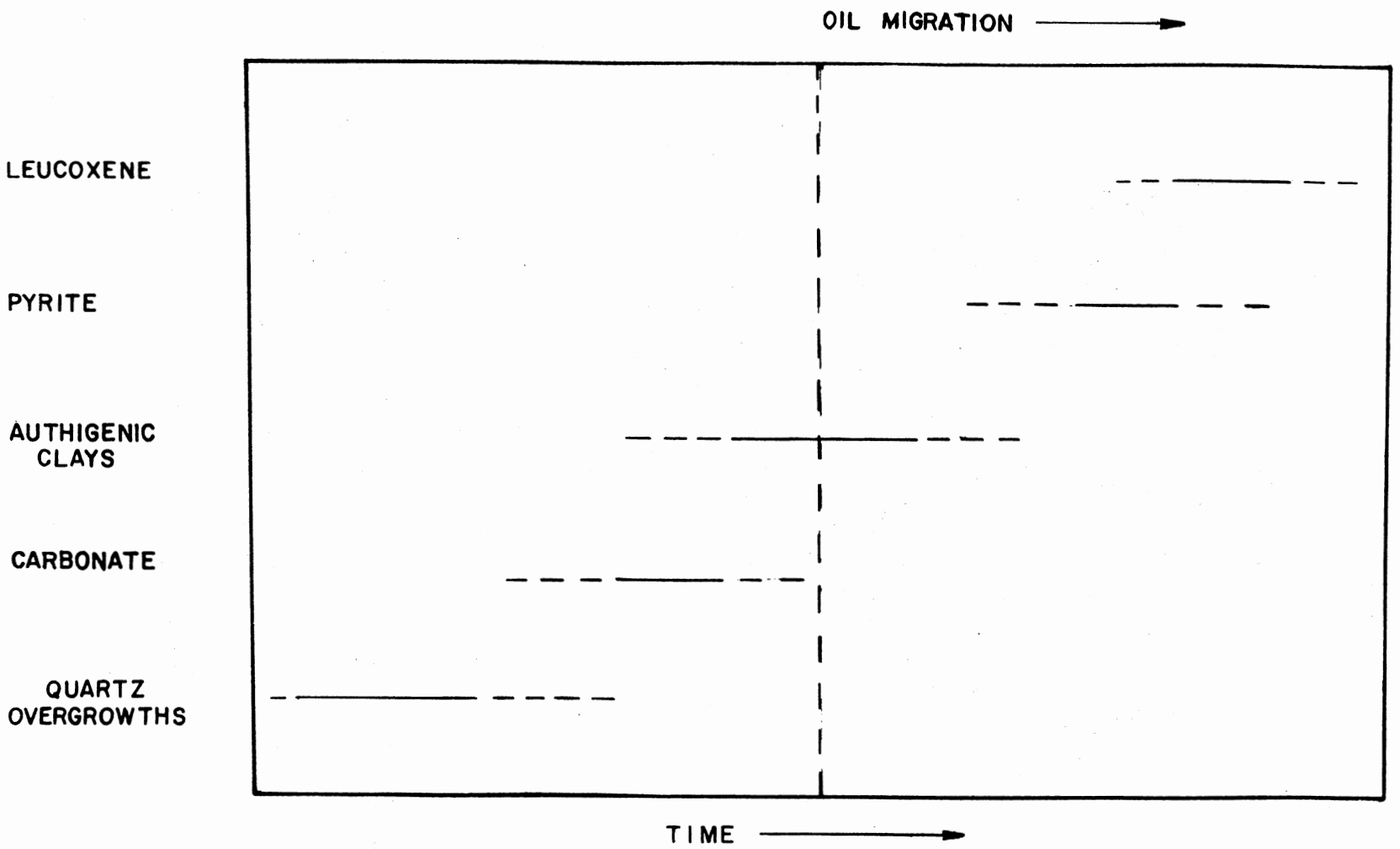

Fig. 60--Paragenetic sequence of the Red Fork sandstone.

shortly after the precipitation of the authigenic clays. The generation and migration of hydrocarbons probably supplied the necessary amount of hydrogen sufide to form authigenic pyrite.

The final diagenetic event of the Red Fork sandstone was the formation of leucoxene. This alteration product was probably formed by dissolution of titanium rich minerals.

CHAPTER X

BURIAL HISTORY AND HYDROCARON GENERATION

Introduction

The generation, migration, and entrapment of hydrocarbons in the Red Fork interval is believed to be a function of the depth of burial, regional tectonics, morphology and lithology of the reservoir. Temperature, lithostatic pressure, and time are important factors governing depth of burial. Regional tectonics assisted in the deposition and burial of the Red Fork. Later tectonic movement during the late Permian provided the mechanism for the migration and entrapment of hydrocarbons. Much of the Red Fork hydrocarbon accumulation is stratigraphically controlled in lenticular sand bodies of various shapes. Limitations on size and extent of sand lenses with good reservoir quality appears to be controlled by original lithology and subsequent diagenetic events. The foci of this chapter are to determine the maximum depth of burial of the Red Fork, to establish a relationship between the depth of burial and the generation of hydrocarbons, and to relate the effect of hydrocabon generation to the diagenetic events of the Red Fork.

Depth of Burial

Deposition of the Red Fork was succeeded by the burial of late Pennsylvannian and early Permian sediments. The increased depth of burial of the Red Fork was a result of continuous subsidence of the Arkoma Basin to the south of the study area. Maximum depth of burial is believed to have occurred during the close of the Permian. Maximum temperatures and pressures are assumed to have been acheived during maximum depth of burial. The present day geothermal gradient of 1.2^{o}C per 100 feet was used in the calculations, because of the relative stable conditions which have prevailed through the developement of the Cherokee Platform. Tissot and Welte (1978, p.514) state that, "Present and ancient geothermal gradients can be about the same in sedimentary basins where no tectonic or magmatic activity has been known since deposition of the potential source rocks." Consequently, vitrinite reflectance values obtained from the Red Fork should provide an accurate measure of the maximum temperature, degree of thermal maturation, and maximum depth of burial of the sediments. Hood (1975, p. 988) concluded that, "Probably one of the most useful measures of organic metamorphism is the reflectance of vitrinite." The most important parameters concerning vitrinite are the nature of the organic matter and the temperature verus time relationship.

Table I shows the mean vitrinite reflectance values and corresponding depths from which the samples were taken. The Cities Service Company, Rhodd #1 (depth 4271.3 feet) has a

TABLE I

VITRINITE REFLECTANCE VALUES FROM THE RED FORK INTERVAL

Red Fork Interval		
Well Name	Depth(feet)	Mean Vitrinite Reflectance Values(%)
Rhodd #1	4271.3'	1.67%
C.Bailey #1	4232.0'	0.95%
C.Bailey #1	4275.0'	0.91%
Rogers #2	3408.9'	0.89%

NOTE: Mean vitrinite reflectance value of the Cities Service Company, Rhodd #1, at a depth of 4271.3' was probably the result of recycled organic debris and was not used in calculating the maximum depth of burial for the Red Fork interval.

Analysis of the samples was preformed by Hagar Laboratories Inc., Denver Colorado.

An average vitrinite reflectance value from the three (3) samples calculated to 0.92%.

mean vitrinite reflectance value of 1.67%. This value is unusually high and was probably the result of recycled organic debris, and was not used in determining the maximum depth of burial. An average of the other vitrinite reflectance values yielded a mean of 0.92%. Figure 61 illustrates the relationship of vitrinite reflectance, to maximum temperature (T_{max}) verus effective heating time (t_{eff}). Hood (1975,p.988) describes effective heating time as, "the time (t_{eff}) during which a specific rock has been within 15°C (27°F) of its maximum temperature (T_{max}).". Using the previous information of effective heating time and a constant geothermal gradient of 1.2°C per 100 feet (1500ft. = 15°C x (100ft./1.2°C)) the combined effective heating time calculates to approximately 100 million years (or less). Maximum temperature of 115°C for the Red Fork interval was attained by using figure 61 (Hood, 1983), an effective heating time of 100 M.Y. and an average vitrinite reflectance value of 0.92%. Correction of the maximum temperature for average mean surface temperature decreases the maximum temperature to 100°C. The maximum depth of burial was determined by assuming a constant geothermal gradient of 1.2°C per 100 feet and a maximum temperature of 100°C, (100°C x (100ft./1.2°C)) = 8333 feet. The maximum depth of burial of the Red Fork interval was determined to be approximately 8300 feet.

Generation of Hydrocarbons

The generation of petroleum hydrocarbons from thermally reactive matter during burial is a part of the overall process

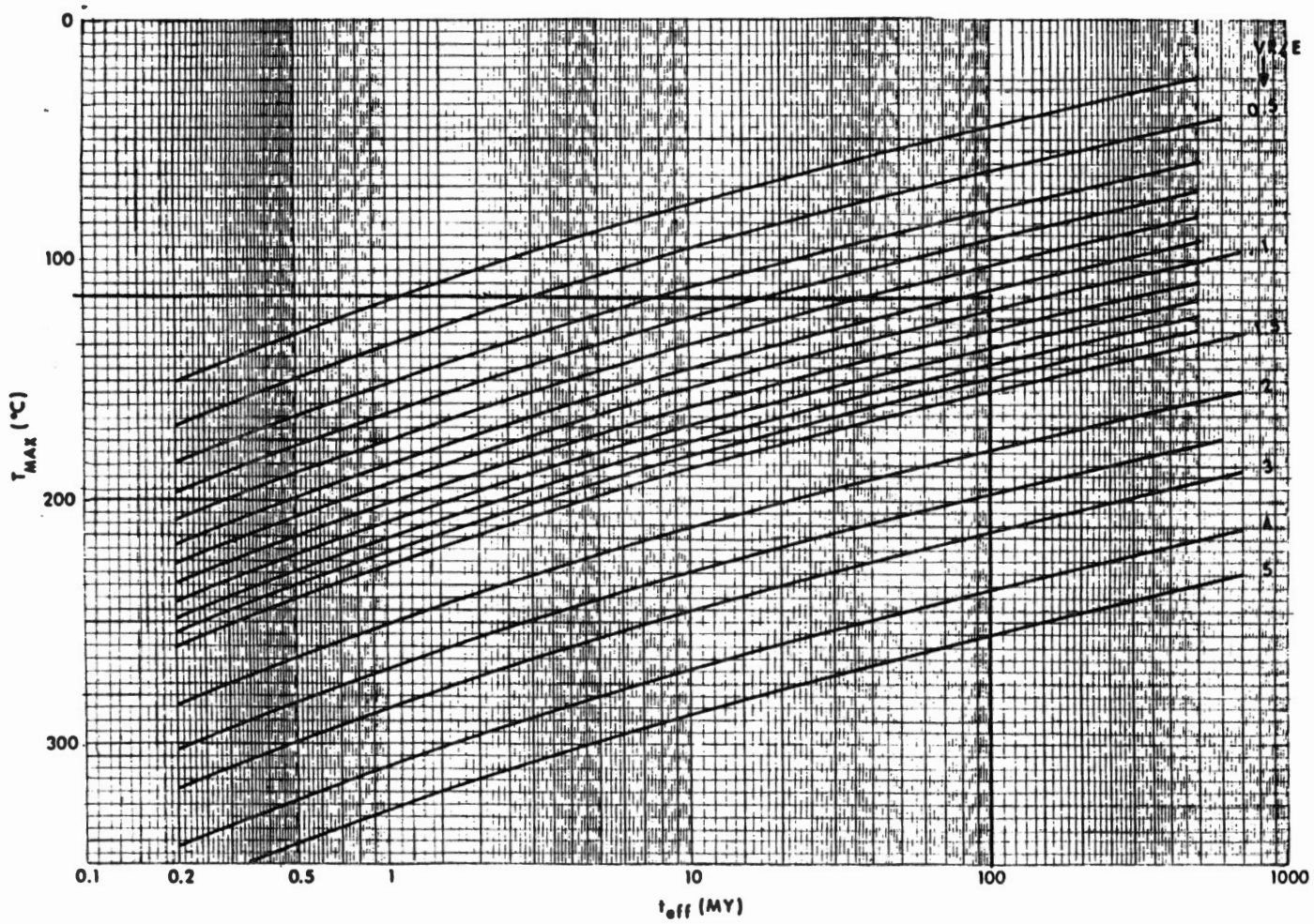

Fig. 61--Diagram depicting effective heating (t_{eff}) versus maximum temperature (T_{max}), (Hood, 1983).

of thermal metamorphism of organic matter. Hood (1975,p.988) states that, "Vitrinite reflectance is directly applicable to the study of temperature histories of source rocks.". The vitrinite reflectance data complied from the Red Fork was used to determine if hydrocarbons had been generated from Cherokee sediments. Generation of hydrocarbons was caused by the transformation of organic matter induced by the increased depth of burial. The threshold corresponding to the begining of significant oil generation varies with geothermal gradient, depth of burial, and duration of burial (effective heating time). The Red Fork sediments were buried to an approximate maximum depth of 8300 feet. This depth was sufficent to generate the necessary pressure and temperature to transform the organic matter to liquid hydrocarbons. Figure 62 illustrates the main stages of evolution of organic matter. By using figure 62 and a mean vitrinite reflectance value of 0.92% obtained from Table I, the main hydrocarbon generated should be oil. Baker (1962) concluded upon examination of the Cherokee sediments that the organic matter contained within the sediments was the source of oil found within the Cherokee reservoirs. Hatch and Leventhall (1982) derived that the organic matter from the black Cherokee shales is very similar to that of the Cherokee oils sampled. The work of these scientists coupled with the findings of this author infer that the Cherokee sediments were the source rocks for hydrocarbons found in the Cherokee reservoirs.

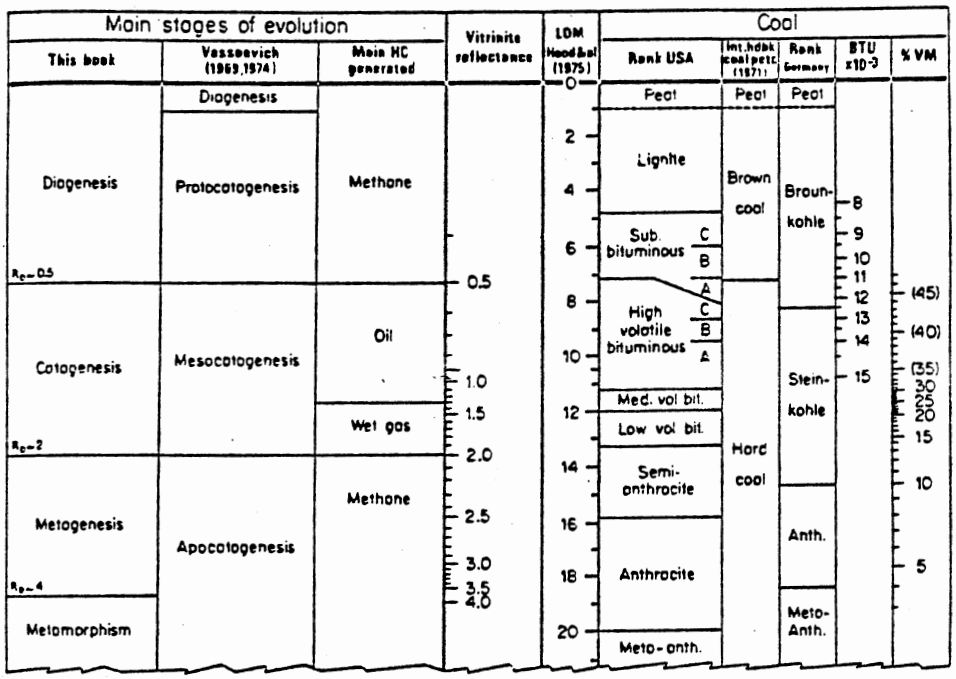

Fig. 62--Illustrates the main stages of evolution (Tissot and Welte, 1978, p. 71). Note the average vitrinite reflectance value was 0.92% and therefore the main hydrocarbon generated should be oil.

Diagenetic Affects Associated with Hydrocarbon Generation

Red Fork sediments were buried by late Pennsylvannian through early Permian sediments to a maximum depth of 8300 feet. The depth of burial was sufficent to generate the necessary pressures and temperatures to transform the organic matter to kerogen and eventually to oil. Figure 63 illustrates the possible modes of primary migration with respect to depth of burial (8300 feet or 2770 meters).

The transformation of organic matter to oil produces CO_2 (gas), H_2O (liquid), and some heavy heteratomic compounds as by-products. The CO_2 gas generated formed with existing pore fluids and created an acidic solution. The acidic pore fluids abetted in the dissolution of feldspar grains, which induced the generation of secondary porosity found throughout the Red Fork sandstone.

Red Fork reservoirs are elongate and or isolated lenses of sandstone, which lie essentially parallel to present day regional dip. Regional tilting during the Permian times facilitated the migration of hydrocarbons updip to the east, and into numerous stratigraphic pinchouts located within the Red Fork.

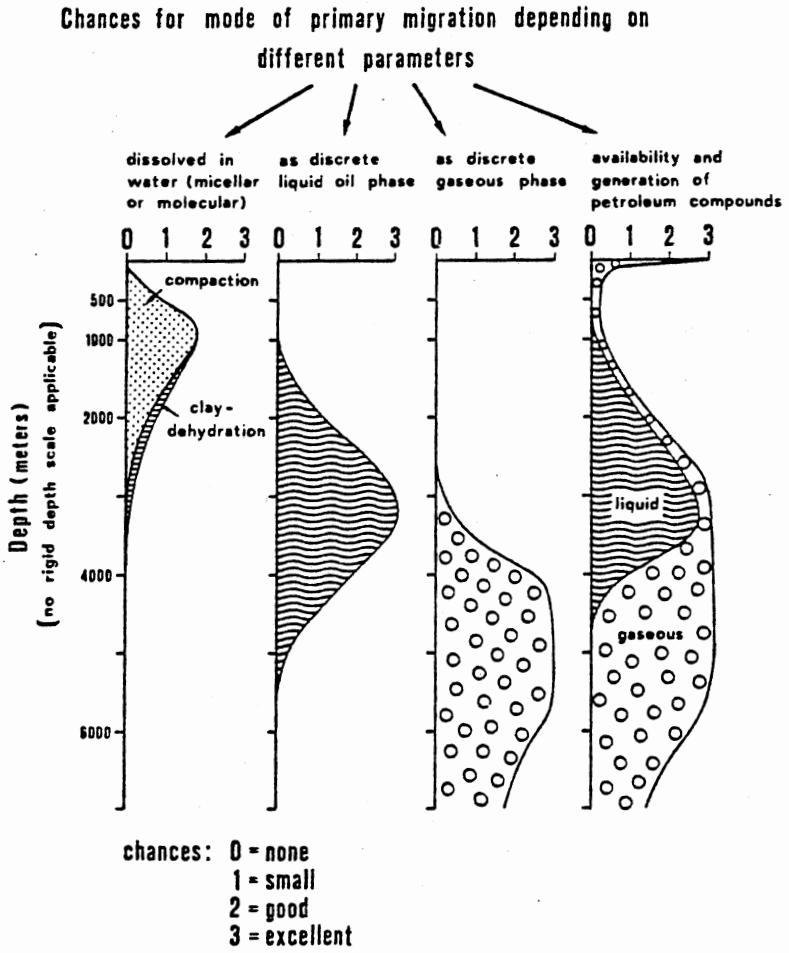

Fig. 63--Illustrates the possible modes of primary migration with respect to depth. Maximum depth of burial calculated to 8300 feet or approximately 2770 meters (Tissot and Welte 1978, p. 293).

CHAPTER XI

SUMMARY

Principle conclusions of this study are as follows:

(1) The Red Fork interval is a regressive deposit defined by two transgressive limestone marker beds. The base of the Pink Limestone defines the upper boundary, while the top of the Inola Limestone delineates the basal boundary of the Red Fork interval.

(2) Isolated absences of the basal Inola Limestone marker bed in areas where the Red Fork sandstone is present and the sharp basal and lateral contacts viewed in the stratigraphic cross sections is highly suggestive of cut-and-fill channel deposition.

(3) Red Fork isopach map and stratigraphic cross sections illustrate a gradual thickening of the interval to the south-southeast, indicating that the paleoslope and receiving basin were to the south-southeast during Red Fork time.

(4) Net-Sand map of the Red Fork sandstone reveals dominant north-south trends. These sand bodies are elongate and perpendicular to depositional strike.

(5) Vertical succession of sedimentary features viewed in each of the cores studied, coupled with the various maps and cross sections generated, supports the interpretation

that the Red Fork sandstone was deposited in a fluvial-deltaic environment.

(6) The Southern region of the study area contains multi-storied and multilateral sand deposits.

(7) The Pink Limestone structure map illustrates an approximate dip of 50 feet to the west.

(8) Petrologic classification of the cores described reveals the Red Fork sandstone of the Cities Service Company, Rhodd #1, and the Ames Oil and Gas Company, Rogers #2 to be a sublitharenite and the Earth Energy Resources, Inc., Coe Bailey #1 as a lithic arkose.

(9) Secondary porosity was the most common type of porosity recognized throughout the intervals studied. The complete and or partial dissolution of chemically unstable constituents (primarily detrital feldspar) was responsible for the generation of the large amounts of secondary porosity.

(10) Authigenic clays identified in the Red Fork sandstone include: kaolinite, illite, and chlorite. The precipitation of these authigenic clays was one of the primary factors which caused a reduction of the effective porosity and permeability.

(11) The paragenetic sequence of the Red Fork sandstone is as follows: 1) reduction of primary porosity and permeability by compaction and precipitation of silica cement initially followed by carbonate cement, 2) enhancement of porosity and permeability by dissolution of chemically unstable constituents (primarily detrital feldspar), 3) reprecipitation

of chemically stable authigenic constituents (primarily authigenic clays).

(12) Red Fork sediments were determined to achieved a maximum depth of burial of 8300 feet. This depth of burial was sufficent to generate the necessary pressure and temperature to transform the available organic matter to kerogen and eventually to oil.

BIBLIOGRAPHY

Almon, W. R., and D. K. Davies, 1977, "Understanding diagenetic zones vital": Oil and Gas Jour., p. 209-216.

Almon, W. R., and D. K. Davies, 1978, "Clay technology and well stimulation": Trans. Gulf Coast Assoc. Geol. Soc, v. 28, p. 1-6.

Al-Shaieb, Z., and J.W. Shelton, 1981, Migration of hydrocarbons and secondary porosity in sandstones: Am. Assoc. Petroleum Geologists Bull., v. 65, No. 11, p. 2433-2436.

Astarita, A. M., 1975, Depositional trends and environments of "Cherokee" sandstone, east-central Payne County, Oklahoma: Unpublished M.S. Thesis, Okla. State Univ., 54 p.

Baker, R. D., 1962, Organic geochemistry of the Cherokee Group in southeastern Kansas and northeastern Oklahoma: Am. Assoc. Petroleum Geologists Bull., v. 46, No. 9, p. 1621-1642.

Bass, N. W., 1934, Origin of Bartlesville shoestring sands, Greenwood and Butler Counties, Kansas: Am. Assoc. Petroleum Geologists Bull., v. 18, p. 1313-1345.

Bass, N. W., et. al., 1937, Origin and distribution of Bartlesville and Burbank shoestring oil sands in parts of Oklahoma and Kansas: Am. Assoc. Petroleum Geologists Bull., v. 21, No. 1, p. 30-66.

Benoit, E. L., 1957, The Desmoinesian Series, Edmond area, central Oklahoma: Okla. City Geol. Soc., Shale Shaker, v. 8, No. 3, p. 16.

Berg, O. R., 1969, Quantitative study of the Cherokee-Marmaton Groups, west flank of Nemaha Ridge, north-central Oklahoma: Okla. City Geol. Soc., Shale Shaker, v. 19, p. 94-110.

Bowman, E. A., 1956, The subsurface geology of southeastern Noble County, Oklahoma: Unpublished M.S. Thesis, Univ. Okla., 42p.

Branson, C. C., 1954, Field Conference on Desmoinesian Rock of north-eastern Oklahoma: Okla. Geol. Surv., Guidebook 11, 41 p.

Busch, D. A., 1959, Prospecting for stratigraphic traps: Am. Assoc. Petroleum Geologists Bull., v. 43, No. 12, p. 2829-2843.

Candler, C. E., 1976, Subsurface stratigraphic analysis of Prue, Skinner and Red Fork sandstones, southern Noble County Oklahoma: Unpublished M.S., Okla. State Univ., 49 p.

Choquette, P. W. and L. C. Pray, 1970, Geologic nomenclature and classification of porosity in sedimentary carbonates: Am. Assoc. Petroleum Geologists Bull., v. 54, p. 207-250.

Clayton, J. M., 1965, Paleodepositional environments of the "Cherokee" sands of central Payne County, Oklahoma: Okla. City Geol. Soc., Shale Shaker, v. 16, p. 50-66.

Clements, K. P., 1961, Subsurface study of the Skinner and Red Fork sand zones, (Pennsylvanian) in portions of Noble and Kay Counties, Oklahoma: Unpublished M.S. Thesis, Univ. Okla., 62 p.

Cole, J.G., 1969, Stratigraphic study of the Cherokee and Marmaton sequences, Pennsylvanian (Desmoinesian), east flank of the Nemaha Ridge, north-central Oklahoma: Okla. City Geol Soc., Shale Shaker, v. 19, p. 134-146, 150-161.

Dogan, N., 1970, Subsurface study of Pennsylvanian Rocks in east-central Oklahoma (From the Brown Limestone to the Checkerboard Limestone): Okla. City Geol. Soc., Shale Shaker, v. 20, p. 192-213.

Folk, R. L., 1968, Petrology of sedimentary rocks: Austin, Texas, Hemphills Book Store, 170 p.

Glass, J. L., 1981, Depositional environments, reservoir trends, and diagenesis of the Red Fork sandstone in Grant and eastern Kay Counties, Oklahoma: Unpublished M.S. Thesis, Okla. State Univ., 99 p.

Graves, J. M., 1955, Subsurface geology of a portion of Lincoln and Payne Counties, Oklahoma: Okla. City Geol. Soc., Shale Shaker, v. 6, p. 1-38.

Hatch, J. R. and J. S. Leventhall, 1982, Comparative organic geochemistry of shales and coals from Cherokee Group and lower part of Marmaton Group of Middle Pennsylvanian Age, Oklahoma, Kansas, Missouri, and Iowa: Am. Assoc. Petroleum Geologists Bull. (Abst.), v. 66, No. 5, p. 579.

Hawissa, I. S., 1965, Depositional environment of the Bartlesville, Red Fork, and the Lower Skinner sandstones in portions of Lincoln, Logan, and Payne Counties, Oklahoma: Unpublished M.S. Thesis, Univ. of Tulsa, 35 p.

Haworth, E., and M. Z. Kirk, 1894, A geologic section along the Noesho River from the Mississippian Formation of the Indian Territory to White City, Kansas, and along the Cottonwood River from Wyckoff to Peabody: Kansas Univ. Quart., v. 2, p. 105-106.

Hood, A., C. M. Gutjhar and J. L. Heacock, 1975, Organic metamorphism and the generation of petroleum: Am. Assoc. Petroleum Geologists Bull., v. 59, p. 986-996.

Hood, A., 1983, Personal communication through Dr. Zuhair Al-Shaieb.

Howe, W. B. 1956, Stratigraphy of Pre-Marmaton Desmoinesian (Cherokee) rock in southeastern Kansas: Kansas Geol. Surv. Bull. 123, p. 123-132.

Hudson, A. S., 1969, Depositional environment of the Red Fork and equivalent sandstones east of the Nemaha Ridge, Kansas and Oklahoma: Unpublished M.S. Thesis, Univ. of Tulsa, 80 p.

Hutchinson, L. L., 1911, Rocks asphalt, asphaltite, petroleum and natural gas in Oklahoma: Okla. Geol. Surv., Bull. 2, p. 230-260.

Jordan, L., 1957, Subsurface stratigraphic names of Oklahoma: Okla. Geol. Surv. Guidebook VI, 220 p.

Krumme, G. W., 1975, Mid-Pennsylvanian source reversal on the Oklahoma Platform: Unpublished Ph. D. Dissertation, Univ. of Tulsa, 1161 p.

Leatherock, C., 1937, Physical characteristics of Bartlesville and Burbank sands in northeastern Oklahoma and southeastern Kansas: Am. Assoc. Petroleum Geologists Bull. , v. 21, No. 2, 246 p.

Lowman, S. W., 1933, Cherokee structural history in Oklahoma: Tulsa Geol. Soc. Dig., v. 1, p. 31-34.

McElroy, M. N., 1961, Isopach and lithofacies study of the Desmoinesian Series of north-central Oklahoma: Okla. City Geol. Soc., Shale Shaker, v. 12, p. 2-22.

Oakes, M. C., 1953, Krebs and Cabaniss Groups of Pennsylvanian age in Oklahoma: Am. Assoc. Petroleum Geologists Bull., v. 37, p. 1523-1526.

Page, K. G., 1955, The subsurface geology of southern Noble County, Oklahoma: Okla. City Geol. Soc., Shale Shaker, v. 5, p. 5-22.

Pittman, E. D., 1979, Porosity, diagenesis, and productive capability of sandstone reservoirs: Soc. of Economic Paleontologists and Mineralogists, Special Pub. No. 26, p. 159-173.

Schmidt, V., D. A. McDonald, and R. L. Platt, 1977, Pore geometry and reservoir aspects of secondary porosity in sandstones: Bull. Canadian Petroleum Geol., v. 25, p. 271-290.

Scholle, P. A., 1978, A color illustrated guide to constituents, textures, cements, and porosities of sandstones and associated rocks: Am. Assoc. Petroleum Geologists, Memoir 28, 201 p.

Scott, J. D., 1970, Subsurface stratigraphic analysis, "Cherokee" Group northern Noble County, Oklahoma: Unpublished M.S. Thesis, Univ. Okla., 56 p.

Shipley, R. D., 1975, Local depositional trends of "Cherokee" sandstones Payne County, Oklahoma: Unpublished M.S. Thesis, Okla. State Univ., 49 p.

Stringer, C. P., 1957, Subsurface geology of western Payne County, Oklahoma: Okla. City Geol. Soc., Shale Shaker, v. 7, p. 3-20.

Tissot, B. P., and D. H. Welte, 1978, Petroleum formation and occurrence: Springer-Verlag, Berlin, 538 p.

Weirich, T. E., 1953, Shelf principle of oil origin, migration, and accumulation: Am. Assoc. Petroleum Geologists Bull., v. 37, No. 8, p. 2027-2045.

Wilson, M. D., and E. D. Pittman, 1977, Authigenic clays in sandstones: recognition and influence on reservoirs properties and paleoenvironmental analysis: Jour. Sed. Petrology, v. 47, p. 3-31.

Withrow, P. C., 1968, Depositional environment of the Pennsylvanian Red Fork sandstones in north-eastern Anadarko Basin, Oklahoma: Am. Assoc. Petroleum Geologists Bull., v. 52, No. 10, p. 198-205.

APPENDIX

No.	Operator and Well Name	Location
	East-West Stratigraphic Section A-A'	
253.	Smith & Cleary Co., Kihega #1	NW SW SW Sec. 7-T17N-R1E
252.	Vierson & Cochran, Cohee #1	NE SE SW Sec. 7-T17N-R1E
247.	Simon & Basset & W.H. Martgan, Lewis #1	NE SE SW Sec. 8-T17N-R1E
244.	Century Drilling Co., Cundiff #1	SW NE SW Sec. 9-T17N-R1E
*241.	Josaline Production Co., Bostlain #1	NW SW SW Sec.10-T17N-R1E
237.	The Texas Co., J.S. Graham #2	E/2SE SE Sec.11-T17N-R1E
218.	The Texas Co., L.M. Graham #4	EL SE SW Sec.12-T17N-R1E
72.	Four States Oil & Gas Co., McCarty #A-1	SE SE SW Sec. 7-T17N-R2E
68.	Federal Petroleum Co., Mileham #1	C SE SW Sec. 8-T17N-R2E
*67	Service Drilling Co., Wall #1	C SW SW Sec.10-T17N-R2E
54.	Anderson Oil & Gas Co., Emma Kent #1	C NE NE Sec.15-T17N-R2E
62.	Federal Petroleum, Inc., Bailey #1	NE NE SW Sec.11-T17N-R2E
66.	Earth Energy Resources, Inc., Coe Bailey #1	NW NW SE Sec.11-T17N-R2E
64.	Pace Petroleum Co., Johnson#1	NW NE SE Sec.11-T17N-R2E
58.	Fred Schonwald, Porter #1	NW NW SE Sec.12-T17N-R2E
	East-West Stratigraphic Section B-B'	
295.	Derby Oil Co., Pershing #1	SE SE NW Sec.19-T18N-R1E
294.	An-Son Petroleum Co., Goodman #1	SW SW NE Sec.20-T18N-R1E
290.	Blackwell Oil& Gas Co., Knight #1	SW SW NE Sec.21-T18N-R1E
289.	Blackwell Oil & Gas Co., Van Brunt #1	SE SE NW Sec.21-T18N-R1E
*285.	Kingwood Oil Corp., Roy E. Downey #1	NW NW NE Sec.22-T18N-R1E

* DENOTE TIE WELLS

Continuation of Section B-B'

284.	Five Star Drlg. Co., Eckert#1	NE NE SW	Sec.24-T18N-R1E
282.	W.H. Martgan, Maguire #4	SW NE SE	Sec.24-T18N-R1E
341.	N.B. Hunt, Higgins #1-B	NE SE SW	Sec.19-T18N-R2E
339.	Massey & MOOre, Poling #1	NE NW SE	Sec.20-T18N-R2E
*337.	Service Drlg. Co., Wolfe #1-21	C NW SE	Sec.21-T18N-R2E
338.	Royal Oil & Gas Co., Kinzie#1	SE NE SE	Sec.21-T18N-R2E
336.	Francis Oil & Gas, Inc., Ross#1	NE NE SE	Sec.22-T18N-R2E
334.	Oklahoma Natural Gas Co., Marshall #1	SW SW SE	Sec.24-T18N-R2E

East-West Stratigraphic Section C-C'

433.	D. & L. Oil Co., U.S. Gov't #1	SW SW NE	Sec.19-T19N-R1E
425.	Dirickson & Lewis, Kern #1	SW SW NW	Sec.29-T19N-R1E
424.	Lawson Petroleum Co., Darby #1	NE NE NW	Sec.29-T19N-R1E
431.	Don Johnson Drlg. Co., McClure #1	SE NW SE	Sec.21-T19N-R1E
*426.	T.N. Berry & Co., McQuain #1	SE SE NW	Sec.27-T19N-R1E
427.	T.N. Berry & Co., George Caukins, Harrow #1	SW SW SW	Sec.26-T19N-R1E
420.	Ketal Oil Prod. Co., Super Bird #1	C NW NE	Sec.36-T19N-R1E
419.	Zephyr Drlg. Co., Stateland #1	SE NE NE	Sec.31-T19N-R1E
393.	Delta Petroleum Corp., Rein #1	SE NE NE	Sec.31-T19N-R2E
*388.	Delta Petroleum Corp., Lester #1	SW NW NW	Sec.32-T19N-R2E
394.	The Texas Co., L.R. Andrews #1	SE SW SE	Sec.28-T19N-R2E
397.	Mitchell & Gauge, Rist #1	SE SW SW	Sec.27-T19N-R2E
399.	T.N. Berry, Patco, W.W. Wolf, Teleford #1	SE SW SW	Sec.25-T19N-R2E

*DENOTES TIE WELL

East-West Stratigraphic Section D-D'

451.	Tennessee Transmission Co., Nora Elgin #4	NE NE NW Sec.19-T20N-R1E
456.	Wilcox Oil Co., Bower #2	SW SW SE Sec.17-T20N-R1E
*458.	Bonray, Rupp #1	C NE SW Sec.15-T20N-R1E
460.	White Shield Oil & Gas Corp., Spillman #1	C SW NW Sec.13-T20N-R1E
488.	Falcon Seaboard Drlg. Co., Downey #1	NE NE SW Sec.17-T20N-R2E
489.	T.W. & J.M.Loffland Jr., State #2	SW SW SW Sec.16-T20N-R2E
*486.	L.B.Jackson Co., Ritter #1	NW NW SW Sec.22-T20N-R2E
485.	Vulcan Energy Corp., Wheatley #1	SE NW SE Sec.23-T20N-R2E
484.	H.E.R. Drlg. Co., R. Peterka #1	NE NE NE Sec.24-T20N-R2E

East-West Stratigraphic Section E-E'

526.	Pipeline Service Co., Detwielder #1	NE NE SW Sec.18-T21N-R1E
527.	Dirickson & Lewis Drlg. Co., Bamberger #1	SE SE SE Sec.18-T21N-R1E
521.	Harry J. Schafer, Tapps #1	NE NE NE Sec.29-T21N-R1E
*524.	Charles R. Bale & Assoc., Wallerstedt #1	C SW NW Sec.27-T21N-R1E
525.	Watchorn Oil & Gas Co., Hirschman #1	SW NW NE Sec.25-T21N-R1E
499.	Baruch & Foster Corp., Ritthaler #1	NE NE SW Sec.29-T21N-R2E
*500.	Jones Shelburne & Pellow & Humprey Oil, Sherrard #1	SW SW SE Sec.28-T21N-R2E
501.	Shippers Warehouse, Schwaltz #1-A	SW SE NW Sec.24-T21N-R2E

*DENOTES TIE WELL

East-West Stratigraphic Section F-F'

549.	United States Smelting, Refining & Mining Co., Sunray Grant #1	SW SE NW	Sec.19-T22N-R1E
548.	Gene Graham Drlg. Co. Foster #1	NE NW SW	Sec.20-T22N-R1E
547.	The Wil-Mc Oil Co.,Loula #2	NW SW SW	Sec.21-T22N-R1E
*544.	Hanlon-Bolye,Inc., L.Wentz #1	SW NE NW	Sec.27-T22N-R1E
545.	Halliburton Oil Producing Co., Black #1	SW NW SW	Sec.26-T22N-R1E
546.	W.R.Yinger, Johnson #1-A	SE SW NE	Sec.25-T22N-R1E
573.	W.F.Eppler, Clifton #1	SW SW NE	Sec.29-T22N-R2E
*574.	D.&L. Oil Co., Marshall #1	NE NE NE	Sec.28-T22N-R2E
577.	C.W.Dobson Oil Co., Mashletter #1	NW SE NE	Sec.24-T22N-R2E

East-West Stratigraphic Section G-G'

644.	Central Oil Co., Harriett #1	SW SW SW	Sec. 7-T23N-R1E
631.	Sam Mizel, Main #1	NW NW NE	Sec.18-T23N-R1E
632.	Phillips Petroleum Co., Foreman #A-1	SW SE NW	Sec.16-T23N-R1E
635.	Continental Oil Co., Sammuel Ellis #1	NW NW SE	Sec.16-T23N-R1E
633.	Continental Oil Co., Dupee #1	SW NE SE	Sec.16-T23N-R1E
*624.	Sundance Energy Corp., Donahoe #1	NW NW NE	Sec.23-T23N-R1E
601.	Roy G. Woods, Pipestem #1	SW SW NE	Sec.19-T23N-R2E
596.	Sunray Mid Continent Oil Co., Williams #1	NE NE NW	Sec.29-T23N-R2E
*597.	La Gorce Oil Co., Peters #1	NW SE NW	Sec.27-T23N-R2E
598.	B.B.Blair, etal., Treeman #1	NW NW NE	Sec.24-T23N-R2E

*DENOTES TIE WELL

North-South Stratigraphic Section H-H'

672.	Javelin Oil Co., Hon #1	NW NW NW Sec. 2-T23N-R1E
640.	B.B.Blair, Selby #1	SW SW NE Sec.10-T23N-R1E
624.	Sundance Energy Corp., Donahoe #1	NW NW NE Sec.23-T23N-R1E
*612.	Russell Cobb Jr., Joe Sewell #1	SE NW NW Sec.35-T23N-R1E
564.	Russell Cobb Jr. Inc., Gerken #1	SW SE SE Sec. 3-T22N-R1E
557.	Blackwell Oil & Gas Co., Pfrimmer #1	NW NW SE Sec.10-T22N-R1E
551.	Summit Drlg. Corp., Pfrimmer #1	NW NW NE Sec.15-T22N-R1E
*544.	Hanlon-Bolye, Inc., L. Wentz #1	SW NE NW Sec.27-T22N-R1E
532.	Shebester, Inc., Reim #1	C SW NW Sec. 3-T21N-R1E
*524.	Charles R. Bale & Assoc., Wallerstedt #1	C SW NW Sec.27-T21N-R1E
517.	Western Pacific Petroleum, Zemp #1-34	E/2SW NW Sec.34-T21N-R1E
472.	Wilcox Oil Co., Johnson #1	NE NE SE Sec. 3-T20N-R1E
*458.	Bonray, Rupp #1	C NE SW Sec.15-T20N-R1E
448.	Publishers Petroleum, Meager #1	C NW SE Sec.22-T20N-R1E
447.	Wilcox Oil Co., Hopkins #1	SE SW SE Sec.27-T20N-R1E
444.	Shell Oil Co. & Wilcox Oil Co., Mary Fillmore #1	NW NW SE Sec.34-T20N-R1E
441.	Dave Morgan, Eades #1	C SE NW Sec.11-T19N-R1E
435.	Ketchum-Whan Drlg. Co., Correll #1	SW SW NE Sec.15-T19N-R1E
*426.	T.N.Berry & Co., McQuain #1	SE SE NW Sec.27-T19N-R1E
422.	T.N.Berry & Co., Oldham #1	SW SW NW Sec.34-T19N-R1E
305.	Davidor & Davidor, U.S.A. #1	NW NE NE Sec.10-T18N-R1E
*285.	Kingwood Oil Corp., Roy E. Downey #1	NW NW NE Sec.22-T18N-R1E
275.	Co-op Refg. Assoc., Wetzel #1	SW SE NW Sec.27-T18N-R1E
270.	Russell Cobb Jr., Frank Phillips #1	SW SE SW Sec.27-T18N-R1E

*DENOTES TIE WELL

Continuation of Section H-H'

242.	Baker & Mundy Drlg. Co.; Basin Oil Co., Longan #1	NW NW NE Sec.10-T18N-R1E
*241.	Josaline Prod. Co., Bostian #1	NW SW SW Sec.10-T17N-R1E
206.	D.F.O'Rourke, State #1	NE NE SE Sec.16-T17N-R1E
177.	Robert Jordan, Campbell #1	NW NW NW Sec.22-T17N-R1E
176.	Gulf Oil Corp., Wilkes #1	SW SW NW Sec.22-T17N-R1E
118.	J.C.Catlett, Clemment #1	NE NE NE Sec.28-T17N-R1E
117.	W.F.Catlett, Woods #1	SE SW SE Sec.28-T17N-R1E
107.	Woods Drilling Co., Webber #1	SW NW SE Sec.33-T17N-R1E

North-South Stratigraphic Section I-I'

610.	Salt Fork Producers, Inc., Otoe School Reserve #1	N/2NE SE Sec. 3-T23N-R2E
606.	Woods Petroleum Corp., Otoe #1	NE SE NE Sec. 9-T23N-R2E
600.	Deep Rock Oil Corp., Black-hawk #1	NW NW NE Sec.21-T23N-R2E
*597.	La Gorce Co., Peters #1	NW SE NW Sec.27-T23N-R2E
594.	Edward P. Baker, Shultz #1	NE NE NW Sec.34-T23N-R2E
592.	Beach & Talbot, Greenshields #1	NW NW SW Sec. 3-T22N-R2E
591.	Derrick Oil Supply Co., Schultz #1	SW NW SE Sec. 9-T22N-R2E
*574.	D & L Oil Co., Marshall #1	NE NE NE Sec.28-T22N-R2E
567.	Sterling Oil of Oklahoma, Inc. Pancoast #1	SW SW NE Sec.33-T22N-R2E
516.	Red Patton Drlg. & G.A.Brown, Scott #1	NE NE SE Sec. 5-T21N-R2E
505.	Big Four Petroleum Co., State -Chessmore #1	NE NE NW Sec.16-T21N-R2E
*500.	Jones Shelbourne & Pellow & Humprey Oil, Sherrard #1	SW SW SE Sec.28-T21N-R2E
493.	T.N.Berry & Co., Earle White #1	SW SW NW Sec.10-T20N-R2E
*486.	L.B.Jackson Co., Ritter #1	NW NW SW Sec.22-T20N-R2E
475.	Wilcox Oil Co., Thompson #1	NW SE NW Sec.33-T20N-R2E

*DENOTES TIE WELL

Continuation of Section I-I'

418.	J.H.Tomlinson, Willman #1	NE	SE	NW	Sec. 4-T19N-R2E
416.	Beard Oil Co., Longan-Daugherty #1	C	NE	SE	Sec. 8-T19N-R2E
412.	Texan Oil Co., Heid #1	SW	NE	SW	Sec.17-T19N-R2E
407.	Fred P. Schowald, Murphy #1	SW	NE	SW	Sec.20-T19N-R2E
*388.	Delta Petroleum Corp., Lester #1	SW	NW	NW	Sec.32-T19N-R2E
389.	Blackwell Oil & Gas Corp., French #1	NW	NW	SW	Sec.32-T19N-R2E
373.	Ketal Oil Producing Co., Driggs #1	NW	NW	SE	Sec. 5-T18N-R2E
363.	The Texas Co., Carl Wetzel #1	SE	NE	SW	Sec. 9-T18N-R2E
347.	Fred Jones Engineering, Schoolland #1	C	NE	SW	Sec.16-T18N-R2E
*337.	Service Drlg.Co., Wolfe #1-21	C	NW	SE	Sec.21-T18N-R2E
329.	Rogers-Fain Drlg. Co., Blumer #1	SW	SW	SE	Sec.28-T18N-R2E
321.	B.M.Heath, J.C.Dudley & B.K. Leach,Downey #1	SE	SE	NE	Sec.33-T18N-R2E
*67.	Service Drlg. Co., Wall #1	C	SW	SW	Sec.10-T17N-R2E
55.	F.P Menager & Portable Drlg. Co., Westfall #1	NW	NW	SW	Sec.15-T17N-R2E
35.	Jones and Pellow Oil Co., J & P Harriet #22-1	C	NE	SW	Sec.22-T17N-R2E
5.	Gilbralter Exploration, Ltd., Close #1	C	NW	SW	Sec.34-T17N-R2E

*DENOTES TIE WELL

VITA

Kenneth Scott Robertson

Candidate for the degree of

Master of Science

Thesis: STRATIGRAPHY, DEPOSITIONAL ENVIRONMENTS, PETROLOGY, DIAGENESIS, AND HYDROCARBON MATURATION RELATED TO THE RED FORK SANDSTONE IN NORTH-CENTRAL OKLAHOMA

Major Field: Geology

Biographical:

Personal Data: Born in Pittsburgh, Pennsylvania, June 14, 1955, the son of Mr. Kenneth H. Robertson and Mrs. Jane H. Fortney.

Education: Gaduated from Moon High School, Coraoplis, Pennsylvania, June, 1973; enrolled as a Chemistry major in the Bachelor of Science program at Waynesburg College, Waynesburg, Pennsylvania, from September, 1973 to May, 1975; completed requirements for Bachelor of Science degree in Geology from Edinboro State University, Edinboro, Pennsylvania, in December, 1977; completed requirements for the Master of Science degree in Geology at Oklahoma State University, Stillwater, Oklahoma, in December, 1983.

Professional Experiece: Well Site Geologist, Geological Logging Company, Oklahoma City, Oklahoma, Febuary 1978 to July, 1979; Contract Geologist, Action Oil, Tulsa, Oklahoma, March, 1980 to June, 1980; Geologist, Bixler Energy Inc., Denver, Colorado, March, 1980 to June, 1980; Geologist, KWB Oil Property Management, Inc., Tulsa, Oklahoma, June, 1980 to September, 1980; Teaching Assistant, Oklahoma State University, Stillwater, Oklahoma, September, 1980 to May, 1981; Geologist, KWB Oil Property Management Inc., Tulsa, Oklahoma, May, 1981 to September, 1981; Junior Member of the American Association of Petroleum Geologists; Member of the Oklahoma City Geological Society.